Identification of molecular mechanisms mediating the adjuvanticity of cyclic di-nucleotides

Von der Fakultät für Lebenswissenschaften
der Technischen Universität Carolo-Wilhelmina zu Braunschweig
zur Erlangung des Grades
einer Doktorin der Naturwissenschaften
(Dr. rer. nat.)
genehmigte

D i s s e r t a t i o n

von Ivana Škrnjug
aus Zagreb, Kroatien

1. Referentin: PD Dr. Simone Bergmann

2. Referent: Prof. Dr. Dieter Jahn

3. Referent: Prof. Dr. Carlos A. Guzmán

eingereicht am: 08.06.2015
mündliche Prüfung (Disputation) am: 22.09.2015

Druckjahr: 2016

Vorveröffentlichungen der Dissertation

Teilergebnisse aus dieser Arbeit wurden mit Genehmigung der Fakultät für Lebenswissenschaften, vertreten durch die Mentorin der Arbeit, in folgenden Beiträgen vorab veröffentlicht:

Publikationen

1. Ivana Škrnjug, Christine Rueckert, Rimma Libanova, Stefan Lienenklaus, Siegfried Weiss and Carlos Alberto Guzmán (2014) **The mucosal adjuvant cyclic di-AMP exerts immune stimulatory effects on dendritic cells and macrophages**. PLoS ONE 9(4): e95728. doi:10.1371/journal.pone.0095728.
2. Ivana Škrnjug, Carlos Alberto Guzmán and Christine Rueckert (2014) **Cyclic GMP-AMP displays mucosal adjuvant activity in mice.** PLoS ONE9(10): e110150. doi:10.1371/journal.pone.0110150.

Posterbeiträge

1. **Innate immune target cells of the candidate mucosal adjuvant c-di-AMP.** Signal transduction Society meeting, Weimar, Germany; November 5th- November 7th, 2014
2. **Cyclic GMP-AMP has mucosal adjuvant activity in mice.** 4th International Conference on Vaccines and Vaccination, Valencia, Spain; September 24th- September 26th, 2014
3. **Innate immune target cells of the candidate mucosal adjuvant c-di-AMP.** 3rd DGfI Translational Immunology School, Potsdam, Germany; March 20th- March 22th, 2014
4. **The mucosal adjuvant c-di-AMP targets macrophages and dendritic cells.** World immune regulation meeting VIII (´´WIRM VIII´´), Davos, Switzerland; March 19th- March 22th, 2014
5. **Identification of molecular mechanisms mediating the adjucvanticity of cyclic di-nucleotides.** EMTRAIN PhD Workshop, Braine-l´Aleud, Belgium; May 11th- May 14th, 2014
6. **Innate immune target cells of the candidate mucosal adjuvant c-di-AMP.** Signal transduction Society meeting, Weimar, Germany; November 4th- November 6th, 2013

7. **The adjuvant c-di-AMP induces activation of dendritic cells independently of IFN-I signaling.** FEBS conference; Sankt Petersburg, Russia; July 6th- July 11th, 2013
8. **IFN-β/IFNAR signaling is activated, but dispensable for c-di-AMP-induced BMDCs activation.** ´´6th International workshop Interferon and Infection´´, Braunschweig, Germany; May 30th- June 1st, 2013
9. **Identification of molecular mechanisms mediating the adjuvanticity of cyclic di-nucleotides.** Hands-On Light Microscopy Workshop, Basic and Advanced Techniques, University of Luxembourg, Luxembourg; January 14th- January 18th, 2013

Präsentation

1. **Identification of molecular mechanisms mediating the adjuvanticity of cyclic di-nucleotides.** International Graduate Student Immunology Conference, Marseille, France; August 29th- August 31st , 2013

ACKNOWLEDGEMENTS

The project elucidating the molecular mechanisms mediating the adjuvanticity of cyclic di-nucleotides was done in the period from 1st of May 2012 to 30th of April 2015. The work was performed at the department of Vaccinology and Applied Microbiology at the Helmholtz Centre for Infection Research in Braunschweig, Germany. I would like to thank all the people who supported this fruitful project, especially the part presented in this thesis.

I sincerely thank my supervisors, Professor Dr. Carlos A. Guzmán and Dr. Christine Rückert.

Dear Carlos and Christine, the guidance provided by you is the one that a graduate student can only wish for. I am grateful for constructive discussions, challenging environment, encouragement, your patience and the given freedom that allowed me to develop as an independent scientist, yet a beginner. I apologize if sometimes my ambitious attitude was difficult to deal with. Thank you for giving me an opportunity to work with you, I feel extremely lucky and honored to be guided by such team of brilliant scientists and humans.

I am grateful to my thesis committee members Prof. Dr. Carlos A. Guzmán, Dr. Christine Rückert, Prof. Dr. Ingo Schmitz and Dr. Simone Bergmann for the invested time, efforts and valuable scientific input supporting the development of the project presented here.

I would like to thank Prof. Dr. Dieter Jahn, Prof. Dr. Carlos A. Guzmán and Dr. Simone Bergmann for acting as the referees of my thesis.

I would also like to thank Prof. Siegfried Weiss, Dr. Stefan Lienenklaus and Prof. Dr. Ulrich Kalinke for collaboration in providing animal models used in my experiments.

A big thank you I would like to say to my working group. *Dear VACs: Dr. Peggy Riese, Dr. Thomas Ebensen, Dr. Kai Schulze, Dr. Sebastian Weissmann, Dr. Dario Lirussi, Ulrike Bröder, Elena Reinhard, Stephanie Trittel, Neha Vashist, Shiwani Agarwal, Hanna Shkarlet, Mathias Neumeyer, Carolin Kanzler, Cornelia Senske and Dr. Blair Prochnow, thank you very much for being so helpful and collaborative. The team spirit that I experienced with you was a driving force for my work!*

Finally, I would like to express my infinite gratefulness to my family and the closest friends: Zrinka, Hanna, Biliana, Marc, Alisha, René, Marina, Goran, Alex, Aida and Mateja, who supported me in many difficult moments.

Dear colleagues and friends, the past three years were very special. Together with me, you took part in the adventure of revealing the ´´dirty little secret´´ of cyclic di-nucleotides. I hope you enjoyed!

Yours sincerely,

Ivana

Mojoj obitelji

TABLE OF CONTENTS

TABLE OF FIGURES

TABLE OF TABLES

ABBREVIATIONS

Abbreviation	Full name
ABTS	2,2´-azino-bis (3-ethylbenzthiazoline-6 sulfonic acid) diammonium salt
ACK	Ammonium chloride-potassium
AEC	3-amino-9-ethyl-carbazole (AEC substrate kit)
APCs	Antigen presenting cells
APC	Allophycocyanin
APRIL	A proliferation-inducing ligand
APS	Ammonium persulfate
BAFF	B cell-activating factor
BMDCs	Bone marrow-derived dendritic cells
BSA	Bovine serum albumin
CD	Cluster of differentiation
c-di-AMP	Bis-(3´,5´)-cyclic dimeric adenosine monophosphate
c-di-GMP	Bis-(3´,5´)-cyclic dimeric guanosine monophosphate
CDN	Bacterial cyclic di-nucleotide
cGAMP	(3',5'-3',5')-cyclic (adenosine monophosphate-guanosine monophosphate)
(2´,5´)-cGAMP	(2',5'-3',5')-cyclic (adenosine monophosphate-guanosine monophosphate)
cGAS	GMP-AMP synthase
Ci	Curie
CMA	10-carboxymethyl-9-acridanone
Cpm	Counts per minute
CR	Complement receptor
CS	Complement system
CTL	Cytotoxic T lymphocyte

DAI	DNA-dependent activator of IFN-regulatory factors
DDX41	DEAD box polypeptide 41
DEAD	Asp-Glu-Ala-Asp
DMSO	Dimethyl sulfoxide
DMXAA	5,6-Dimetylxanthenone-4-acetic acid
DNA	Deoxyribonucleic acid
ds	Double stranded
ECL	Enhanced chemiluminescence
EDTA	Ethylenediaminetetraacetic acid
e.g.	*Exempli gratia*
ELISA	Enzyme-linked immunosorbent assay
ELISPOT	Enzyme-linked immunospot assay
ER	Endoplasmatic reticulum
ERK	Extracellular signal-regulated kinases
FCS	Fetal calf serum
FITC	Fluorescein-isothiocyanate
GM-CSF	Granulocyte-macrophage colony stimulating factor
Gt	Goldenticket
HEK	Human embryonic kidney
HEPES	4-(2-hydroxyethyl)-1-piperazineethanesulfonic acid
h.i.	Heat inactivated
HRP	Horseradish peroxidase
i.e.	*Id est*
IFI	Interferon-inducible myeloid differentiation transcriptional activator
IFN	Interferon
IFNAR	Interferon-α/-β receptor
Ig	Immunoglobulin

IL	Interleukin
i.n.	Intranasal
IRF	Interferon regulatory factor
ISG	IFN-stimulated gene
Jak	Janus kinase
ko	Knock out
LPS	Lipopolysaccharide
M cells	Microfold cells
MHC	Major histocompatibility complex
min	Minute
MyD88	Myeloid differentiation primary response gene 88
NALT	Nose-associated lymphoid tissue
NF-κB	Nuclear factor kappa-light-chain-enhancer of activated B cells
NLR	NOD-like receptor
NOD	Nucleotide-binding oligomerization domain
n. s.	Non-significant
OVA	Ovalbumin
PAGE	Polyacrylamide gel electrophoresis
PAMP	Pathogen-associated molecular pattern
PBS	Phosphate-buffered saline
PCR	Polymerase chain reaction
PE	Phycoerythrin
PerCP	Peridinin-chlorophyll-protein complex
PE-Cy7	Phycoerythrin-cyanin 7
PFA	Paraformaldehyde
PMSF	Phenylmethanesulfonyl fluoride
PRR	Pathogen recognition receptor
RIG	Retinoic acid-inducible gene

RLR	RIG-like receptor
RNA	Ribonucleic acid
SC	Secretory component
SDS	Sodium dodecyl sulfate
SEM	Standard error of the mean
Stat	Signal transducer and activator of transcription
Sting	Stimulator of interferon genes
TAE	Tris-acetate-EDTA
TBK-1	Tank-binding kinase-1
TBS	Tris-buffered saline
TBS-T	Tris-buffered saline Tween 20
TCR	T cell receptor
TEMED	Tetramethylethylenediamine
TGF	Transforming growth factor
Th	T helper
TIR	Toll/interleukin-1 receptor
TLR	Toll-like receptor
TNF	Tumor necrosis factor
TNFR	Tumor necrosis factor receptor
Trif	TIR-domain-containing adapter-inducing interferon-β
UV	Ultraviolet
wt	Wild type

ABSTRACT

Infectious diseases cause millions of deaths every year worldwide, resulting also in overwhelming direct and indirect costs. Thus, they represent a major problem in primary human health care. In this regard, vaccination is one of the most cost-efficient strategies for their prevention. Successful vaccines should be highly effective in evoking immune responses able to protect against specific pathogens while at the same time leading to negligible adverse reactions. To circumvent safety issues associated with the use of whole pathogen containing vaccines, the development of vaccines containing pathogen subunits should be favored. However, they are usually poorly immunogenic, making necessary to incorporate adjuvants in the formulation. The cyclic di-nucleotides (CDNs) bis-(3´,5´)-cyclic dimeric guanosine monophosphate (c-di-GMP) and bis-(3´,5´)-cyclic dimeric adenosine monophosphate (c-di-AMP) are promising candidate adjuvants, capable of enhancing the stimulation of balanced humoral and cellular immune responses after systemic or mucosal administration. However, their immune regulatory properties and their molecular mode of action remain to be fully characterized as a precondition for their application in vaccines leading to predictable immune responses in humans.

In the first part of this thesis, the mucosal adjuvant activity of the newly discovered CDN (3',5'-3',5')-cyclic (adenosine monophosphate-guanosine monophosphate) (cGAMP) was demonstrated in mouse immunization studies and was compared to the adjuvant activity of c-di-AMP to identify possible differences in their immune stimulatory potency. Based on immunization experiments using ovalbumin as model antigen, it was shown that c-di-AMP and cGAMP enhance the stimulation of antigen-specific humoral responses (*e.g.* mucosal IgA and systemic IgG), T helper (Th) 1 and Th2 responses to a similar extent. In contrast, c-di-AMP was shown to be a stronger enhancer of the Th17 response, as compared to cGAMP. *In vitro* experiments using bone marrow derived dendritic cells also demonstrated a stronger induction of IL-12/IL-23p40 by c-di-AMP than by cGAMP, whereas their capacity to up-regulate the surface expression of the activation markers MHC class II, CD86 and CD80 were similar.

It is known that CDNs induce the production of cytokines (*e.g.* type I interferon (IFN) and tumor necrosis factor (TNF)-α) via the stimulator of interferon genes (Sting). The downstream signaling of type I IFN is mediated by the IFN-α/-β receptor (IFNAR). In the second part of this thesis, the relevance of the type I IFN induction and signaling pathways for the adjuvanticity of c-di-AMP and cGAMP was evaluated *in vivo*. To this

end, immunization studies were performed using mice lacking functional Sting or IFNAR and the immune responses were compared to the response in wild type animals. The results suggested that the adjuvanticity of c-di-AMP and cGAMP is dependent on Sting, whereas the function of IFNAR is dispensable.

The findings described in this thesis demonstrate the potential of CDNs to be used in vaccine formulations as a tool for evoking effective and predictable immune responses. In addition, they shed light on the role played by type I IFN signaling in the development of adaptive immune responses post vaccination. First, IFNAR deficiency did not abolish the enhancement of adaptive immune responses by c-di-AMP or cGAMP, thereby indicating that type I IFN is dispensable for the adjuvant efficacy of c-di-AMP or cGAMP. Instead, IFNAR signaling seems to modulate the extent of c-di-AMP and cGAMP-enhanced immune responses. Second, the results demonstrate that not the classically described function of Sting in the induction of type I IFN but rather alternative pathways are required for the adjuvant activity of c-di-AMP and cGAMP. To this end, the CDN-induced NF-κB-TNF-α signaling axis that is known to play a role in the adjuvanticity of c-di-GMP may be considered as a possible alternative pathway.

1 INTRODUCTION

1.1 The immune system

The immune system of mammals is composed of organs, tissues, cells and molecules that form a complex network evolutionary developed to fight dangerous entities, such as infectious agents and transformed cells. There are two branches of the immune system: the innate and the adaptive immunity. Each branch contains humoral and cellular components, as shown in **figure 1,** and acts via many mechanisms protecting the host from for example, colonization and/or invasion by pathogens, as well as the subsequent progression of infections.

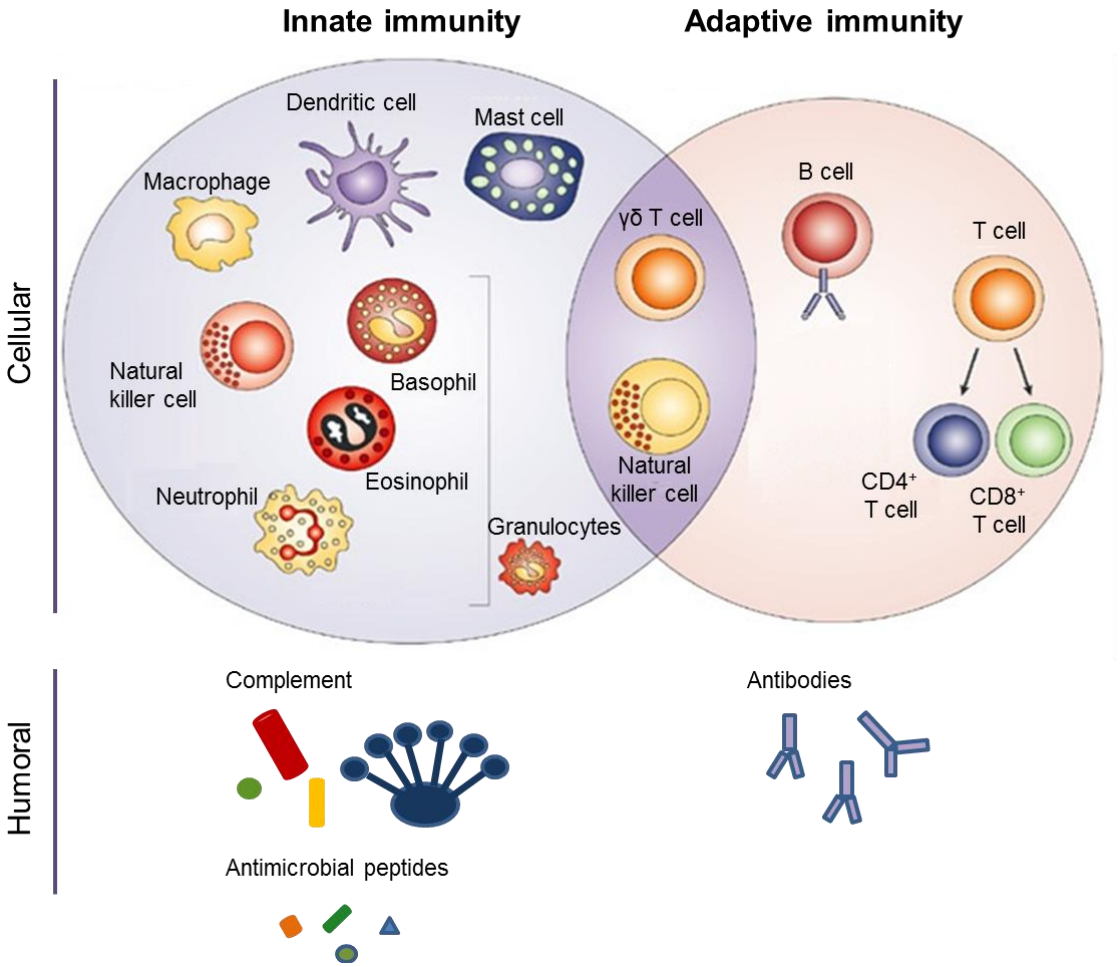

Figure 1: Components of the immune system. Each of the branches, innate and adaptive immunity is composed of cellular and humoral components that differ based on their effector characteristics and the pattern of their surface receptors expression. γδ T cells and natural killer T cells are classified as cells that bridge the innate and adaptive immunity because they not only show characteristics of innate cells, but as well express antigen-specific receptors (modified from [1]).

1.1.1 The innate immune system

The innate immune system is enrolled in the immediate early phase of a pathogen encounter. Its effector strategies are not antigen-specific and do not develop long lasting memory. The main components of the humoral innate immune response are proteins of the complement system (CS). There are several cascades of CS activation, which results in activation of C3 convertase, leading to different effector strategies of pathogen clearance. For example, once triggered by binding of *e.g.* C1q to the surface of a pathogen, CS activation triggers the enzymatic activity of C3 convertase, generating C3a and C3b proteins. C3a acts as a local pro-inflammatory molecule and C3b binds to the pathogen surface, labeling it for destruction by antigen presenting cells (APCs). APCs express complement receptor (CR) C3b on their surface. They recognize C3b bound to the surface of pathogens, resulting in elimination of these immune complexes, in a process called opsonization. In a similar fashion, due to surface expression of Fc receptors, APCs can recognize immune complexes of antibodies bound to pathogens, allowing their clearance [2].

Major cell types acting at this level of immunity are macrophages and dendritic cells, which function as APCs. They are required for the elicitation of adaptive immune responses [3, 4] and can be activated by pathogen associated molecular patterns (PAMPs) such as pathogen specific proteins, lipids, carbohydrates and deoxyribonucleic acid (DNA) or ribonucleic acid (RNA) molecules. They recognize PAMPs via specific pathogen recognition receptors (PRRs) expressed at the cell surface or in intracellular compartments. Major families of PRRs are: Toll-like receptors (TLRs), retinoic acid-inducible gene (RIG)-like receptors (RLRs), nucleotide binding domain (NOD)-like receptors (NLRs), and C-type lectins [5, 6]. APCs endocytose the encountered antigens, digest and load their peptides on major histocompatibility complex (MHC) class II molecules, forming immune complexes recognized by T cells. In addition, dendritic cells can act as a delivery vehicle of intact antigens to naïve B cells, for example via CR1/2-mediated surface binding of immune complexes containing antigens and complement components [7-9]. Activation of APCs by PAMPs enhances the surface expression of the MHC class II molecules and the co-stimulatory molecules cluster of differentiation (CD)80 (B7-1) and CD86 (B7-2). Once activated, APCs also start producing pro-inflammatory cytokines [6, 10] and migrate to lymph nodes to activate specific T or B cells.

1.1.1.1 Type I interferons

Type I interferons (IFNs) (IFN-α1-13, IFN-β) are important cytokines produced early after pathogen encounter and PAMP-mediated activation of APCs. Tank binding kinase-1 (TBK-1) and the transcription factors IFN regulatory factor (IRF) 3 and IRF7 are the central players of pathways mediating IFN-α and/or IFN-β production. TBK-1 activates IRF3/IRF7 by phosphorylation, which triggers their dimerization and translocation to the nucleus where they bind to type I IFN promoters [2]. Depending on the type of PAMP, the IRF-mediated activation of type I IFN promoters can be enhanced by nuclear factor kappa-light-chain-enhancer of activated B cells (NF-κB), strengthening the up-regulation of type I IFNs [11-13] . The TBK-1-IRF3/IRF7 axis can be triggered by various PAMPs that are recognized by for example foreign double stranded (ds) DNA sensors, such as DNA-dependent activator of IFN-regulatory factors (DAI), IFN-inducible myeloid differentiation transcriptional activator (IFI16), DEAD (Asp-Glu-Ala-Asp) box polypeptide 41 (DDX41) and cyclic GMP-AMP synthase (cGAS) [14-18] or by different TLR receptors. These molecules recruit adaptors, such as stimulator of interferon genes (Sting), TIR-domain-containing adapter-inducing interferon-β (Trif) or myeloid differentiation primary response gene 88 (MyD88) that recruit TBK-1 resulting in the activation of IRF3/IRF7-mediated IFN-β up-regulation **(figure 2)**.

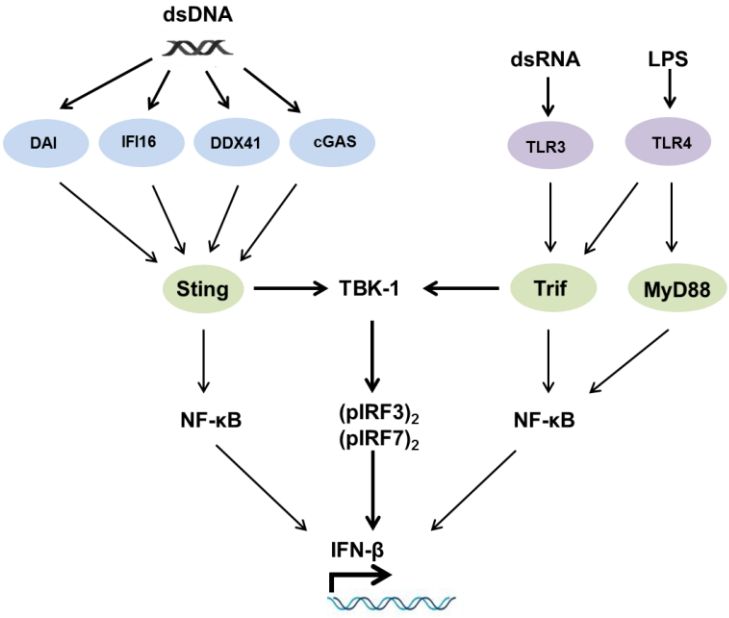

Figure 2: Activation of the IFN-β promoter. The central activator of the IFN-β promoter is the TBK-1 and IRF3/IRF7 mediated signaling axis and NF-κB can enhance the activation of IFN-β production. Various PAMPs, such as dsDNA, dsRNA and lipopolysaccharide (LPS) are recognized by different sensors (DAI, IFI16, DDX41, cGAS, TLR3, TLR4). This results in activation of adaptor proteins such as Sting, Trif and MyD88, which recruit the TBK-1 and NF-κB, thereby resulting in activation of IFN-β expression.

Type I IFNs signal via the Interferon-α/β receptor (IFNAR)1/2, which is expressed in all cell types [19, 20], and activate the Janus kinase/signal transducer and activator of transcription (Jak/Stat) signaling cascade. As a result, IFN stimulated genes (ISGs) are induced, which are crucial for the establishment of antiviral responses at the cellular level [2] **(figure 3)**.

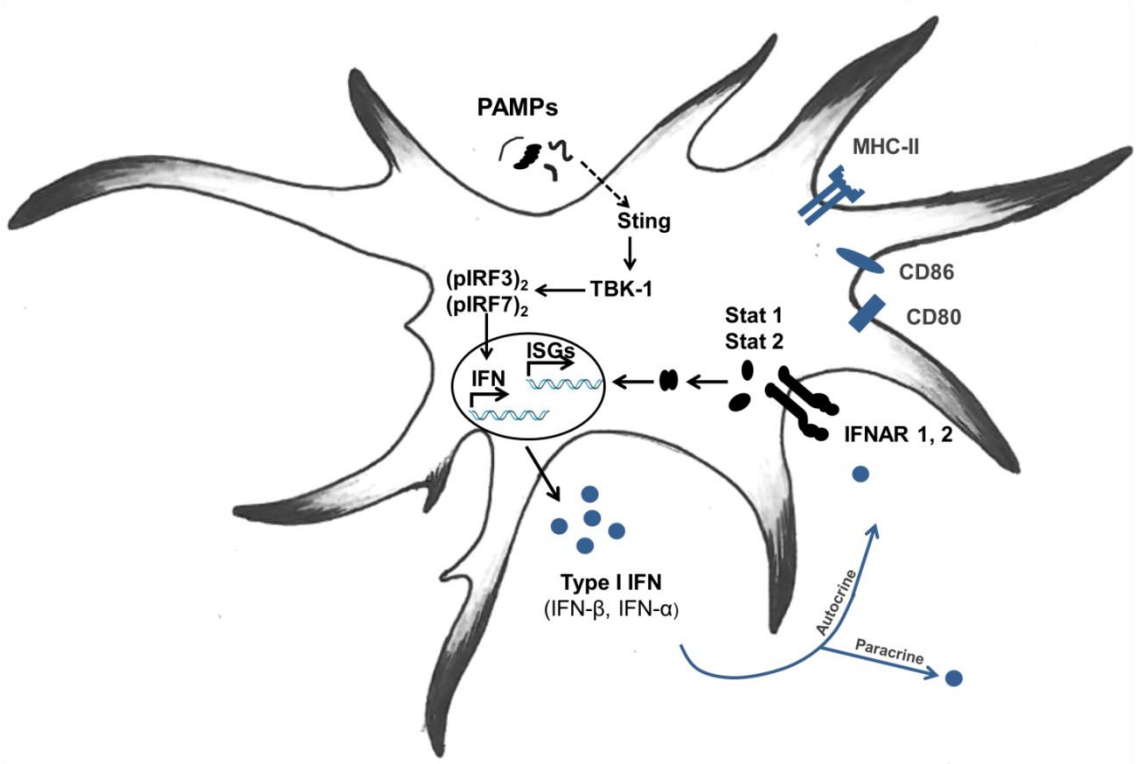

Figure 3: Type I IFN-associated pathways. APCs sense pathogens via detection of PAMPs. Type I IFNs production can be upregulated for instance upon PAMP-triggered Sting activation. Type I IFNs are secreted and bind to the IFNAR, which triggers Stat1/Stat2-mediated activation of ISGs, thereby inducing antiviral activity.

1.1.1.2 Sting

Sting (also known as ERIS, MYPS, MITA, TMEM173 and NET23) is a transmembrane protein located predominantly in the endoplasmic reticulum (ER) [21, 22]. Once activated, Sting oligomerizes, traffics from ER to perinuclear vesicles via the Golgi apparatus and interacts with TBK-1 that is recruited from the cytoplasm [21-23]. This can result in activation of transcription factors IRF3 or NF-κB, which translocate to the nucleus and induce IFN-β and/or tumor necrosis factor (TNF)-α production [21, 24, 25]. In addition, Sting can activate extracellular signal-regulated kinases (ERK) [26] and Stat6 [27]. Sting-mediated IFN-β production is under control of different regulators that induce Sting degradation [28], and affect its dimerization [29] or translocation to the

perinuclear region [30, 31]. There are several stimuli for Sting activation, such as: i) activation of cytosolic sensors of foreign dsDNA (*e.g.* DAI, IFI16, DDX41 and cGAS, see chapter 1.1.1.1) and ii) cell membrane fusion-related signals [32]. In addition, some cytosolic DNA sensors produce molecules that activate Sting. For example, the mammalian enzyme cGAS after binding of cytosolic dsDNA catalyzes the production of (2',5'-3',5')-cyclic (adenosine monophosphate-guanosine monophosphate) ((2',5')-cGAMP). (2´,5´)-cGAMP is a non-canonical cyclic di-nucleotide so far described only in eukaryotes. Once produced, it binds to Sting and induces IFN-β production [17, 18, 33-36]. Most of the reports are focused on Sting as a central molecule in the induction of type I IFNs and point to its role in the early immune response against pathogens. However, the fine regulation of Sting activity and its role in the development of an adaptive immune response still remain to be elucidated.

1.1.2 The adaptive immune system

The adaptive immune response can fight pathogens by: i) antibodies targeting the antigens outside the host cells and ii) cell-mediated killing of the infected host cells, resulting in a strong specific reaction against the pathogen and formation of memory cells, ensuring a long-term protection. The adaptive immune system is principally composed of T and B lymphocytes that recognize specific pathogens. T and B lymphocytes are characterized by the surface expression of T and B cell receptors, respectively. The variability of T and B lymphocyte receptors results from recombination in germ-line genes during their development. T lymphocytes acting exclusively in the adaptive immune response are T helper ($CD4^+$) cells and cytotoxic ($CD8^+$) T cells. $CD4^+$ T helper (Th) lymphocytes regulate cellular and humoral adaptive immune responses, whereas $CD8^+$ cytotoxic T lymphocytes (CTL) are effectors of cell mediated killing of infected cells. B cells mediate humoral adaptive immune responses by antibody production [2].

Activation of naïve antigen-specific T cells requires two signals, which are only present upon activation of the APC with PAMPs to prevent unnecessary T and B cell activation by presented self-antigens [37]. The first signal is the binding of an antigen presented by MHC class II for $CD4^+$ cells or MHC class I for $CD8^+$ cells to a corresponding T cell receptor (TCR) on the surface of a T cell. The second is the co-stimulatory signal, provided by the interaction of CD80 and CD86 at the surface of APCs with the co-receptor CD28 on the surface of T cells [38]. Beyond these main players, there are

several other surface molecules involved in fine-tuning the interaction between APCs and T cells, which from part of the so-called immune synapsis [39-41]. In addition, the activation of naïve antigen-specific T cells is supported by the local cytokine milieu originating from APCs and T cells [2].

Naïve B cells process antigens in a manner similar to other APCs. The intact antigens may be taken directly from the environment or can be delivered by dendritic cells to naïve B cells [8, 42, 43]. Naïve B cells express on their surface immunoglobulin (Ig)M and IgD, which act as antigen receptors. After the antigen is recognized by those receptors it becomes endocytosed and digested. Its peptides are loaded to MHC class II molecules and are transported to the surface of B cells where they can be recognized by Th2 cells. Then the interaction of CD40 on the B cell surface and CD40L on the surface of the interacting T cell provides the co-stimulatory signal [44]. This triggers the development of B cells to antibody-producing plasma cells. There are five classes of antibodies: IgD, IgM, IgG, IgA and IgE. After the first encounter with a pathogen, plasma cells produce the IgM isotype which forms pentamers and is characterized by its low affinity binding to an antigen. However, B cells can undergo a class switch, leading to the production of high affinity IgG and IgA subclasses, which is regulated by other APCs and Th cells [8, 45-47]. Systemic humoral responses are characterized by IgG production, in mice present in a form of isotypes IgG1, IgG2a-c and IgG3, whereas IgA secretion is the hallmark of mucosal antibody-mediated protection [2]. Secretory IgA exists in a form of at least two IgA molecules, which are connected through the short J-chain polypeptide [48, 49]. The J-chain polypeptide in a complex with IgA is recognized by the secretory component (SC), a protein located at the basolateral surface of secretory epithelial cells [50]. Binding of this ligand to SC triggers transcytosis, resulting in a transport of the secretory IgA from basolateral side of epithelium to the mucosal surface [51]. Despite the fact that secretory IgA is the major mucosal Ig, monomeric IgA and some other Ig subclasses originating from serum can be found at mucosal sites due to transudation and the proportions of different Ig subclasses there differ according to a specific mucosal territory [52-54].

Activation of naïve T cells results in T cell proliferation, enhancement in their surface expression of adhesion molecules and promotes cell survival. The local cytokine milieu provides signals that promote differentiation into different $CD4^+$ effector T cell phenotypes, such as Th1, Th2, Th17 or regulatory T cells [55]. For example, IFN-γ and interleukin (IL)-12 produced by activated APCs have been described as important

cytokines that promote the differentiation of $CD4^+$ effector T cells into the Th1 phenotype [45, 56]. Th1 cells are characterized by IFN-γ and IL-2 production leading to the development of a CTL response. CTL induce apoptosis of infected cells by different mechanisms (*e.g.* granzyme release into target cells, binding of Fas ligand on the surface of CTL to Fas receptor on the target cell) [57-61]. This is important for clearing infections caused by intracellular pathogens, such as viruses, *Toxoplasma gondii* [62] or certain fungal infections [63]. Increased IL-4 and decreased IFN-γ production by APCs and B cells [64] promote $CD4^+$ T cell differentiation into the Th2 phenotype. These cells are characterized by IL-4 production and promote the adaptive humoral immune response. This branch of the immune response is important for resolving infections caused by extracellular pathogens, such as some extracellular bacteria and helminths [65]. Activation of naïve $CD4^+$ T cells in the presence of IL-6, IL-21, IL-1β and transforming growth factor (TGF)-β results in differentiation into the Th17 phenotype [66, 67], which is maintained by APC-secreted IL-23 [68, 69]. $CD4^+$ T cells of the Th17 phenotype secrete IL-17A, IL-17F, IL-21 and IL-22 [70] and are indispensable to fight extracellular pathogens, such as *Klebsiella pneumoniae* [71]. Taken together, relative amounts of different cytokines induced by a pathogen modulate the differentiation of naïve T cells and therefore the profile of the final adaptive immune response [2].

1.2 Mucosal vaccination

Infectious diseases are one of the major health problems worldwide, being directly responsible for millions of deaths every year [72, 73]. Pathogens use various strategies to colonize human hosts and cause diseases [74-78]. Treatment of infections is rendered difficult by the lack of highly effective drugs against many agents (*e.g.* Ebola virus, influenza), as well as the rapid emergence and spread of anti-microbial resistant strains [79]. Thus, vaccination remains as one of the most effective prevention strategy to fight infections. In addition, the potential use of vaccines as a therapeutic tool against infections has also gained considerable interest [80]. However, there are still many infections for which there is no available vaccine or the existing vaccine is suboptimal [81]. This is particularly true for diseases in which the simulation of cellular immunity would be needed in order to confer efficient protection. Therefore, new vaccines able of promote long-term protection are urgently needed. Most pathogens are restricted to or need transit across the mucosal barriers (*e.g.* gastrointestinal, respiratory and urogenital mucosa) [82]. Therefore, ensuring local pathogen-specific immune protection at the

mucosa would be advantageous for controlling the pathogen early upon the encounter with the host. However, most of the currently available parenterally administered vaccines elicit mainly systemic responses, while they are less effective at mucosal sites [83]. The mucosal administration of vaccine antigens induces not only systemic immune response, but also a mucosal response at the pathogen´s port of entry [84, 85].

1.2.1 Basic principles of mucosal immune responses

The local mucosal immune response against infections is based on unspecific mechanisms of defense and pathogen-specific immune responses largely mediated by secretory IgA [86-90]. The unspecific mucosal defense is mediated by physical and chemical barriers. The physical barrier is composed by the mucosal epithelium which prevents penetration of pathogens into the host. The epithelial cells can form a single layer or multilayers and their integrity defines the access of antigens to dendritic cells, crucial for initiating a pathogen-specific adaptive immune response [91]. Mucociliary clearance in the airways of the host is one of the most important non-specific mechanisms against pathogen colonization. The respiratory mucosa is composed of a mucus layer and special ciliary epithelial cells that provide the clearance of the pathogens from the mucosal surface by constant mechanical movements. Mucosal chemical barriers are composed of mucins, inhibitors of pathogen growth and anti-microbial peptides, such as defensins, which are secreted by epithelial cells [92].

Antigen-specific secretory IgA is the central mediator of the pathogen-specific mucosal immune response and is produced at the basolateral side of the mucosal epithelium [51]. B cells become activated by antigen recognition followed by interaction with Th2 cells and mature under the influence of local cytokines, such as APRIL (a proliferation-inducing ligand) and BAFF (B cell-activating factor) originating from dendritic cells [47]. They undergo a class switch driven towards the IgA isotype and become plasma cells that secrete dimeric or polymeric IgA [93]. IgA is taken up at the basolateral side of the epithelium and transported across epithelial cells via transcytosis to the mucosal surface where it neutralizes foreign antigens [94].

1.2.2 Evoking immune responses by mucosal vaccines

Antigen-specific secretory IgA prevents the colonization of mucosal surfaces by pathogens and can be evoked by vaccination [95]. Mucosal vaccines can be administered orally or applied directly on the mucosal surface of the respiratory and

urogenital tracts as liquids or aerosols. The existence of a mucosal network allows the stimulation of mucosal responses at distant mucosal territories after vaccination at a particular mucosal site [96]. However, there is a certain degree of compartmentalization in the mucosal immune system and it should be considered when defining the vaccination route to evoke immune responses at specific mucosal areas [97, 98]. Mucosal vaccines delivered by the same route as their target pathogen evoke immune responses that mimic those observed after natural infections. For example, the live attenuated vaccine against the polio virus is administered orally and this virus enters the host via the intestinal tract, where the primary infection takes place [99]. On the other hand, vaccine candidates against air-borne pathogens, such as influenza virus [100], respiratory syncytial virus [101] and nontypeable *Haemophilus influenzae* [102] are administered by the intranasal (i.n.) route and promote stronger responses than those administered via the oral route.

Although there are clear advantages of evoking a mucosal adaptive immune response via vaccination, the efficacy of the administered vaccine depends on the ability to deliver the antigen to APCs across the mucosa. This is hampered by the natural barrier functions of the mucosa, such as: i) physical clearance of antigens via ciliary epithelial cells ii) chemical degradation of antigens due to enzymes and low pH and iii) limited transport through mucosal barrier [103, 104]. Therefore, to improve the efficacy of mucosal vaccines it is necessary to develop formulations capable of the delivery of antigens to APCs by crossing the epithelial layer. From this point of view, the administration of antigens through the nasal mucosa seems to be more attractive than the oral route, where the higher abundance of enzymes increases the risk of degradation of the administered vaccine components. Furthermore, i.n. applied vaccine formulations can take advantage of the nose-associated lymphoid tissues (NALT) that would provide compact immune responsive cell populations in close proximity to the site of administration [105].

1.2.3 Evoking adaptive immune responses *via* the NALT

As shown by Wu *et al.*, the central site of mucosal immune response induction upon i.n. immunization in rodents is the NALT, an equivalent of the Waldeyer´s ring in humans [106]. The NALT is composed of lymphoid tissue enveloped in an epithelial layer which contains microfold (M) cells [107]. The epithelium prevents dendritic cells to directly access the nasal cavity and sample for antigens. Instead, the M cells are enrolled in the

delivery of the antigens from the apical to the basolateral surface of the mucosal tissue. There, dendritic cells take up and deliver antigens to T or B cells to stimulate them locally or migrate to draining lymph nodes to initiate their proliferation and migration to distal mucosal tissues [86] **(figure 4)**.

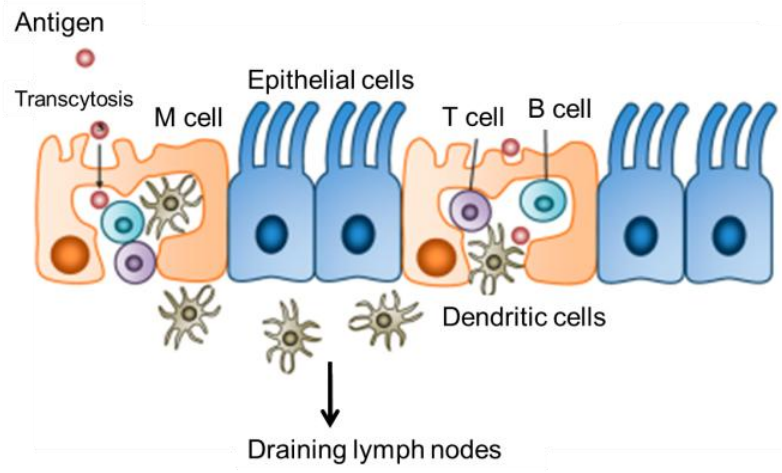

Figure 4: The initiation of an immune response at the nasal mucosa. Antigens are taken up by M cells and are transported via transcytosis to dendritic cells located at the basolateral site of the mucosal tissue. Dendritic cells initiate adaptive responses via presentation of antigens to resident T or B cells or migrate from the mucosal site to draining lymph nodes (modified from [108]).

1.2.4 Formulations of mucosal vaccines

Most of the antigens in mucosal vaccines nowadays are delivered as live attenuated organisms (*e.g.* polio, cholera, influenza, typhoid vaccine) [109, 110]. Although live-attenuated vaccines have proven to induce effective immune responses, their limitations become evident when specific groups of patients do not respond or show unexpected adverse effects. Mostly, it is not known which specific vaccine component has to be modified to solve these problems. For example, a live attenuated vaccine against rotavirus gastroenteritis administered via the oral route was withdrawn from the market due to cases of intussusception in patients [111], but the exact cause has never been identified. Notably, the empirical formulation of vaccines does not allow benefiting from knowledge gained from failed vaccine clinical trials, which makes vaccine development costly in the long term. Furthermore, the attenuation of pathogens sometimes does not exclude risks, such as back reversion to virulence. Knowing the exact composition of vaccines would allow controlling the risks of applying compounds with toxic, allergenic or autoimmune potential. In addition, a defined vaccine composition would help to ensure that the evoked immune profile is suitable to fight multiple strains by incorporation of

antigens specific for multiple strains of a pathogen [112]. To this end, recombinant attenuated pathogens, DNA constructs, pathogen subunits or synthetic peptides can be used as antigens. Since their immunogenicity is usually weak, adjuvants can be incorporated in such formulations. Adjuvants are compounds that enhance and modulate adaptive immune responses to co-administered antigens [113].

1.2.5 Mucosal adjuvants

Cholera toxin and heat-labile *Escherichia coli* enterotoxin are well studied mucosal adjuvants in animal experimental systems. However, their application in humans requires the attenuation of their toxicity [114-116], as became apparent in the case of the virosomal-subunit influenza vaccine where *E. coli* heat-labile toxin was used as a mucosal adjuvant. This vaccine was withdrawn from clinical use due to the correlation of cases of Bell´s palsy in patients with vaccine administration [117].

Most of the adjuvanted vaccine formulations which are commercially available today are administered parenterally and contain alum-based adjuvants. A list of licensed adjuvants is given in **table 1**. It has been suggested that alum-induced activation of the Th2 response suppresses Th1 development [118], finally evoking a dominant humoral immune response to vaccination [119, 120]. Interestingly, a recent report described the use of alum in mucosal vaccine where it enhanced the Th1 and antibody responses, when compared to the response profile evoked by a formulation containing cholera toxin as adjuvant [121]. Although alum-based adjuvants are the most used, there are several problems related to their stability, costly shipping and long term storage [122]. To make vaccines available that evoke effective Th1 responses and can be distributed at low costs, alternative adjuvants would be needed. Furthermore, it would be desirable that the molecular mechanisms underlying the immune modulatory potency of adjuvants are well understood to meet the following requirements for the development of novel vaccines:

- Improved efficacy accomplished by combining compatible antigens, adjuvants and the optimal route of administration
- Options to rationally design formulations eliciting predictable immune responses, which provide effective protection against the target pathogen
- Better prediction of risk of potential undesired effects, based on the knowledge about adjuvant-triggered pathways that are not directly involved in evoking the immune response

Taken together, it is necessary to perform preclinical studies to identify immune modulators and characterize their patterns of immune response elicitation and safety profiles to develop safe vaccine formulations with the efficacy of live attenuated vaccines.

Table 1: Adjuvants licensed for use in human vaccines. (adapted from [123])

Adjuvant name (year licensed)	Adjuvant class	Components	Vaccines (diseases)
Alum* **(1924)**	Mineral salts	Aluminium phosphate or aluminium hydroxide	Various
MF59 **(Novartis; 1997)**	Oil-in-water emulsion	Squalene, polysorbate (Tween 80; ICI Americas), sorbitan trioleate (Span 85; Croda International)	Fluad (seasonal influenza), Focetria (pandemic influenza), Aflunov (pre-pandemic influenza)
ASO_3 **(GSK; 2009)**	Oil-in-water emulsion	Squalene, Tween 80, α-tocopherol	Pandremix (pandemic influenza), Prepandrix (pre-pandemic influenza)
Virosomes **(Berna Biotech; 2000)**	Liposomes	Lipids, hemagglutinin	Inflexal (seasonal influenza), Epaxal (hepatitis A)
ASO4* **(GSK; 2005)**	Alum-absorbed TLR 4 agonist	Aluminium hydroxide , MPL	Fendrix (Hepatitis B), Cervarix (human papilloma virus)

* The only adjuvants licensed in the United States.

1.3 Bacterial cyclic di-nucleotides

The cyclic di-nucleotides (CDNs) bis-(3´,5´)-cyclic dimeric guanosine monophosphate (c-di-GMP), bis-(3´,5´)-cyclic dimeric adenosine monophosphate (c-di-AMP) and (3',5'-3',5')-cyclic (adenosine monophosphate-guanosine monophosphate) (cGAMP) are well known bacterial second messengers, involved in processes such as biofilm formation, regulation of virulence and motility [124-126] **(figure 5)**. The cGAMP is the latest

discovered CDN [126] and represents the prokaryotic isoform of the already mentioned (2',5')-cGAMP (section 1.1.1.2). CDNs have been described as important factors of pathogens to colonize hosts. For example, c-di-GMP can decrease the pathogenicity of *Listeria monocytogenes*, *Mycobacterium tuberculosis* and *Vibrio cholerae* [127-129]. Overproduction of c-di-AMP seems to be involved in the regulation of *L. monocytogenes* [130, 131] and *M. tuberculosis* virulence [132]. cGAMP is known to increase host colonization by *V. cholerae* [126].

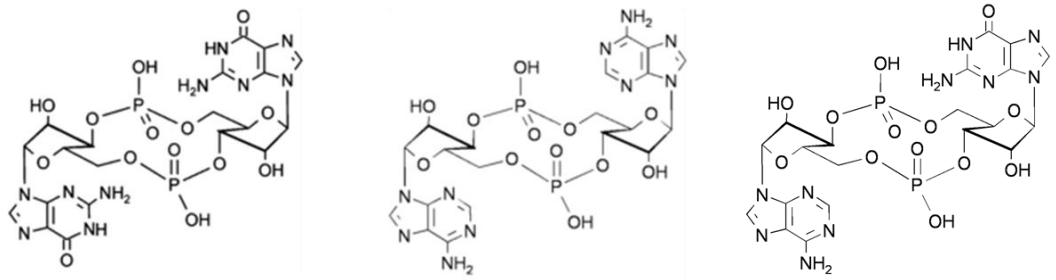

Figure 5: Chemical structure of bacterial cyclic di-nucleotides. (adapted from [133])

As many PAMPs, CDNs induce the production of IFN-β via Sting [134-137]. However, cGAMP cannot be considered as a classical PAMP since its isoform is present in mammalian cells. The interest in CDNs for the application in mucosal vaccines has been growing due to the proven ability of c-di-GMP and c-di-AMP to enhance balanced humoral and cellular responses to the model antigen ovalbumin (OVA) in murine models [138, 139]. Therefore, it would be interesting to test if cGAMP shows immune modulatory potential and if it is equivalent to the already described immune modulatory potential of the candidate adjuvant c-di-AMP. This question will be addressed in this thesis [140].

Although a series of adjuvant effects of CDNs have been well described, the molecular basis of their activity on the host immune system still remains to be elucidated. Current knowledge does not allow extrapolation of conclusions based on findings with one of the CDNs to all of them. For example, X-ray crystal structures of direct binding to Sting have been resolved for c-di-GMP [141, 142], cGAMP and (2´,5´)-cGAMP [36], whereas the attempts of crystalizing c-di-AMP bound to Sting have been so far unsuccessful. This leaves the option of alternative sensor(s) of c-di-AMP that interact with Sting to induce IFN-β production. For instance, Parvatyar *et al*. [137] described that the cytosolic dsDNA

sensor DDX41 can act as a direct sensor of c-di-GMP and c-di-AMP and pointed to the role of Sting as an adaptor in triggering the production of IFN-β. In addition, it cannot be excluded that different CDNs trigger signals from different domains of Sting, activating cascades that differentially contribute to their adjuvanticity. Having in mind that CDNs induce the production of IFN-β, it would be interesting to see if type I IFN pathways play a role in their adjuvanticity. Although the induction of type I IFNs early upon virus encounter is essential for the host defense, in bacterial infections the activity of type I IFNs depends on the invading pathogen and is not always beneficial to defend the host. For example, type I IFNs have been described as an important factor for fighting several gram positive bacteria [143-145], but its production upon *L. monocytogenes* infection seems to be the pathogen´s strategy to down-regulate the long term immune response of the host [146]. These observations point to the activity of type I IFNs as an important factor in development of immunity against specific pathogens and could be also assumed to be relevant for immune responses evoked by vaccination. The biological effects of type I IFNs are mediated by their receptor IFNAR. Blaauboer *et al.* reported that Sting, but not IFNAR plays a crucial role in enhancing the responses in immunization studies using c-di-GMP as an adjuvant [147]. Therefore, it would be interesting to investigate if the c-di-AMP and cGAMP-triggered type I IFN pathways play a role in their adjuvanticity and if the outcome of this study would differ from the findings published for c-di-GMP.

1.4 The aims of this thesis and experimental strategies

The thesis presented here was designed to contribute to the characterization of CDNs as candidate mucosal adjuvants. It aims at the investigation of the immune response profiles associated with the application of CDNs *in vivo* and the *in vitro* identification of cellular activation profiles that could be used as surrogate markers to predict immune responses evoked by CDNs. These activation markers can be further used as readouts for biochemical studies elucidating the pathways triggered by CDNs and their actual relevance for the adjuvanticity of CDNs can be addressed. To fulfill these overall aims, the experimental activities are focused on four specific areas.

First, the characterization of the recently discovered cGAMP in terms of its adjuvant potential should be performed by carrying out immunization studies in which the model antigen OVA should be administered alone or together with cGAMP by i.n. route to mice according to a three dose-immunization schedule. Two weeks after the third

immunization indicators of adaptive immune responses should be measured in serum and tissue samples from the immunized animals. Antigen-specific humoral responses should be determined by enzyme-linked immunosorbent assay (ELISA). To assess cellular responses, spleen cells should be re-stimulated with OVA. The proliferation of re-stimulated spleen cells should be measured by ^{3}H-thymidine incorporation assays. The cytokine production of re-stimulated spleen cells, indicative for Th1, Th2 or Th17 responses should be measured by enzyme-linked immunospot assays (ELISPOT) or flow cytometry. Then, the OVA-specific immune responses obtained in groups of animals immunized with the antigen alone or co-administered with cGAMP should be compared to assess the potential of GAMP as adjuvant.

Second, if cGAMP shows adjuvant properties, the efficacy of cGAMP and c-di-AMP to enhance adaptive immune response should be compared to explore their potential at inducing differential immune response profiles. To this end, immunization studies using experimental groups immunized with the model antigen OVA alone or co-administered with cGAMP or c-di-AMP should be measured as described above and resulting evoked immune responses should be compared side-by-side.

Third, if any differences at the effector level of the c-di-AMP and cGAMP activity are found, *in vitro* systems should be established to derive hypotheses explaining their differential activities. To this end, bone marrow-derived dendritic cells (BMDCs) should be used as a model system for CDN-responsive innate immune cells, and the surface expression of the activation markers MHC class II, CD86 and CD80, together with the production of key cytokines (*e.g.* type I IFNs, IL-6, IL-12/IL-23p40) should be measured as indicators of CDN-induced activation. To this end, flow cytometry or ELISA should be applied.

Fourth, to address the relevance of type I IFN induction and signaling pathways for the adjuvanticity of c-di-AMP and cGAMP, their efficacy in animals lacking functional components of these pathways should be tested. The lack of Sting impairs the CDN-triggered production of type I IFNs. The lack of functional IFNAR impairs the signaling mediating the biological activities of type I IFNs, such as up-regulation of ISGs. Therefore, to test if any of these type I IFN pathways are involved in mediating the adjuvanticity of c-di-AMP or cGAMP, immunization studies using wild type (wt) animals and mice lacking functional Sting or IFNAR should be performed as described above. OVA-specific immune responses should be compared in animals immunized with OVA alone or OVA co-administered with CDN. This should allow assessing if the CDN-

mediated enhancement of OVA-specific immune response observed in wt animals is impaired in any of the animals with a dysfunctional type I IFN pathway, thereby enabling to draw conclusions on the role played by a particular molecule on the adjuvanticity of a specific CDN.

2 MATERIALS AND METHODS

2.1 Materials

2.1.1 Technical equipment

Table 2: Technical equipment

Equipment	Manufacturer/ country
Cell counter, Z2 Coulter counter	Beckman Coulter, Germany
Cell culture dishes	Greiner, Germany
Cell harvester	Inotech, Switzerland
Centrifuge, 5417 R	Eppendorf, Germany
Centrifuge, Multifuge 3 S-R	Thermo Scientific, Germany
ChemiDocTM MP Imaging System	Bio-Rad, Germany
CTL ELISPOT reader	Cellular Technology, Ltd., Germany
Electrical source for agarose electrophoresis	Pharmacia LKB, Sweden
ELISA washer	Biotek, Germany
Falcon tubes	Greiner, Germany
Flow cytometry measurement tubes 1.2 ml	MP Biomedicals, France
Flow cytometry measurement tubes 5 ml	BD Bioscience, USA
Heraeus Multifuge x3R	Thermo scientific, Germany
High binding ELISA plates	Greiner, Germany
Incubator, Heracell 240i	Thermo Scientific, Germany
LSR-II SORP	BD Biosciences, USA
MultiScreen HTS filter plates	Milipore, Germany
Nitrocellulose membrane	Bio-Rad, Germany
pH-meter	Hannah Instruments, Germany
96F plates	TPP, Switzerland
PTC-100^{TM} Programmable Thermal controller	MJ Research, Inc., USA

Precision 2000 automated microplate pipetting system	Biotek, Germany
Serological pipets	Roth, Germany
Sterile hood, LaminAir	Heraeus, Germany
Synergy 2 Multi-Mode Microplate Reader	Biotek, Germany
Semi-dry blotter	Biometra, Germany
T Filtermat A filters	PerkinElmer, USA
Thermomixer compact	Eppendorf, Germany
Tumbling table	Analytik Jena, Germany
γ scintillation counter (1450 Microbeta Trilux)	Wallach Sverige, Sweden
Water bath	Köttermann, Germany

2.1.2 Chemical substances

Table 3: Chemical substances

Chemical substance	Manufacturer
2,2´-azino-bis (3-ethylbenzthiazoline-6 sulfonic acid) diammonium salt (ABTS)	Sigma-Aldrich, Germany
3-amino-9-ethyl-carbazole (AEC) substrate kit	BD Pharmingen, USA
Amersham enhanced chemiluminescence (ECL) Prime Western Blotting Detection Reagent	GE-Healthcare, Germany
Ampuwa	Serumwerk, Germany
Ammonium persulfate (APS)	Bio-Rad, Germany
Avidin-horseradish peroxidase (HRP)	BD Pharmingen, USA
β-mercaptoethanol	Merck, Germany
Bromophenolblue	Sigma-Aldrich, Germany
Bovine serum albumin (BSA)	Carl Roth, Germany
Calyculin A	Cell Signaling, Netherlands
Citric acid	Sigma-Aldrich, Germany
c-di-AMP	Biolog, Germany

c-GAMP (3´,3´)	Biolog, Germany
Dimethyl sulfoxide (DMSO)	Applichem, Germany
Ethanol 100%	Roth, Germany
Ethylenediaminetetraacetic acid (EDTA)	Roth, Germany
Fetal calf serum (FCS)	Biochrom, Germany
GeneRuler DNA ladder mix	Thermo Scientific, Germany
Gentamicine	Gibco, UK
L-Glutamine	Gibco, UK
Glycerol	Sigma-Aldrich, Germany
Granulocyte-macrophage colony stimulating factor (GM-CSF)	eBioscience, Germany
4-(2-hydroxyethyl)-1-piperazineethanesulfonic acid (HEPES)	Serva, Germany
Hydrogen peroxide (H_2O_2)	Sigma-Aldrich, Germany
^{3}H-thymidine	PerkinElmer, USA
Isotone II	Coulter-Beckman, USA
Kaleidoscope Prestained standard	Bio-Rad, Germany
Lipopolysaccharide (LPS)	Sigma-Aldrich, Germany
Magnesium chloride ($MgCl_2$)	Carl-Roth, Germany
Methanol	J. T. Baker, Germany
2-Mercaptoethanol (50 mM)	Gibco, UK
Midori green advanced green DNA stain	Nippon Generics, Germany
Milk powder	Roth, Germany
My TaqTMHS Redmix 2x	Bioline, Germany
NEEO Ultra Quality Roti Agarose	Roth, Germany
OVA protein	EndoGrade, Hyglos, Germany
Paraformaldehyde (PFA)	Riedl-de-Hän, Germany
Phenylmethanesulfonyl fluoride (PMSF)	Sigma-Aldrich, Germany

Ponceau S	Sigma, Germany
Penicillin/streptomycin (100x concentrated, 10000 IU penicillin, 10000 µg/ml streptomycin)	Gibco, UK
Potassium bicarbonate ($KHCO_3$)	Sigma, Germany
Potassium dihydrogen phosphate (KH_2PO_4)	Merck, Germany
Precision Plus Protein Kaleidoscope	Bio-Rad, Germany
Protease Inhibitor Cocktail	Sigma-Aldrich, Germany
Proteinase K	Bioline, Germany
Rotiphorese gel 30 (30% acrylamide, 0.8% bisacrylamide)	Carl-Roth, Germany
RPMI 1640	Gibco, UK
Saponin	Sigma-Aldrich, Germany
Sodium dodecyl sulfate (SDS)	Sigma-Aldrich, Germany
Sodium hydrogen carbonate ($NaHCO_3$)	Merck, Germany
Sodium chloride (NaCl)	Carl-Roth, Germany
Streptavidin-HRP	Sigma-Aldrich, Germany
Streptavidin-HRP, BD ELISPOT	BD Bioscience, USA
Tetramethylethylenediamine (TEMED)	Carl-Roth, Germany
Tween 20	Carl-Roth, Germany

2.1.3 Antibodies

Table 4: Antibodies used in flow cytometry analyses

Antibody conjugated with a fluorochrome*	Clone	Dilution	Catalog number	Manufacturer
Rat, anti-mouse CD16/CD32 (Fc-block)	93	1:1000	101319	Biolegend, Germany
Rat, anti-mouse CD11b (eFluor450-conjugated)	M1/70	1:400	48-0112-82	eBioscience, Germany
Hamster, anti-mouse CD11c (Pe-Cy7-conjugated)	N418	1:800	117317	BD Pharmingen, USA

Mouse, anti-mouse I-A^b MCH-II (FITC-conjugated)	AF6-120.1	1:100	553551	BD Pharmingen, USA
Rat, anti-mouse CD86 (PE-conjugated)	GL1	1:500	553692	BD Pharmingen, USA
Hamster, anti-mouse CD80 (APC-conjugated)	16-10A1	1:1200	17-0801-82	eBioscience, Germany
Rat, anti-mouse CD3 (FITC-conjugated)	145-2c11	1:300	553062	BD Pharmingen, USA
Rat, anti-mouse CD4 (PE-Cy7-conjugated)	RM4-5	1:1000	25-0042-82	eBioscience, Germany
Rat, anti-mouse CD8 (APC-conjugated)	53-6.7	1:500	17-0081-81	eBioscience, Germany
Rat, anti-mouse IL-17 (V450-conjugated)	TC11-1 8H10	1:200	560522	BD Bioscience, USA
Rat, anti-mouse TNF-α (PerCP-eF710-conjugated)	MPG-XT22	1:200	46-7321-82	eBioscience, Germany
Rat, anti-mouse IL-6 (PE-conjugated)	MP5-20F3	1 :200	12-7061-71	eBioscience, Germany
Rat, anti-mouse IL-12/IL-23p40 (Alexa647-conjugated)	C17.8	1:400	51-7123-80	eBioscience, Germany

*phycoerythrin-cyanin 7 (Pe-Cy7), fluorescein-isothiocyanate (FITC), phycoerythrin (PE), allophycocyanin (APC), peridinin-chlorophyll-protein complex (PerCP)

Table 5: Antibodies used in Western blot

Antibody	Clone	Dilution	Catalog number	Manufacturer
Primary				
Rabbit, anti-mouse Sting	--	1:2000	3337S	Cell Signaling, Germany
Secondary				
Goat, anti-rabbit-HRP	--	1:20000	111-035-144	Jackson Immunoresearch, USA

Table 6: Antibodies used in ELISA

Antibody	Dilution	Catalog number	Manufacturer
Elisa capture antibodies			
Goat, anti-mouse IgA	1:500	M-8769	Sigma-Aldrich, Germany
Elisa biotinylated detection antibodies			
Goat, anti-mouse IgA	1:5000	1040-08	Southern Biotech, USA
Goat, anti-mouse IgG	1:5000	B7022-1ml	Sigma-Aldrich, Germany
Goat, anti-mouse Ig1	1:5000	1072-08	Southern Biotech, USA
Goat, anti-mouse IgG2c	1:5000	1079-08	Southern Biotech, USA

Table 7: Antibodies used in ELISPOT

Antibody	Dilution	Catalog number	Manufacturer
ELISPOT capture antibodies			
Anti-mouse IFN-γ	1:200	51-2525KZ	BD Bioscience, USA
Anti-mouse IL-2	1:200	51-1816KZ	BD Bioscience, USA
Anti-mouse IL-4	1:200	51-1819KZ	BD Bioscience, USA
Anti-mouse IL-17A	1:250	16-7175-68	eBioscience, USA
ELISPOT biotinylated detection antibodies			
Anti-mouse IFN-γ	1:250	51-1818KZ	BD Bioscience, USA
Anti-mouse IL-2	1:250	51-1817KZ	BD Bioscience, USA
Anti-mouse IL-4	1:250	51-1804KZ	BD Bioscience, USA
Anti-mouse/rat IL-17A	1:250	13-7177-68C	eBioscience, USA

2.1.4 Solutions and buffers

Table 8: Solutions and buffers

Solution/ buffer	Composition
Ammonium chloride-potassium (ACK) lysis buffer	0.1 mM EDTA, 1mM $KHCO_3$, 155 mM NH_4Cl, pH 7.3
Antibody storage solution	2% (w/v) BSA, 0.02% (w/v) NaN_3 in TBS

Blotting buffer	24.8 mM Tris, 19.2 mM glycine, 2% (v/v) methanol
Cell lysis buffer for sodium dodecyl sulfate polyacrylamide gel electrophoresis (SDS-PAGE)	20 mM HEPES, 50 mM KCl, 2 mM $MgCl_2$, 1% (v/v) Triton X-100, 100 nM calyculin A, 0.03% (v/v) protease inhibitor cocktail, 1 mM PMSF
Flow cytometry permeabilization buffer	0.5% (w/v) BSA, 0.5% saponin in PBS
Flow cytometry fixation buffer	2% (v/v) PFA in PBS
ELISA coating buffer	0.05 M carbonate buffer, pH 8.2
ELISA blocking buffer	3% (w/v) BSA in PBS
ELISA washing buffer	0.1% (v/v) Tween20 in PBS
ELISA sample dilution buffer	3% (w/v) BSA in PBS
ELISA antibody dilution buffer	1% (w/v) BSA/0.1% (v/v) Tween 20 in PBS
ELISA substrate solution	0.5 mM ABTS, 0.03% H_2O_2 in 0.1 M citrate-phosphate buffer, pH 4.35
Lysis buffer for tissue biopsies	0.45% nonidet P40, 0.45% tween 20, 0.1% gelatine, 50 mM KCl, 1.5 mM $MgCl_2$, 10 mM Tris HCl, pH 8.5 Proteinase K freshly added: 2.76 U per 500 µl of lysis buffer
4x Loading buffer (Protein Solubilization buffer)	40% (v/v) glycerol, 240 mM Tris HCl pH 6.8, 8% (w/v) SDS, 0.08% (w/v) bromophenol blue (3',3",5',5"-tetrabromophenolsulfonphthalein), 4% (v/v) 2-mercaptoethanol
Nasal wash buffer	5% FCS (v/v) in PBS
Phosphate-buffered saline (PBS)	0.27 mM KCl, 0.18 mM KH_2PO_4, 13.7 mM NaCl, 1mM Na_2HPO_4, pH 7.4
Tris-acetate-EDTA (TAE) buffer	0.04 M Tris, 1 mM EDTA, 0.04 M acetic acid, pH 8.0
Tris-buffered saline (TBS)	20 mM Tris, 0.5 M NaCl, pH 7.4
Tris-buffered saline Tween 20 (TBS-T)	20 mM Tris, 0.5M NaCl, 0.05% (v/v) Tween 20, pH 7.4
SDS-Running buffer	24.8 mM Tris, 19.2 mM glycine, 0.1% (w/v) SDS
Stacking gel buffer	0.5 M Tris, pH 6.8
Separation gel buffer	1.5 M Tris, pH 8.8
Western blot blocking solution	5% (v/v) milk in TBS

2.1.5 Cells

Table 9: Cell line used in experiments

Cell type	Description
Human embryonic kidney (HEK)-Blue mTLR4	Cell line purchased from InvivoGen, stably transfected to express murine TLR4 at high levels and alkaline phosphatase reporter gene under the control of a promoter inducible by transcription factor NF-kB

2.1.6 Cell culture media

Table 10: Cell culture media

Media	Supplements
RPMI 1640 complete	10% v/v FCS heat inactivated (h.i.), 100 U/ml penicillin, 50 µg/ml streptomycin, 2-mercaptoethanol 50 µM, 2 mM L-glutamine
RPMI 1640 for BMDCs	10% v/v FCS heat inactivated, 100 U/ml penicillin, 50 µg/ml streptomycin, 2-mercaptoethanol 50 µM, 2 mM L-glutamine, 50 µg/ml gentamicin
HEK-Blue growth medium	DMEM high glucose (4.5 g/l), 10% v/v FCS heat inactivated, 100 U/ml penicillin, 50 µg/ml streptomycin, 1 x normocin
HEK-Blue selection medium	HEK blue growth medium supplemented with HEK-Blue Selection
HEK-Blue detection medium	1 pouch of HEK-blue detection in 50 ml endotoxin-free H_2O, sterile filtered through 0.2 µm pore membrane

2.1.7 Mice

Table 11: Mice used in experiments

Mouse	Description	Provider
wt	C57/BL6	Harlan, Germany
IFNAR1$^{-/-}$	Animals lacking functional IFNAR1, developed on C57/BL6 background [148]	Kindly provided by Prof. Dr. U. Kalinke (Twincore, Hannover, Germany)
Sting$^{Gt/Gt}$	Animals lacking functional Sting, *Sting*$^{Gt/Gt}$ (Sting goldenticket, C57BL/6J-Tmem173gt/J) [135]	Jackson Laboratory, USA

2.1.8 Primers for genotyping IFNAR$^{-/-}$ mice

Table 12: Primers used in PCR for genotyping (Provided by Eurofins)

Primer	Sequence
1	5´CCA AGC GAA ACA TCG CAT CG3´
2	5´GTT CCC TTC CTC TGC TCT G3´
3	5´ACA AAA GAC GAG GCG AAG TG3´

2.1.9 Kits used for cytokine detection and live/dead cell stain

Table 13: ELISA, ELISPOT and live/dead cell stain kits

Kit	Manufacturer
IFN-β Biolegend Max ELISA kit	Biolegend, Germany
VeriKine™ Mouse Interferon Alpha ELISA kit	PBL, USA
Mouse IFN-γ, IL-2, IL-4 or IL-17 ELISPOT pair kit	BD Biosciences, USA
Live/Dead® Fixable dead cell stain Kit	Life technologies, Germany

2.2 Methods

2.2.1 LPS detection using the HEK-blue™ LPS detection Kit

Stock solutions of the components used in immunization experiments were tested for the presence of LPS contaminations higher than 1.6 ng/ml using the HEK-blue™ LPS detection Kit according to the manufacturer´s instructions. The detection limit of this method for *E. coli K12* LPS is 0.3 ng/ml. Briefly, the HEK-Blue-4 cells were cultured in HEK-Blue growth medium at 37°C, 5% CO_2 in a humidified atmosphere until 50–80% confluence was reached. Then, the cells were detached using trypsin, transferred into HEK-Blue selection medium and passaged twice a week. When the confluence of 60–80% was reached, the cells were detached using trypsin and diluted in pre-warmed HEK-Blue detection medium to a concentration of 1 x 10^5 cells/ml. To a 96-well sterile flat-bottomed cell culture plate were added 20 µl/well of each sample to be tested (c-di-AMP, cGAMP and OVA stock solutions used in immunization formulations), and 20 µl/well of endotoxin-free water as a negative control. As a positive control, 20 µl/ well of

E. coli K12 LPS at a concentration of 1.625, 3.125, 6.25, 12.5, 25, 50 and 100 ng/ml were added. Then, 200 µl/ well of cell suspension was added and the plate was incubated for 24 h at 37°C, 5% CO_2. HEK-Blue-4 cells express at high levels stably transfected murine LPS receptor TLR4, which makes them very sensitive to LPS. In addition, they are stably transfected to express an alkaline phosphatase reporter gene, which is controlled by NF-κB. In presence of LPS, the signaling axis from TLR4 via NF-κB induces expression of alkaline phosphatase, which is secreted and reacts with the substrate HEK-Blue detection in the growth medium, giving a blue colored product. Spectrophotometric measurement of the absorbance at 630 nm 24 h upon the treatment allows semi-quantification of alkaline phosphatase activity, which is correlated to up-regulation of its expression due to presence of LPS. The minimal dose of LPS potentially inducing innate immune cell priming *in vivo* is 0.1 ng [149]. To cause innate immune cell priming by LPS contamination in the immunization experimental system described in 2.2.7, LPS would be required in a minimal concentration of 33 ng/ml in OVA or 20 ng/ml in c-di-AMP and cGAMP stock solutions. Based on the comparison of the absorbance values of the samples with cells incubated with CDN or OVA stock solution with to the absorbance values of the blank and LPS in defined concentrations, presence of LPS in immunization stock solutions in minimal concentrations potentially causing immune stimulatory effects *in vivo* was estimated.

2.2.2 *IFNAR*$^{-/-}$ genotyping by PCR

DNA samples obtained from supernatants of lysed tail biopsies of mice were analyzed by polymerase chain reaction (PCR). Briefly, the biopsies were lysed in tail lysis buffer containing proteinase K, overnight at 56°C under constant shaking at 800 rpm. Proteinase K is a serine protease that is used here to degrade native as well as denatured proteins. Proteinase K was deactivated by exposing the samples to 96°C for 10 min after the lysis procedure. Then, the samples were cooled down and 2 µl of sample suspensions were used for a PCR reaction of a total volume 25 µl. A single reaction contained 12.5 µl of DNA Pol Redmix, 1µl DMSO, 2µl H_2O and 2.5 µl of each of the primers given in **table 12**, at the final concentration of 10 µM. The protocol of PCR cycles is given in **figure 6.**

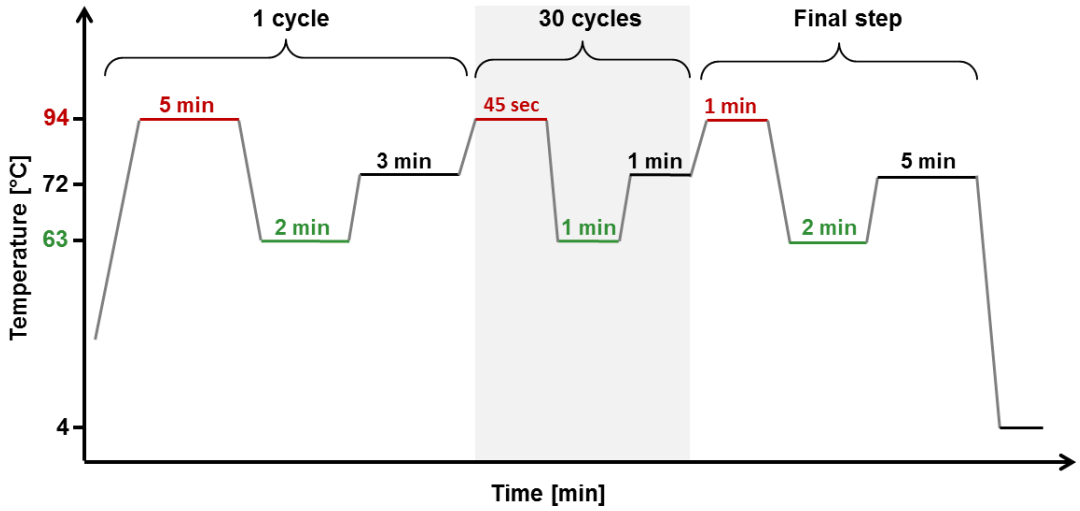

Figure 6: PCR temperature cycles for IFNAR genotyping. Tissue lysate samples were used for PCR performed with the temperature cycles shown.

The PCR products were analyzed by agarose gel electrophoresis. To this end, 2% (w/v) agarose gels were prepared in TAE buffer containing Midori Green (60 µl/l), a nucleic acid dye which, upon exposure to ultraviolet (UV) light, emits green fluorescence when bound to DNA and therefore allows the visualization of DNA bands. PCR samples were loaded onto the gel and the GeneRuler LadderMix was used as a DNA fragment size standard. The gel electrophoresis was performed for 1 h at 120 V and the DNA was visualized by exposing the gels to UV light of 270 nm wavelength and the detection of emitted light at wavelength 530 nm using the GelDocXRS system.

2.2.3 Sting detection by Western blot

2.2.3.1 Cell lysis

BMDCs ($3x10^5$) from wt, $IFNAR^{-/-}$ or $Sting^{Gt/Gt}$ mice were lysed in 10 µl lysis buffer for Western blot. The lysis was performed on ice for 10 min and the samples were thoroughly stirred after 5 min. Then, 4 µl of 4 x concentrated loading buffer and β-mercaptoethanol at final concentration 4% (v/v) were added. The lysates were boiled for 7 min at 96°C and spun down prior to SDS-PAGE.

2.2.3.2 SDS-PAGE

The SDS-PAGE is a method for the separation of proteins based on their molecular weight. SDS-denatured polypeptides carry amounts of the negatively charged anionic detergent SDS proportional to their molecular weight. They move in an electric field towards the positively-charged electrode (anode). Differential electrophoretic mobility of

polypeptides in PAGE is defined by the pore size in the gel that allows faster movement of smaller polypeptides, resulting in their separation in the gel and highly depends on the concentration of acrylamide. Polymerization of acrylamide and bisacrylamide monomers requires presence of free radicals in a polymerizing gel mixture, which is ensured by adding APS and TEMED. APS spontaneously decomposes to form free radicals and therefore initiates the polymerization. TEMED is a free radical stabilizer and is included to promote the polymerization. The gel was prepared in two phases: stacking (4.2% acrylamide) and separation phase (10% acrylamide). The gel running was done in a gel chamber Mini-PROTEAN II, First, the samples were run through the stacking gel at 15 mA for approximately 45 min. This step was followed by running the samples in the separation gel, where was applied constant current of 20 mA for approximately another 1 h. When the front dye bromophenolblue reached the end of the separation gel, the SDS-PAGE was stopped and the Western blot was performed in order to detect specific proteins on a nitrocellulose membrane.

2.2.3.3 Western blot

First, the proteins from the gel were blotted on a nitrocellulose membrane. The procedure was done in a semi-dry manner, where Whatman paper and a nitrocellulose membrane were first equilibrated in blotting buffer. Then, a sandwich of 3 layers of Whatman paper, the nitrocellulose membrane, the polyacrylamide gel and another 3 layers of Whatman paper were placed on the blotter with paying attention that the membrane is positioned between the SDS gel and the positive electrode, towards which the proteins will move. The protein transfer from the SDS gel to the nitrocellulose membrane was performed for 1 h at constant current of 45 mA. Then the Ponceau S staining of the proteins transferred to nitrocellulose membrane was performed to verify if approximately equal amount of proteins was loaded per lane.

Next, the unspecific binding sites on the membrane were blocked by incubation in 5% TBS-T-milk, overnight at 4°C with constant shaking. Then, the membrane was washed in 4 cycles of 10 min shaking in TBS-T and incubated with specific antibody diluted in a storage solution for 2h at room temperature on a shaker. After 6 cycles of 10 min washing in TBS-T, the membrane was incubated with the HRP-conjugated secondary antibody diluted in blocking solution for 1 h at room temperature with constant shaking. The membrane was washed in 4 cycles of 10 min in TBS-T and rinsed with water. The membrane was incubated with ECL-detection reagent for 5 min and exposed to the

ChemiDocXRS camera to detect the light emitted upon the reaction of the HRP with its substrate contained in the ECL reagent.

2.2.4 Generation of BMDCs

Bone marrow cells were isolated from bones (femur and tibia) of 6-8 weeks old C57BL/6 mice. Briefly, mice were euthanized using CO_2 and hind legs were dissected. The bones were cleaned from muscle tissue and incubated for 1-2 min in 70% (v/v) ethanol. Then, the bones were rinsed in fresh RPMI medium and the ends of the bones were removed. The bone marrow was flushed by fresh RPMI medium pressed through the medullary cavity of femur and tibia. The cell suspension was transferred into falcon tubes and centrifuged for 10 min at 300 x g at room temperature. The supernatant was discarded and the pellet was re-suspended in ACK lysis buffer for 3 min. Next, 10 ml RPMI medium were added to stop the lysis of erythrocytes, which was followed by another centrifugation step for 10 min at 300 x g, at room temperature. The supernatant was discarded and the cell pellet was re-suspended in 10 ml RPMI medium and pressed through a 100 µm filter mesh. The cell number was determined as described in section 2.2.10, adjusted to a final concentration of $1x10^6$ cells/ml and distributed in $5x10^6$ cells per well on a 6 well plate. Cell differentiation towards dendritic cells was directed by the presence of 5 ng/ml mouse GM-CSF in the growth RPMI medium. The cells were incubated at 37°C in a humidified atmosphere containing 5% CO_2, with exchanging half of the volume per well with fresh medium every second day until day 7, when the cells were treated.

2.2.5 Treatment of BMDCs

BMDCs were treated on day 7 after the isolation from bones of mice, in GM-CSF-free medium. Briefly, the culture medium of cells was gently removed and replaced by fresh medium supplemented with 1 µg/ml LPS, 5 µg/ml c-di-AMP or cGAMP or left in medium without additive. Cells were incubated for 24 h at 37°C in a humidified atmosphere containing 5% CO_2, and the cytokines present in the supernatant, surface expression of activation markers and intracellular presence of cytokines was analyzed.

2.2.6 Analysis of type I IFN production by BMDCs

The supernatants from treated BMDCs were collected, spun down and 50 µl (for IFN-β analysis) or 100 µl (for IFN-α analysis) of the supernatants were used per ELISA

reaction or the samples were stored at -20°C until the analysis. The presence of IFN-α and -β in supernatants from treated BMDCs was evaluated using the commercially available IFN-β Biolegend Max ELISA kit and the VeriKine™ Mouse Interferon Alpha ELISA kit, according to the manufacturer´s instructions.

2.2.7 Mouse immunization experiments

Four or five animals per group of 9-14 weeks old mice were immunized i.n. on days 0, 14 and 28. Animals were anesthetized with Isofluorane and 10 µl of immunization solution were administered per nostril. Immunization solutions were formulated in Ampuwa containing 15 µg OVA alone or co-administered with 5 µg of the corresponding CDN per dose. The control group received Ampuwa without any supplements. Animals were sacrificed 14 days after the third immunization and samples were collected, as shown in **figure 7.**

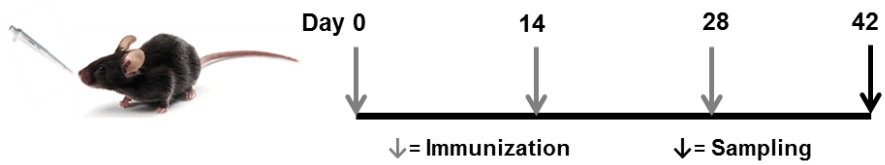

Figure 7: A schematic overview of mouse immunization experiments. The picture of the mouse is adapted from [150].

2.2.8 Sample collection

On day 42, animals were anesthetized with Isoflurane and blood samples were collected from the retro-orbital complex, centrifuged for 5 min at 8,000 x g, and sera were stored at -20°C. The mice were euthanized by exposure to CO_2 and spleens and nasal lavages were collected. Briefly, the abdominal surface area was soaked in ethanol and the spleens were removed. Isolated spleens were pooled per group, transferred to complete RPMI medium and processed, as described in 2.2.9. The samples for analysis of IgA in the nasal cavity were collected by nasal washes: the lower jaw was cut and the nasal cavity was flushed twice with 150 µl of lavage buffer. Briefly, 200 µl pipette tip was inserted into a posterior opening of the nasopharynx and the wash buffer was pressed through the nasal cavity towards the nose entrance where it was collected in a 1.5 ml tube prefilled with 10 µl of 40 mM PMSF. Then, the samples were centrifuged at 7,000 x g for 10 min and the supernatants were stored at -20°C.

2.2.9 Spleen processing

Pooled spleens of each immunization group were homogenized in complete sampling medium and the suspension was centrifuged for 10 min at 300 x g at room temperature. The supernatant was removed; the cell pellet was re-suspended and kept in ACK buffer for 3 min in order to lyse the erythrocytes. After 3 min, fresh medium was added to the suspension in order to stop the lysis and the cell suspension was centrifuged for 10 min at 300 x g at room temperature. Cells were re-suspended in 10 ml of fresh medium, pressed through a 100 µm pore cell mesh and counted.

2.2.10 Cell counting

The cytometer was used to determine the numbers of cells in suspensions. The cells were diluted with Isotone II in a ratio of 1:1000 and measured using the multisize analyzer and Multi32 Coulter Z2® Accu Comp® software. Everything of a size below 5 µm was considered as debris and was not counted. Cells with a diameter between 5-16 µm were counted.

2.2.11 Cell proliferation assay

Spleen cells were seeded in complete medium on 96F plates ($4x10^5$/well) in presence or absence of OVA (40 µg/ml), and further incubated for 72 h at 37°C in a humidified atmosphere containing 5% CO_2. For additional 16 h cells were incubated in the presence of 20 µg/ml ^{3}H-thymidine and harvested on Filtermat A filters using a cell harvester. Incorporated ^{3}H-thymidine was measured by a γ scintillation counter. The values obtained with non-stimulated cells were subtracted from values obtained with re-stimulated cells and the average value of replicates for each group was calculated.

2.2.12 Detection of cytokine production in spleen cells from immunized mice by ELISPOT

The production of IFN-γ, IL-2 and IL-4 by spleen cells was assessed using MultiScreen HTS filter plates and mouse ELISPOT pair antibodies according to the ELISPOT kit manufacturer´s instructions. Briefly, the plates were coated with anti-mouse IFN-γ, IL-2, IL-4 or IL-17 capture antibodies diluted in PBS, overnight at 4°C. Then, complete RPMI medium was used for washing the plates three times and blocking for 2 h at room temperature. Spleen cells were distributed on plates ($4x10^5$/well) and incubated in

complete medium with or without OVA (30 µg/ml) for 24 h (IFN-γ analysis) or 48 h (IL-2, IL-4, IL-17 analyses) at 37°C in a humidified atmosphere containing 5% CO_2. The detection steps were performed according to the manufacturer´s instructions. The plates were scanned using a CTL ELISPOT reader and the spots were quantified using the ImmunoSpot image analyzer software v3.2. Spot number values of the cells without re-stimulation were subtracted from the spot number values of the OVA-re-stimulated cells. The average spot number value of triplicates was calculated for each group. The background was always below five percent for the spot number value of the samples from immunization groups with OVA co-administered with adjuvants.

2.2.13 Preparation of samples for flow cytometry analysis

Cells for flow cytometry measurements were prepared at 4°C. The cells were incubated with the specified fluorophore containing reagents for 30 min. Washing steps were performed in PBS (except the first washing step following the intracellular staining) and included centrifugation for 5 min at 300 x g and 4°C.

2.2.13.1 Preparation of spleen samples for flow cytometry analysis

Spleen cells ($12x10^6$/well) were incubated in complete medium with or without 40 µg/ml OVA for 16 h at 37°C in a humidified atmosphere containing 5% CO_2. For additional 8 h, the inhibitors of secretion brefeldin A (5 µg/ml) and monensin (6 µg/ml) were added to the cell suspensions. Then, cells were collected in PBS and stained with a blue fluorescent amine-reactive dye as a live/dead cell marker and fluorescently labeled antibodies: anti-mouse CD3, FITC-conjugated and CD4, PE-Cy7-conjugated. Afterwards, the cells were washed, fixed overnight in flow cytometry fixation buffer, washed again, and incubated in flow cytometry permeabilization buffer for 1 h. Intracellular staining was performed using anti-mouse IL-17, V-450-conjugated, and anti-mouse TNF-α, PerCP-eFluor710-conjugated antibodies, diluted in permeabilization buffer. After the intracellular staining, the cells were washed in permeabilization buffer and two times in PBS (1 ml each wash).

2.2.13.2 Preparation of BMDC samples for flow cytometry analysis

BMDCs were collected in PBS and incubated for 20 min with anti-mouse CD16/32 in order to block the binding of fluorescently-labeled antibodies to Fc receptors present on the surface of the cells. For flow cytometry analysis of the surface expression of the activation markers, the cells were decorated with a blue fluorescent amine-reactive dye

as a live/dead cell marker and following fluorescent-labeled antibodies directed against surface markers: anti-mouse CD11c, PE-Cy7-conjugated, CD11b, eFluor450-conjugated, MHC class II, FITC-conjugated, CD86, PE-conjugated and CD80, APC-conjugated, diluted in PBS. Afterwards, the cells were washed three times and analyzed. To detect intracellular IL-6 or IL-12/IL-23p40 after 24 h of BMDC stimulation, the secretion inhibitors brefeldin A (5 µg/ml) and monensin (6 µg/ml) were added to the culture medium 16 h after starting the treatment and the cells were incubated for additional 8 h. Then, the cells were collected in PBS and the Fc receptors were blocked, as described above. The cells were stained with a blue fluorescent amine-reactive dye as a live/dead cell marker and fluorescently labeled antibodies: anti-mouse CD11c, PE-Cy7-conjugated and CD11b, eFluor450-conjugated, diluted in PBS. The procedure following the surface staining was the same as described in 2.2.13.1 for spleen cells. Intracellular staining was performed using antibodies anti-mouse IL-6, PE-conjugated, and IL-12/IL-23p40, Alexa647-conjugated.

2.2.14 Flow cytometry analysis

Flow cytometry analysis was performed using an LSR-II instrument operated with the software FACSDiva and data was evaluated using the software FlowJo Mac v9.6. Single cells were gated based on their forward and sideward scatter characteristics. Live cell populations were identified based on their lower fluorescent signal intensity of the live/dead cell marker. Live $CD3^+/CD4^+$ (in the spleen cell samples) or $CD11c^+$ (in the BMDC samples) single cells were selected according to the gating strategy illustrated in **figure 8** and analyzed for enhanced fluorescence intensity indicating the antibody-detected presence of surface activation markers MHC class II, CD86 and CD80, or intracellular cytokines IL-17, TNF-α, IL-6 or IL-12/IL-23p40.

.

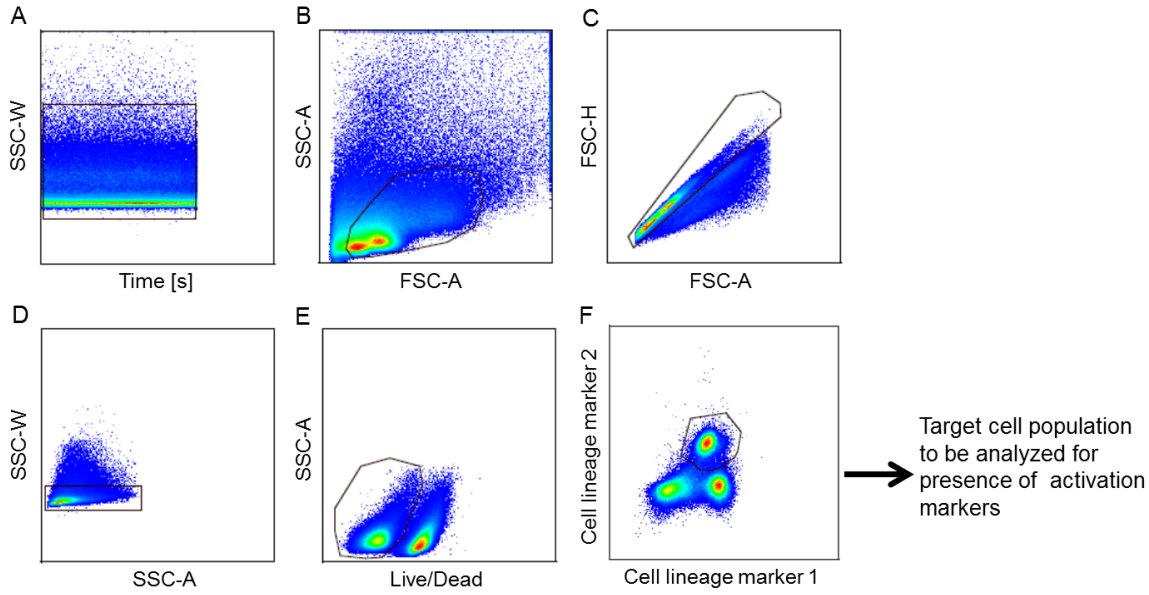

Figure 8: Gating strategy for flow cytometry data analysis. Cells measured in a constant flow rate were determined by gating on side scatter width (SSC-W) distribution over time (A) and were used for further analysis. Cell debris was excluded by gating on forward scatter area (FSC-A) versus side scatter area (SSC-A) (B). Doublets are characterized by high forward scatter area and side scatter width values. To exclude doublets based on forward scatter characteristics, cells were plotted FSC-A vs. FSC-H (C). The exclusion of doublets based on side scatter, cells were plotted for SSC-W versus SSC-A (D). Single cells were characterized by the same proportion of height and area. Live cells were determined based on lower fluorescence signal intensity of the live/dead marker, which is more intensive in necrotic cells due to penetration through the membranes and staining of both, cell surface and intracellular structures (E). Live cells were gated for cell lineage determination markers ($CD11c^+$ for dendritic cells or $CD3^+$/$CD4^+$ for T cells) and were analysed for activation marker expression (surface markers or cytokine production) (F).

2.2.15 ELISA measurement of OVA-specific IgG, IgG1 and IgG2c titers

The OVA-specific IgG, IgG1 and IgG2c titers were measured by specific ELISA. High-affinity binding 96-well plates were coated overnight at 4°C with 2 µg/ml OVA in ELISA coating buffer (100 µl per well) and blocked with ELISA blocking buffer for 1 h at 37°C (200 µl per well). Serial 2-fold dilutions of the samples (100 µl per well) were prepared in ELISA blocking buffer and incubated for 2 h at 37°C. ELISA blocking buffer was used as a blank sample. The plates were washed six times with ELISA wash buffer. The biotinylated detection antibody goat, anti-mouse IgG was diluted at the ratio of 1:5000 in ELISA diluting buffer and distributed on plates at 100 µl per well. The plates were incubated for 2 h at 37°C and washed again six times with ELISA wash buffer. Streptavidin-HRP, diluted at 1:1000 in ELISA dilution buffer was added (100 µl per well) and plates were incubated for 30 min at 37°C. Then, plates were washed again six times

with ELISA wash buffer and incubated in the dark for 15 min at room temperature with 100 µl per well of ELISA substrate solution. The absorbance of light at 405 nm wavelength was measured using a Synergy 2 Multi-Mode Microplate Reader. Titers were determined as the highest dilution factors of the analyzed samples with at least twice the average readout value of the blank.

2.2.16 ELISA measurement of total IgA and OVA-specific IgA

The OVA-specific IgA titer was measured by ELISA with OVA-coated plates and total IgA titer was measured by ELISA with anti-mouse IgA-coated plates. High-affinity binding 96-well plates were coated overnight at 4°C with 2 µg/ml OVA or 2 µg/ml anti-mouse IgA in ELISA coating buffer, 100 µl per well. The detection steps were performed as described in 2.2.15 for the measurement of IgG titers, but using a goat, anti-mouse IgA biotinylated antibody diluted in ELISA dilution buffer at the ratio 1:5000. ELISA blocking buffer was used as a blank sample. Titers were determined as the highest dilution factors of the analyzed samples with at least twice the average readout value of the blank sample (*i.e.* ELISA blocking buffer). Normalization was done by calculating the percentage of OVA-specific IgA titer of the total IgA titer determined for each sample.

2.2.17 Statistical analysis

Statistical analysis was performed using the unpaired t-test in GraphPad Prism 4 software. n. s. indicates non-significant, *** indicates $p<0.001$, ** indicates $p<0.01$, whereas * indicates $p<0.05$.

3 RESULTS

3.1 Ruling out artifacts due to LPS contamination of key immunization components

False positive results in immunization studies can be obtained due to the presence of contaminations with PAMPs in immunization components. In this regard, LPS is a common concern as a contaminant in vaccine components. To avoid immune responses falsely attributed to CDN activity due to LPS contamination in stock solutions of the antigen OVA or adjuvants (*i.e.* c-di-AMP and cGAMP), the corresponding stock solutions were examined. To this end, a HEK-Blue^{TM} test was applied. The reporter HEK-Blue^{TM}-4 cells were incubated for 24 h in medium containing the OVA, c-di-AMP or cGAMP stock solution. The blank sample contained endotoxin-free water. Spectrophotometric measurement of the absorbance at 630 nm wavelength allowed semi-quantification of alkaline phosphatase reporter activity, indicative for activation of the LPS-sensing pathway in HEK-Blue^{TM}-4 cells. According to the report of Inagawa *et al*. [149], intravenous administration of 0.1-1 ng of LPS to mice is non-toxic, but induces a priming stage of innate immune cells. In our experimental model 3 µl of the OVA stock solution and 5 µl of the CDN stock solutions are used per immunization dose. Therefore, to administer the minimum reported dose of LPS that induces immunogenic effects *in vivo* (0.1 ng LPS), its concentration in the OVA stock solution would have to be higher than 33 ng/ml or 20 ng/ml in CDN stock solutions, in case the potential LPS contamination would origin either from OVA or CDN stock solution. The lowest concentration of LPS tested in this assay was 1.6 ng/ml and the absorbance value of the samples with cells incubated with it was approximately three magnitudes higher than the absorbance measured with the cells incubated with the blank. The absorbance of the samples with cells incubated with immunization stock solutions were similar to the absorbance values of the blank **(figure 9)**. Therefore, it was concluded that LPS was not present in stock solutions of OVA or CDN used in immunization studies in a concentration that could potentially induce immune stimulatory effects *in vivo*.

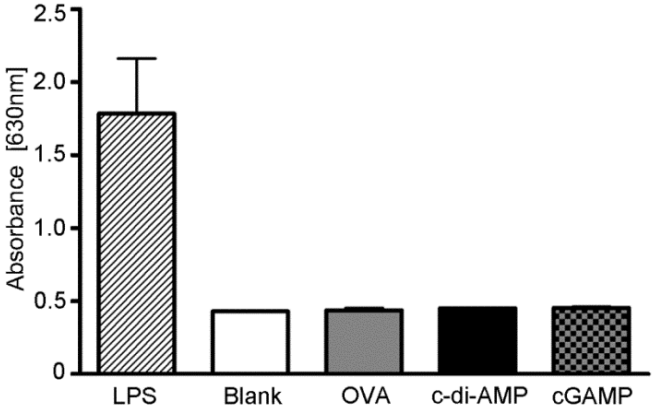

Figure 9: Absence of LPS contamination in OVA and CDN stock solutions. Stock solutions of OVA and CDNs were tested for the presence of LPS contamination using the HEK-Blue™ test. Upon 24 h incubation of the reporter HEK-Blue™-4 cells with either LPS at a concentration 1.6 ng/ml, endotoxin-free water (blank) or the indicated substances, the absorbance of light at 630 nm wavelength was measured. Error bars represent standard deviation of duplicates.

3.2 cGAMP enhances OVA-specific humoral and cellular immune responses

The immunization experiments presented in this thesis were set up in a time frame of 42 days, where animals received primary immunization and two boosts by i.n. route, separated by two weeks from each other. On day 42 samples from immunized animals were collected and analysis of the immune response was performed. The experimental groups in the *in vivo* studies contained five animals per group. To evaluate the immune stimulatory potency of cGAMP, immunization studies were performed where mice were treated with Ampuwa, OVA alone (15 µg) or OVA (15 µg) co-administered with cGAMP (5 µg). Six weeks after the first application, animals were sacrificed and the samples were analyzed for indicators of humoral (IgG and IgA production) and cellular (spleen cell proliferation and cytokine production) adaptive immune responses. A schematic overview of the procedures is given in **figure 10**.

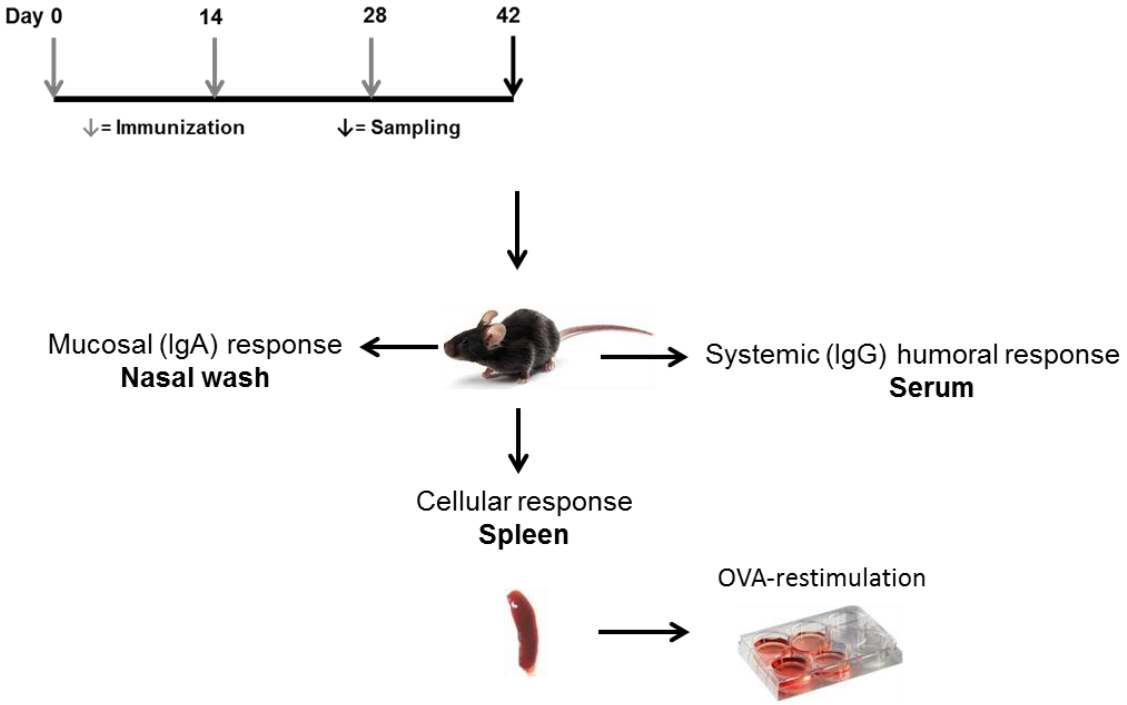

Figure 10: A schematic overview of the adaptive immune response evaluation strategy. Mice were immunized on days 0, 14 and 28. Sampling was performed on day 42 after the initial immunization. Nasal washes were collected for measurement of the humoral response at the nasal mucosa (IgA production). Serum samples were collected in order to analyse systemic humoral responses (IgG production). Spleen cells were re-stimulated with the antigen and their proliferation or cytokine production capacity was evaluated.

OVA-specific immune response in animals treated with Ampuwa was barely detectable. The animals treated only with the antigen OVA developed a basal level of OVA-specific responses. The antigen-specific immune response in animals immunized with OVA and cGAMP was multifold enhanced, as compared to the response evoked by OVA alone **(figure 11-13)**.

Nasal wash samples from the immunized mice were analyzed to see if cGAMP co-administration with the antigen OVA also results in enhanced OVA-specific mucosal IgA production. To this end, total and OVA-specific IgA were measured by ELISA and the amount of OVA-specific IgA was given as a percentage of total IgA. The titer of OVA-specific IgA in nasal washes from the animals treated with OVA and cGAMP was significantly higher when compared to samples from animals that received OVA alone **(figure 11 D).** This finding clearly indicates the potency of cGAMP to act as a mucosal adjuvant. The titers of OVA-specific IgG and its sub-classes IgG1 and IgG2c were then

measured in serum samples of immunized animals by ELISA **(figure 11 A-C)**. When the OVA-specific IgG titers were determined in serum from animals immunized with OVA and cGAMP, a clear trend of enhanced responses in comparison to the samples from the animals immunized with OVA alone was observed **(figure 11 A)**. However, the differences were not statistically significant. In contrast, the OVA-specific IgG1 titer was significantly enhanced in serum samples from animals immunized with OVA and cGAMP when compared to samples from animals that received only OVA **(figure 11 B)**. Similarly, the titer of IgG2c in the samples derived from animals immunized with OVA co-administered with cGAMP was significantly enhanced, as compared to the samples of mice immunized with OVA alone **(figure 11 C)**. Elevated titers of IgG1 and IgG2c are indicators Th2 and Th1 cell activity, respectively [151]. Thus, the efficacy of cGAMP in enhancing OVA-specific IgG1 and IgG2c production implied its potency to enhance the activity of Th2 and Th1 cells.

To explore the potency of cGAMP to enhance cellular responses, pooled spleen cells from immunized groups of animals were isolated and re-stimulated *in vitro* with OVA. First, the proliferation of spleen cells was measured using the ^{3}H-thymidine incorporation assay. The cells from the animals that received OVA co-administered with cGAMP proliferated significantly stronger when compared to the cells from the animals that were immunized with OVA alone **(figure 12)**. IFN-γ and IL-2 cytokine production are characteristic of Th1 cell activity, whereas IL-4 is indicative for the Th2 and IL-17 for the Th17 phenotype. Thus, to characterize the potential of cGAMP in enhancing Th responses, the production of cytokines IFN-γ, IL-2, IL-4 and IL-17 by OVA-re-stimulated spleen cells was measured by ELISPOT **(figure 13)**. The numbers of IFN-γ, IL-2 and IL-17-producing cells were significantly enhanced in samples from animals immunized with OVA co-administered with cGAMP when compared to cell samples derived from animals immunized with OVA alone **(figure 13 A, B, D)**. Similarly, a trend of an enhanced number (although statistically not significant) of IL-4-producing cells was observed in samples from animals immunized with OVA and cGAMP, when compared to samples derived from animals that received OVA alone **(figure 13 C)**. Enhanced numbers of antigen-specific IFN-γ, IL-2, IL-4 and IL-17-producing cells in the animals immunized with OVA and cGAMP in comparison to the response in mice receiving only OVA indicate the ability of cGAMP to enhance Th1, Th2 and Th17 responses.

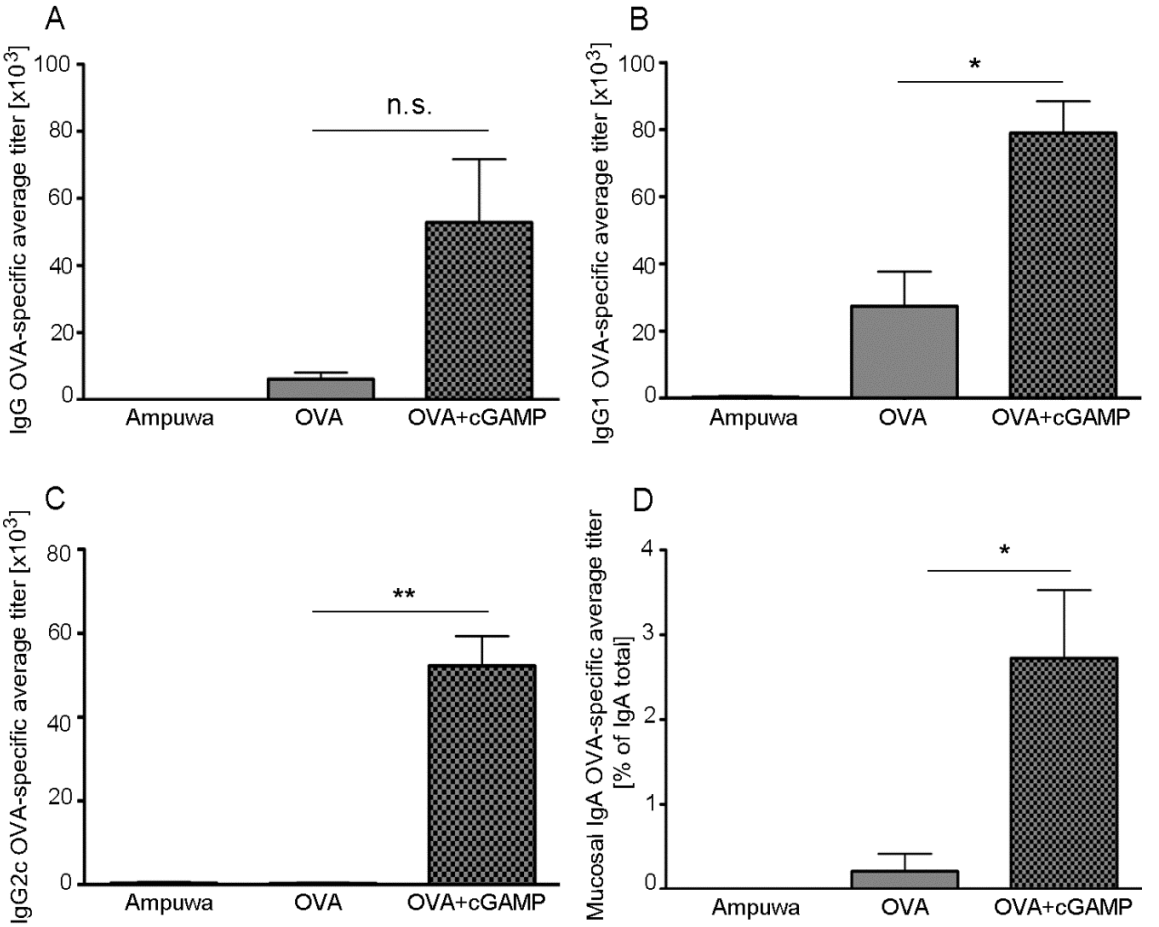

Figure 11: cGAMP enhances antigen-specific humoral responses in immunized mice. Mice were treated with Ampuwa injection water or OVA alone or OVA co-administered with cGAMP. Serum samples of these mice were analyzed for the presence of OVA-specific (A) total IgG, (B) IgG1, and (C) IgG2c by ELISA. The titer gives the dilution factor of the assay sample with twice the readout value of the blank (absorbance of light of 405 nm wavelength). (D) Mucosal IgA was analyzed in nasal lavage samples by ELISA and OVA-specific IgA titers are expressed as percentage of the total IgA titers. The error bars represent the standard error of the mean (SEM) of three independent experiments with five mice per group per experiment. Significant differences between select groups are indicated with * for $p<0.05$ and ** for $p<0.01$, whereas n. s. indicates non-significant.

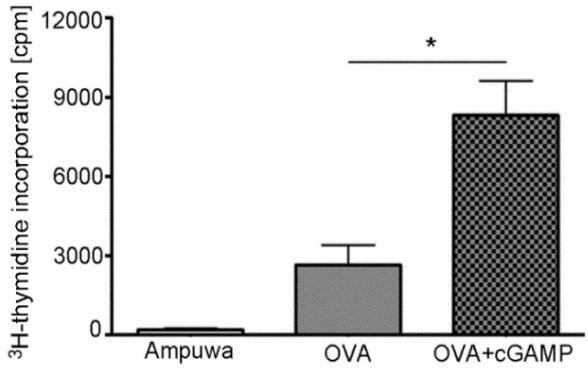

Figure 12: cGAMP enhances the antigen-specific proliferative capacity of re-stimulated spleen cells from immunized mice. The proliferation of antigen-stimulated spleen cells from mice treated with Ampuwa injection water or OVA alone or OVA co-administered with cGAMP was measured by a ^{3}H-thymidine incorporation assay. The error bars represent the SEM of three independent experiments with five mice per group per experiment. Significant differences between select groups are indicated with * for $p<0.05$.

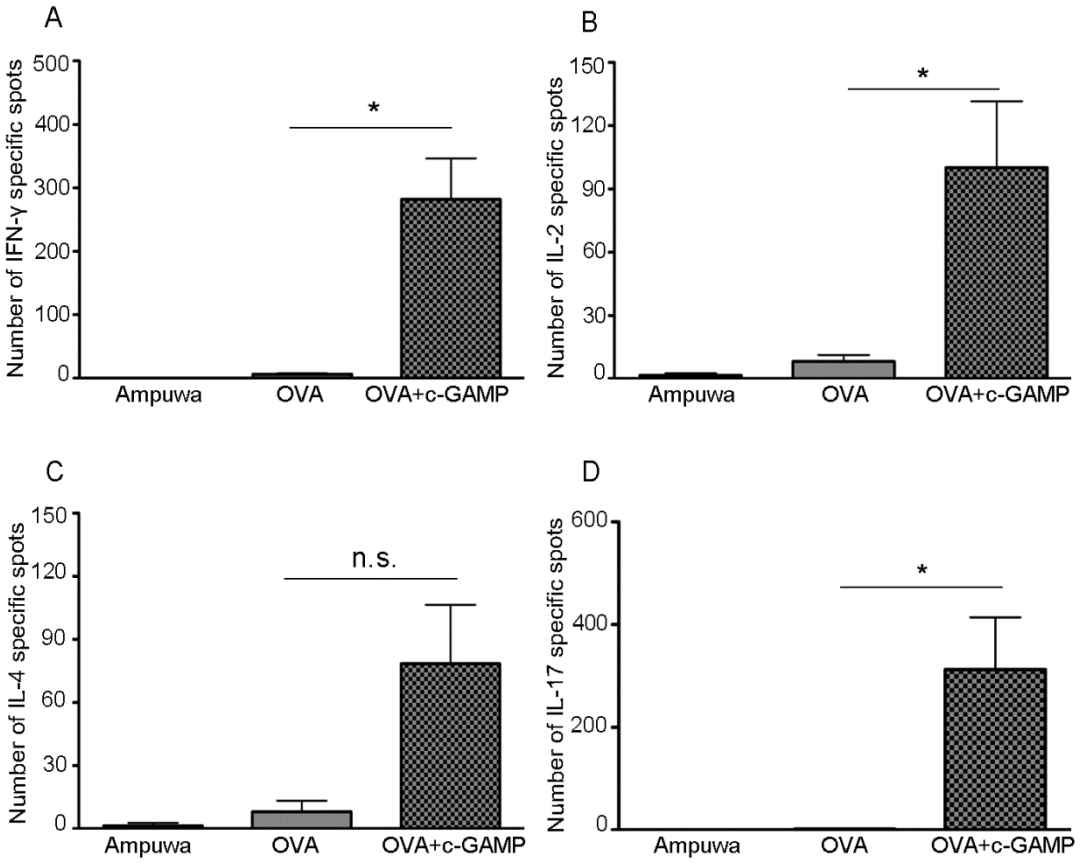

Figure 13: cGAMP enhances IFN-γ, IL-2, IL-4 and IL-17 production of antigen-re-stimulated spleen cells from immunized mice. Mice were treated with Ampuwa injection water or OVA alone or OVA co-administered with cGAMP. Spleen cells of these mice were re-stimulated with OVA and analysed for the production of the cytokines (A) IFN-γ, (B) IL-2, (C) IL-4 and (D) IL-17 in ELISPOT assays. The results are expressed as number of spots per 10^6 cells. The error bars represent the SEM of three independent experiments with five mice per group per experiment. Significant differences between select groups are indicated with * for $p<0.05$, whereas n. s. indicates non-significant.

3.3 Comparison of c-di-AMP and cGAMP immune stimulatory potencies

To compare the immune stimulatory potencies of c-di-AMP and cGAMP, additional immunization studies were performed. Experimental groups were immunized with OVA alone or OVA co-administered with either c-di-AMP or cGAMP. Then, antigen-specific humoral and cellular responses were assessed according to the protocol shown in **figure 10**.

3.3.1 C-di-AMP and cGAMP promote a similar enhancement of humoral responses

Nasal wash samples from the immunized mice were analyzed to compare the capacity of c-di-AMP and cGAMP to enhance OVA-specific mucosal IgA production. To this end, total and OVA-specific IgA were measured by ELISA. The amount of OVA-specific IgA is given as a percentage of total IgA. The titers of OVA-specific IgA in nasal wash of mice that received CDN with OVA were significantly enhanced when compared to samples of mice immunized with OVA alone **(figure 14 D).** The extent to which c-di-AMP enhanced OVA-specific IgA titer was slightly higher than that observed for cGAMP **(figure 14 D)**.

Serum samples of immunized animals were analyzed to assess humoral responses at systemic level, as defined by the presence of OVA-specific IgG and its sub-classes IgG1 and IgG2c. The titers of OVA-specific IgG in serum of mice immunized with c-di-AMP and OVA were significantly higher than those observed in mice immunized with OVA alone. A similar enhancing effect on IgG production (although statistically not significant) was observed in samples from animals that received the cGAMP-adjuvanted formulation **(figure 14 A)**. The extent of the c-di-AMP-mediated enhancement of OVA-specific IgG response was slightly higher than that observed for cGAMP **(figure 14 A)**. The titers of OVA-specific IgG1 in serum of mice that received either of the tested CDN with OVA were significantly enhanced when compared to serum of mice immunized with OVA alone **(figure 14 B)**. The extent of c-di-AMP-enhanced OVA-specific IgG1 response was slightly higher than that observed in animals that received cGAMP as adjuvant **(figure 14 B)**. A clear trend of enhanced OVA-specific IgG2c titer was also observed in serum of mice immunized with OVA and c-di-AMP when compared to samples from mice immunized with OVA alone. The titer of IgG2c in serum of mice that received OVA and cGAMP was significantly higher as compared to samples of mice that received only

OVA **(figure 14 C)**. However, the extent of c-di-AMP-mediated enhancement of OVA-specific IgG2c response was slightly higher than that observed when using cGAMP as adjuvant **(figure 14 C).** Taken together, both candidate adjuvants enhanced the production of OVA-specific IgG, IgG1 and IgG2c as compared to the response observed in the animals immunized with the antigen OVA alone. The extent of their enhancing effect was comparable, with c-di-AMP being a slightly stronger enhancer of IgG, IgG1 and IgG2c production than cGAMP. Elevated titers of IgG1 and IgG2c are indicators of Th2 and Th1 cell activity, respectively [151]. Thus, the capacity of c-di-AMP and cGAMP to promote the enhanced IgG1 and IgG2c production reported here implies that these candidate adjuvants promote balanced Th1/Th2 responses.

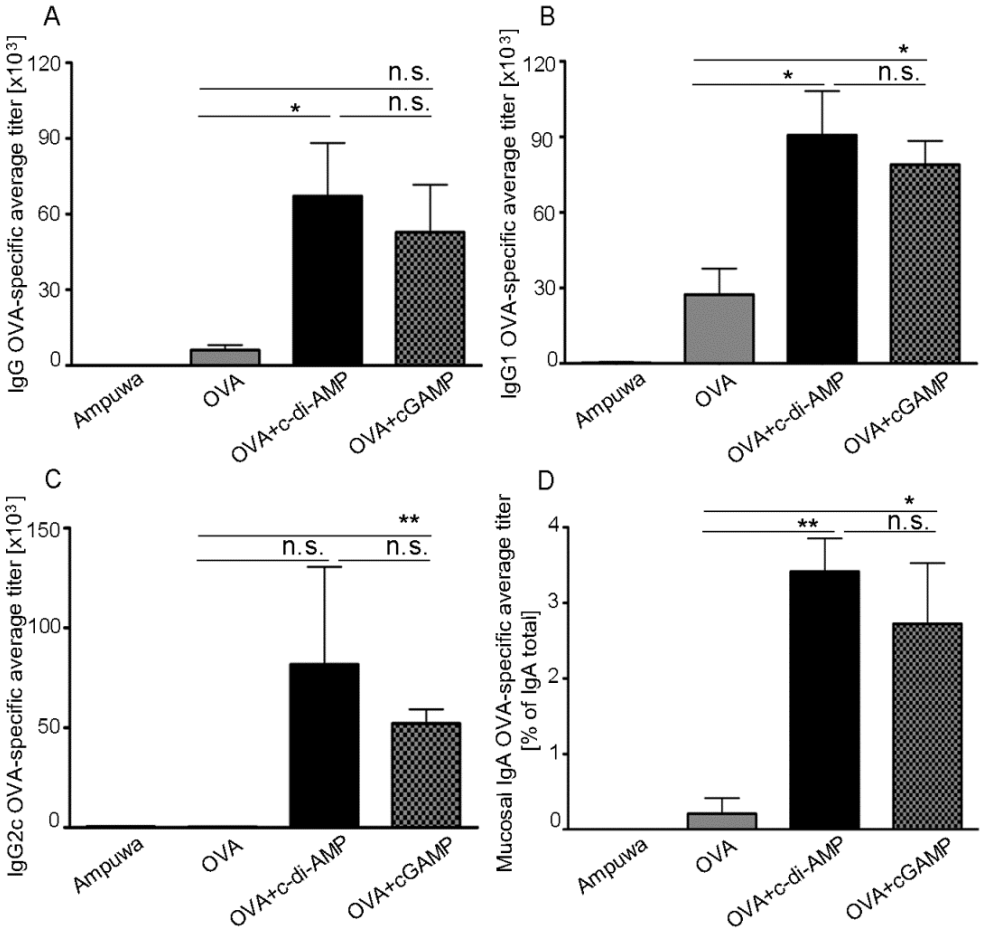

Figure 14: Humoral response in immunized mice that received c-di-AMP or cGAMP as an adjuvant. Mice were treated with Ampuwa injection water OVA alone or OVA co-administered with either c-di-AMP or cGAMP. Serum samples of these mice were analyzed for the presence of OVA-specific (A) total IgG, (B) IgG1, (C) IgG2c titers by ELISA. The titers are expressed as the dilution factor of the assay sample with twice the readout value of the blank (absorbance of light of 405 nm wavelength). (D) Mucosal IgA responses were analyzed in nasal lavage samples by ELISA. OVA-specific IgA titers are expressed as percentage of total IgA titers. The error bars represent the SEM of three independent experiments with five mice per group per experiment. Significant differences between select groups are indicated with * for $p<0.05$ and ** for $p<0.01$, whereas n. s. indicates non-significant.

3.3.2 C-di-AMP mediates a slightly stronger enhancement of the proliferation capacity of spleen cells than cGAMP

Next, cellular responses upon i.n. administration of the formulations containing OVA alone or co-administered with one of the two tested CDNs were measured. To this end, spleen cells of immunized mice were isolated and re-stimulated *in vitro* with OVA. The proliferation of cells was evaluated using the ^{3}H-thymidine incorporation assay. The proliferation of OVA-re-stimulated spleen cells from mice immunized with OVA and either of the candidate adjuvants was significantly enhanced when compared to cell samples from mice immunized with OVA alone. The extent of c-di-AMP-enhanced cell proliferation was slightly higher than that observed for cGAMP **(figure 15)**.

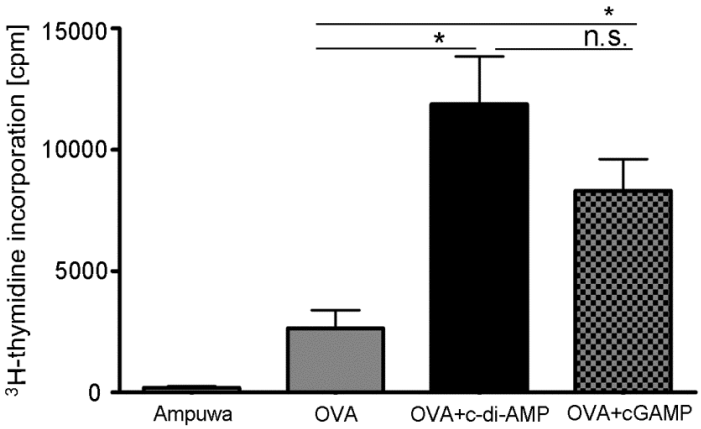

Figure 15: Proliferation of re-stimulated spleen cells from OVA-immunized mice that received c-di-AMP or cGAMP as an adjuvant. The proliferation of antigen-stimulated spleen cells from mice treated with Ampuwa injection water, OVA alone or OVA co-administered with either c-di-AMP or cGAMP was measured by a ^{3}H-thymidine incorporation assay. The error bars represent the SEM of three independent experiments with five mice per group per experiment. Significant differences between select groups are indicated with * for $p<0.05$, whereas n. s. indicates non-significant.

3.3.3 C-di-AMP and cGAMP promote a similar enhancement of Th1 and Th2 responses, but a differential activation of Th17 cells

Cellular responses of the animals treated by i.n. route with OVA alone or combined with CDN were evaluated by measurement of the produced cytokines. To this end, spleen cells from immunized animals were re-stimulated with OVA and the production of cytokines was measured using ELISPOT **(figure 16)**. The co-administration of either c-di-AMP or cGAMP with OVA resulted in significantly enhanced numbers of IFN-γ and IL-2-producing cells, when compared to samples derived from mice immunized with OVA alone **(Figure 16 A-B)**. The number of IFN-γ-producing cells was slightly higher in

samples from mice that received c-di-AMP than in those receiving cGAMP as adjuvant, whereas the numbers of IL-2-producing cells were similar for samples derived from both groups **(figure 16 A-B)**. The number of IL-4-producing cells derived from mice immunized with c-di-AMP and OVA was significantly higher than that observed in mice receiving OVA alone. A similar enhancing trend for IL-4-secreting cells (although not statistically significant) was observed in samples from animals that received the cGAMP-adjuvanted formulation. Similar numbers of IL-2-producing cells were observed in mice receiving the c-di-AMP- and cGAMP-adjuvanted formulations **(16 C)**. The numbers of IL-17-producing cells were also significantly enhanced in samples from animals immunized with OVA and CDN when compared to samples derived from mice immunized with OVA alone. However, the number of IL-17-producing cells was significantly higher in mice receiving c-di-AMP than that observed in mice receiving the cGAMP-containing formulation. **(Figure 16 D)**.

The observation of the differential effect of c-di-AMP and cGAMP on Th17 polarization by ELISPOT was further investigated at the T cell subset level using flow cytometry. For this, OVA-re-stimulated spleen cells from mice belonging to different immunization groups were stained for $CD3^+$ and $CD4^+$ T cell surface markers and intracellular IL-17. This experimental approach confirmed that c-di-AMP is a stronger enhancer of the number of IL-17-producing cells than cGAMP. Furthermore, the application of gates for $CD4^+$ cells allowed the identification of Th cells as those responsible for the differential production of IL-17. The frequency of IL-17-producing cells in OVA-re-stimulated splenocytes from mice immunized with OVA co-administered with c-di-AMP was higher as compared to samples derived from animals that received cGAMP as adjuvant **(figure 17).** This finding indicates a clear difference in the immune stimulatory capacity of the two candidate adjuvants.

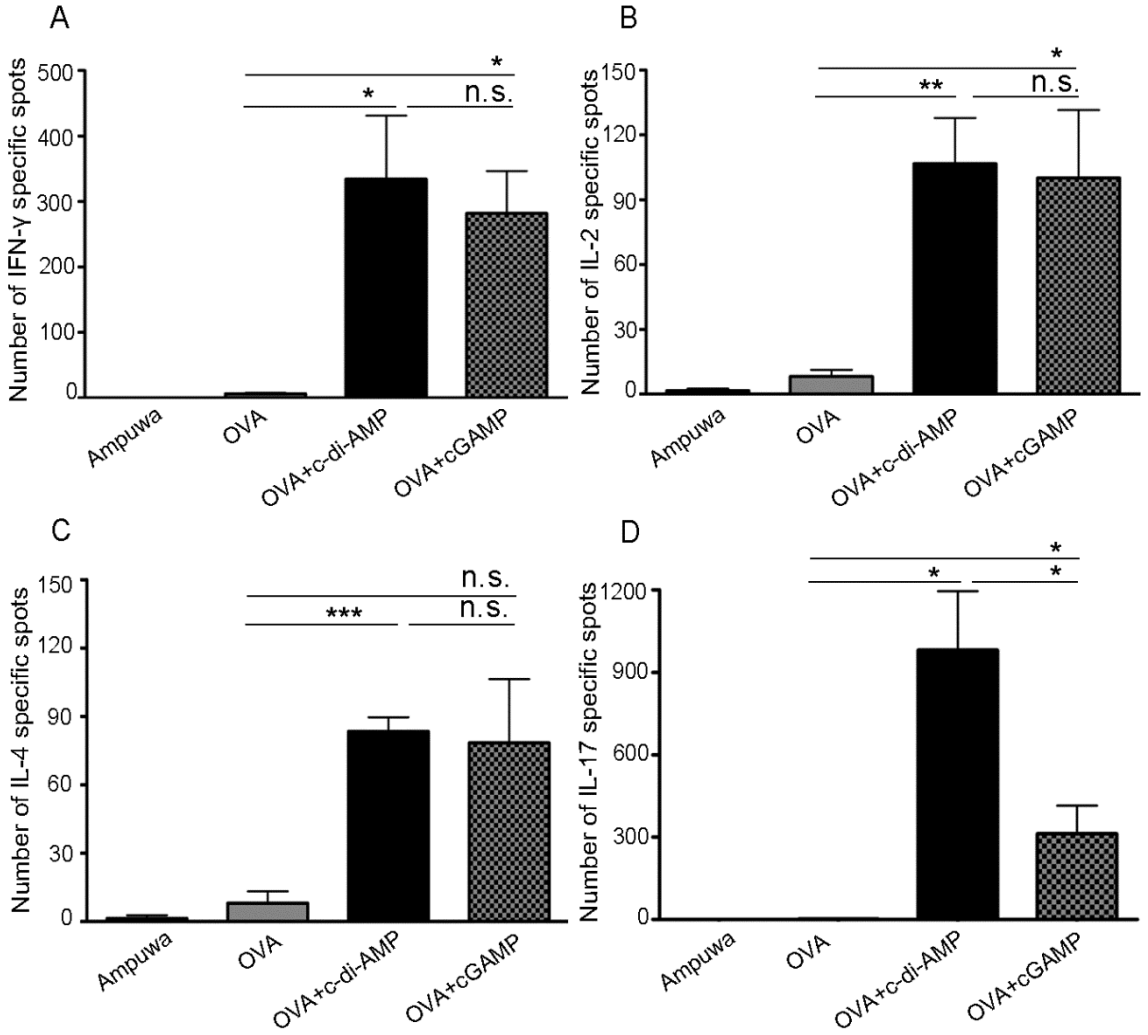

Figure 16: IFN-γ, IL-2, IL-4 and IL-17 production of re-stimulated spleen cells from OVA-immunized mice that received c-di-AMP or cGAMP as an adjuvant. Mice were treated with Ampuwa injection water or OVA alone or OVA co-administered with either c-di-AMP or cGAMP. Spleen cells of these mice were re-stimulated with OVA and analysed for the production of the cytokines (A) IFN-γ, (B) IL-2, (C) IL-4 and (D) IL-17 in ELISPOT assays. The results are expressed as number of spots per 10^6 cells. The error bars represent the SEM of three independent experiments with five mice per group per experiment. Significant differences between select groups are indicated with * for $p<0.05$ and *** for $p<0.001$, whereas n. s. indicates non-significant.

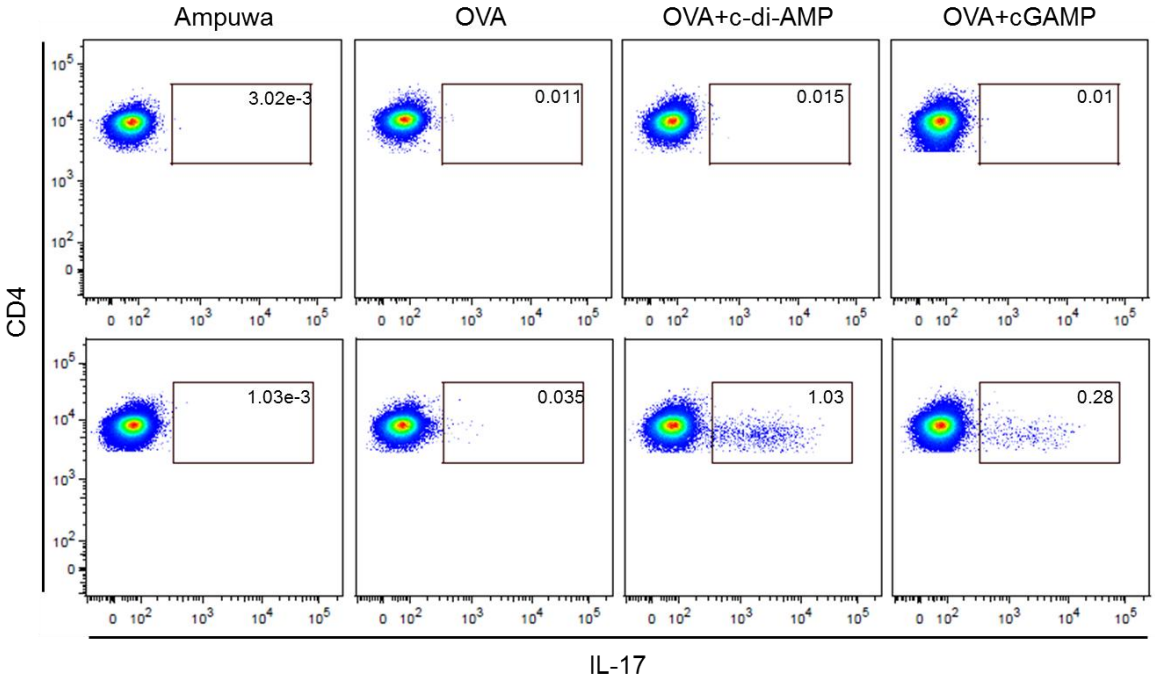

Figure 17: Flow cytometry analysis of IL-17 production by re-stimulated spleen cells from OVA-immunized mice. Mice were treated with Ampuwa injection water or OVA alone or OVA co-administered with either c-di-AMP or cGAMP. Pooled spleen cells from five immunized mice per group were re-stimulated *in vitro* with OVA (lower panel) or left in medium (upper panel) for 24 h and then IL-17 production was measured by flow cytometry and results were displayed as dot plots. The numbers in the rectangles give the percentage of gated IL-17-producing cells among gated $CD3^+/CD4^+$ splenocytes.

3.4 Identification of *in vitro* parameters indicative for c-di-AMP and cGAMP activity

Some of the responses usually evoked by PAMPs at the cellular level were screened to identify if they can be used as surrogate *in vitro* parameters indicative for c-di-AMP or cGAMP activity using BMDCs as a model system. Hallmarks of dendritic cell activation are up-regulation of the surface expression of components of the immune synapsis, such as MHC and co-stimulatory molecules, and production of cytokines involved in immune activation. It was previously reported that IL-6 and IL-23, both produced by dendritic cells, are involved in development or maintenance of the Th17 phenotype [69, 152]. Thus, guided by the finding that c-di-AMP and cGAMP differentially enhance Th17 responses *in vivo*, it was tested if c-di-AMP and cGAMP differ in their *in vitro* capacity to induce the expression of IL-6 or IL-12/IL-23p40. In addition, it was evaluated the production of type I IFNs after *in vitro* treatment with c-di-AMP or cGAMP. To this end,

bone marrow cells were cultured for seven days in the presence of GM-CSF to promote the generation of BMDCs, and on day 7 c-di-AMP or cGAMP was added to the culture medium for 24 h. The surface expression of the activation markers MHC class II, CD86 and CD80, and the production of IL-6, IL-12/IL-23p40 and type I IFNs were then assessed as shown in **figure 18**.

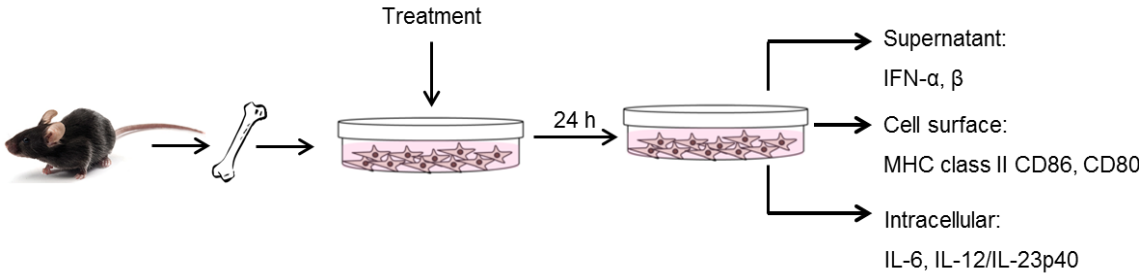

Figure 18: A scheme of *in vitro* experiments with BMDCs stimulated with c-di-AMP or cGAMP. Murine bone marrow cells were cultured for 7 days in the presence of GM-CSF. The cells were then treated with c-di-AMP (5 µg/ml), cGAMP (5 µg/ml) or LPS (1 µg/ml) for 24 h. Untreated cells were used as controls. Then, BMDCs were decorated with fluorophore-conjugated antibodies specific for dendritic cell activation markers or intracellular cytokines and further analysed by flow cytometry. The presence of type I IFNs was determined in supernatant fluids by ELISA.

3.4.1 C-di-AMP and cGAMP exhibit a similar capacity to induce the surface expression of the activation markers MHC class II, CD86 and CD80

Treatment of BMDCs with c-di-AMP or cGAMP for 24 h led to a clear trend of the up-regulated surface expression of MHC class II and the T cell co-stimulatory molecule CD86 as compared to non-stimulated cells **(figure 19)**. The surface expression of CD80 by the BMDCs treated with c-di-AMP or cGAMP was also increased in comparison to non-stimulated cells, but to a lesser extent **(figure 19)**. No significant differences were observed between the patterns of up-regulation of the activation markers expressed by BMDCs treated with c-di-AMP and cGAMP.

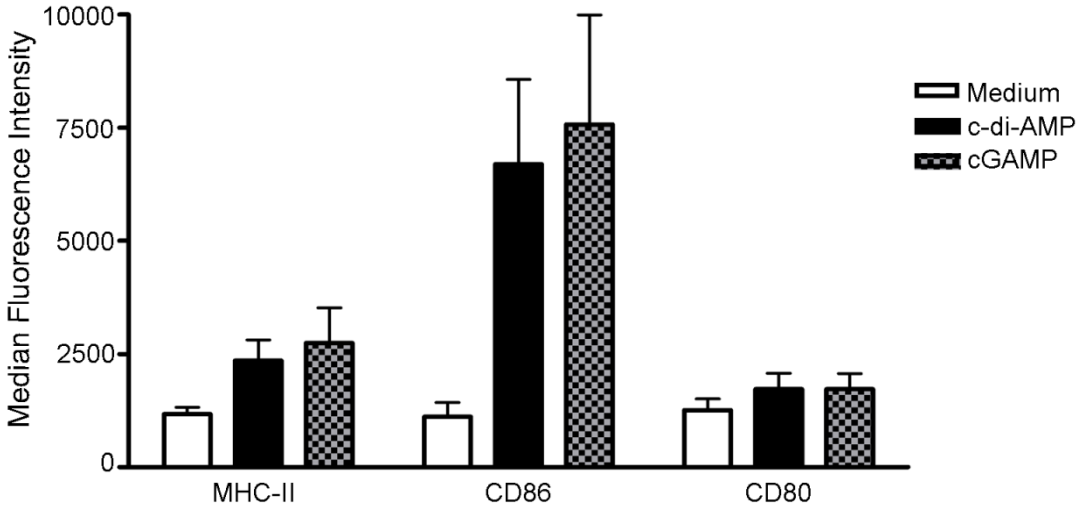

Figure 19: Analysis of the surface expression of activation markers on murine BMDCs following treatment with c-di-AMP or cGAMP by flow cytometry. BMDCs were stimulated *in vitro* with c-di-AMP (5 µg/ml) or cGAMP (5 µg/ml) or left untreated for 24 h. The cells were then decorated with fluorophore-conjugated antibodies specific for dendritic cell activation markers MHC class II (I-Ab), CD86 or CD80 and analysed by flow cytometry. Shown are the values of median fluorescence intensity signals measured for activation markers on $CD11c^+$ cells. Error bars represent the SEM of four independent experiments.

3.4.2 C-di-AMP is a stronger inducer of IL-12/IL-23p40 expression in BMDCs than cGAMP

Next, the potential of c-di-AMP and cGAMP to induce production of IL-6 and IL-12/IL-23p40 by BMDCs was investigated. To this end, BMDCs were treated with 5 µg/ml of c-di-AMP or cGAMP for 24 h. Untreated cells were used as controls. During the last 8 h of incubation, cells were treated with inhibitors of secretion brefeldin A (5 µg/ml) and monensin (6 µg/ml). Subsequently, cells were processed and the fluorescence signals indicating the presence of cell-specific activation markers, IL-6 and IL-12/IL-23p40 were detected by flow cytometry. To avoid false positive results, gates indicating the cytokine-specific signals on the $CD11c^+$ population were set according to the position of the signals observed in PE (IL-6) and PE-Cy7 (CD11C)-detecting channels for non-stained cell samples **(figure 20 B)**. As it is seen from the upper panel in **figure 20 A**, IL-6 production in BMDCs was not observed after CDN treatment for 24 h. Nevertheless, the frequency of IL-12/IL-23p40$^+$ cells in samples treated with c-di-AMP was four times the frequency of IL-12/IL-23p40$^+$ cells in untreated control samples **(figure 20 A, lower panel)**. In contrast, the frequency of IL-12/IL-23p40$^+$ cells in cGAMP-treated samples was only double the value observed in untreated controls **(figure 20 A, lower panel)**. This observation was confirmed in three independent experiments and the statistically

significant difference in the potency of c-di-AMP and cGAMP to induce IL-12/IL-23p40$^+$ production by BMDCs is given in **figure 21**. It is important to mention that p40 is a common subunit shared by IL-23 and IL-12. However, currently available immuno-assays do not allow a clear distinction between these two cytokines. Therefore, it remains to be assessed which specific cytokine(s) (*i.e.* IL-12 or IL-23) is differentially induced by c-di-AMP and cGAMP.

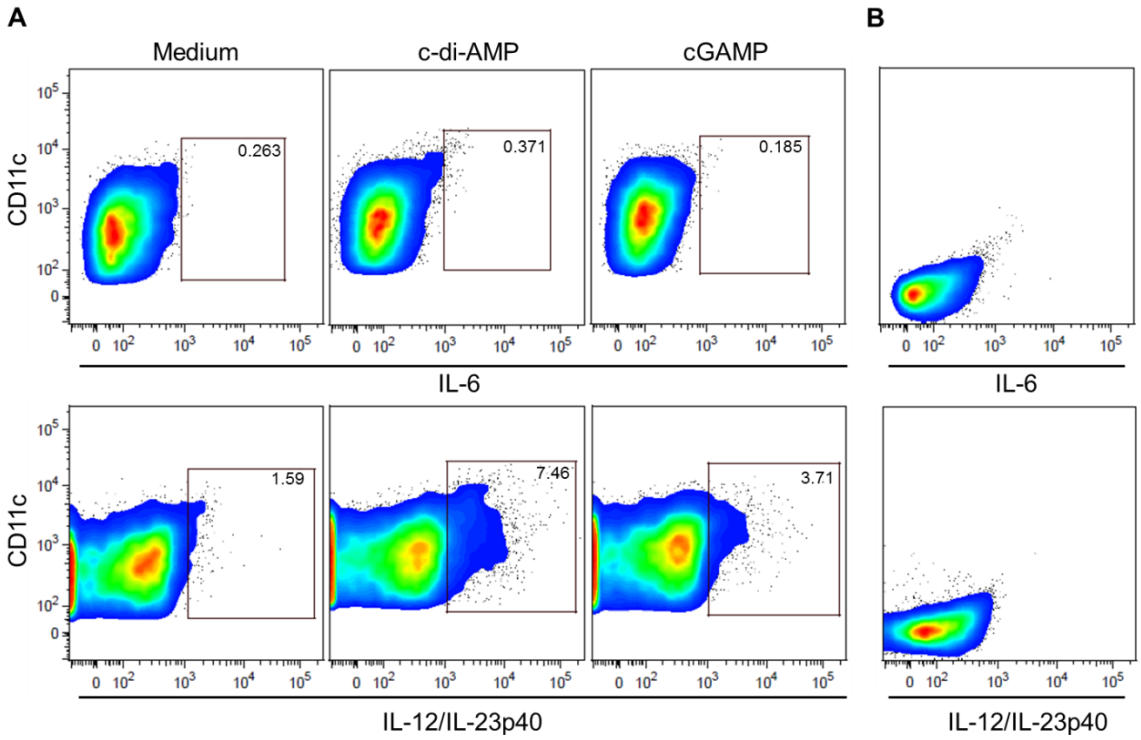

Figure 20: Analysis of IL-12/IL-23p40 induction in BMDCs upon treatment with c-di-AMP or cGAMP by flow cytometry. BMDCs were stimulated *in vitro* with c-di-AMP (5 µg/ml) or cGAMP (5 µg/ml) or left untreated (Medium) for 24 h. Then, BMDCs were decorated with fluorophore-conjugated antibodies against the dendritic cell marker CD11c, as well as intracellular IL-6 (upper panel) an IL-12/IL-23p40 (lower panel), and cells were analysed by flow cytometry. The numbers in the rectangles represent the percentage of IL-6 or IL-12/IL-23p40 producing cells within the CD11c$^+$ cell subpopulation.

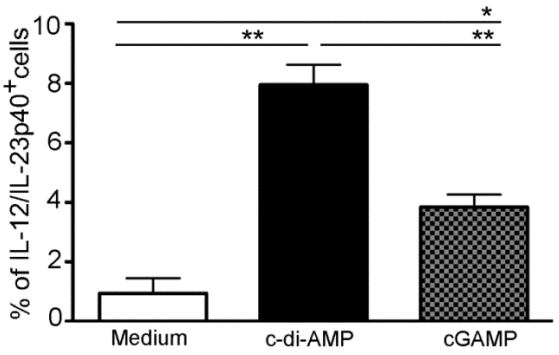

Figure 21: Analysis of IL-12/IL-23p40 induction in BMDCs upon treatment with c-di-AMP or cGAMP by flow cytometry. BMDCs were stimulated *in vitro* with c-di-AMP (5 µg/ml) or cGAMP (5 µg/ml) for 24 h. Untreated cells were used as controls (Medium). The BMDCs were then decorated with fluorophore-conjugated antibodies against the dendritic cell marker CD11c and IL-12/IL-23p40, and analysed by flow cytometry. Results are expressed as a percentage of $CD11c^+$ cells with intracellular expression of IL-12/IL-23p40. The error bars represent the SEM of three independent experiments. Significant differences between select groups are indicated with * for $p<0.05$ and ** for $p<0.01$, whereas n. s. indicates non-significant.

3.4.3 The cGAMP is a stronger inducer of type I IFNs production by BMDCs than c-di-AMP

In order to compare the capacity of c-di-AMP and cGAMP to induce expression of type I IFNs, BMDCs were treated with CDN and their supernatants were analyzed for the presence of IFN-α and IFN-β. LPS was used as a positive control of type I IFN induction. BMDCs were treated for 24 h with 1 µg/ml LPS (positive control), 5 µg/ml CDN or left in medium without additives (negative control). Supernatants were collected after 24 h treatment and analyzed by ELISA. BMDCs treated with LPS produced increased amounts of IFN-α (although the differences were not statistically significant) and significantly higher amounts of IFN-β, as compared to untreated controls. BMDCs treated with c-di-AMP produced significantly higher amount of IFNs, as compared to untreated samples. Similar results were obtained with BMDCs treated with cGAMP, which produced increased amounts of IFN-α (statistically not significant) and IFN-β, as compared to untreated samples. The cGAMP exhibited a slightly stronger capacity to induce type I IFNs expression in BMDCs than c-di-AMP, although the differences were not statistically significant **(figure 22)**.

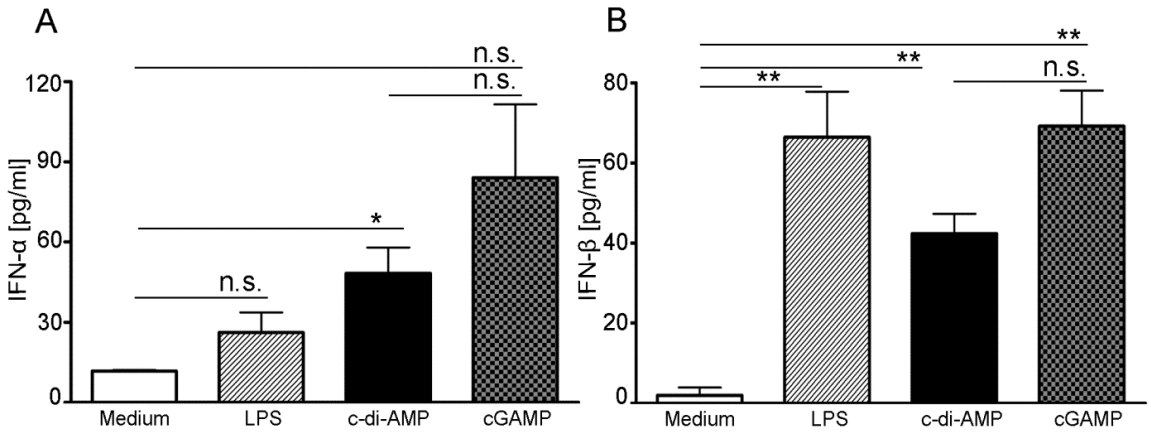

Figure 22: IFN-α and IFN-β production by BMDCs stimulated with c-di-AMP or cGAMP. BMDCs were stimulated *in vitro* with 1 µg/ml LPS, 5 µg/ml c-di-AMP or cGAMP or left in medium without additives for 24 h. Supernatants were then collected and analysed for the presence of IFN-α or IFN-β by ELISA. The error bars represent the SEM of three independent experiments. Significant differences between select groups are indicated with * for $p<0.05$, ** for $p<0.01$, whereas n. s. indicates non-significant.

3.5 Investigation of molecular mechanisms mediating the adjuvanticity of CDNs

The results obtained in BMDCs **(figure 22)** together with a previous study from our team showing the *in vivo* activity of c-di-AMP in IFN-β reporter mice [153] clearly demonstrate the capacity of c-di-AMP and cGAMP to induce type I IFNs production. This raises the issue of whether the stimulation of the type I IFN induction and signaling pathways is critical for the adjuvant properties of c-di-AMP and cGAMP. Thus, to investigate the impact of the type I IFN pathways on the adjuvanticity of c-di-AMP and cGAMP, immunization experiments were conducted using mice lacking functional Sting or IFNAR. This experimental approach allowed dissecting the CDN-triggered type I IFN pathways, namely the Sting-dependent induction of type I IFNs and IFNAR-mediated downstream signaling of type I IFNs resulting in the activation of ISGs. The experimental groups contained four or five animals and were treated with OVA or OVA co-administered with CDN. Adaptive immune responses were assessed as described in **figure 10**.

3.5.1 Sting phenotyping and IFNAR$^{-/-}$ genotyping

To confirm that the experimental *in vivo* models really lack functional components of the type I IFN pathways, phenotyping of the *Sting*$^{Gt/Gt}$ mice **(Figure 23 B)** and genotyping of the IFNAR$^{-/-}$ animals **(figure 23 A)** were performed. *Sting*$^{Gt/Gt}$ animals carry a single point mutation (T596A) of *Sting* that functions as a null allele and fails to produce functional, detectable protein [135]. This was confirmed by Western blot. SDS-PAGE/ Western blot analysis for Sting presence was performed on lysates of BMDCs generated from wt, IFNAR$^{-/-}$ and *Sting*$^{Gt/G}$ mice. Sting was detected in samples from wt and IFNAR$^{-/-}$ mice, but not in the *Sting*$^{Gt/Gt}$ samples **(figure 23 A)**. Total protein staining on the nitrocellulose membrane using Ponceau indicated that the absence of the Sting band in the *Sting*$^{Gt/Gt}$ sample was not due to much lower total protein amounts loaded on the gel in comparison with the wt and IFNAR$^{-/-}$ samples **(figure 23 B)**.

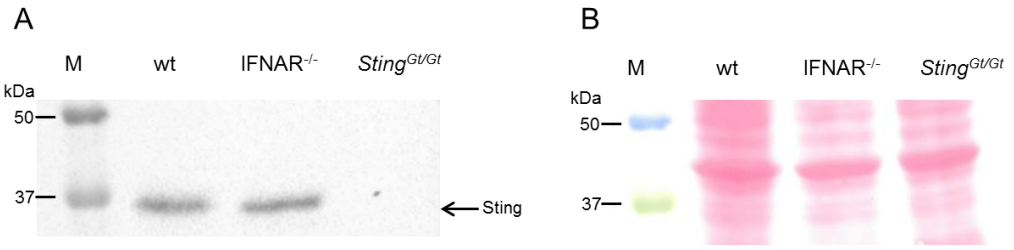

Figure 23: Western blot analysis of Sting expression in BMDC lysates from wt, IFNAR$^{-/-}$ and *Sting*$^{Gt/Gt}$ mice. (A) Image of ECL-signals recorded upon membrane exposure to a ChemiDocXRS camera for 39.1 sec. The arrow head indicates the Sting-specific band. (B) BMDCs lysates, SDS-PAGE in 10% polyacrylamide, Ponceau stained membrane.

The IFNAR$^{-/-}$ genotype was examined by PCR and agarose gel electrophoretic analysis. The IFNAR1 gene disruption is characterized by a neomycin resistance gene insertion into the exon III in the IFNAR1 gene [148]. This resulted in sequence features that can be used for the identification of the knock out (ko) genotype by a detection of a specific PCR product **(figure 24 B)**. DNA material was obtained from tail biopsies of wt and IFNAR$^{-/-}$ animals, which was used as template for the PCR amplification. A negative control, a PCR reaction containing water instead of biopsy lysate gave no detectable bands. Homozygous IFNAR1 gene disruption was confirmed by the presence of a 500 bp band, whereas in wt samples a band appeared at 154 bp running distance **(figure 24 A)**, as expected according to the schematic overview shown in the **figure 24 B**.

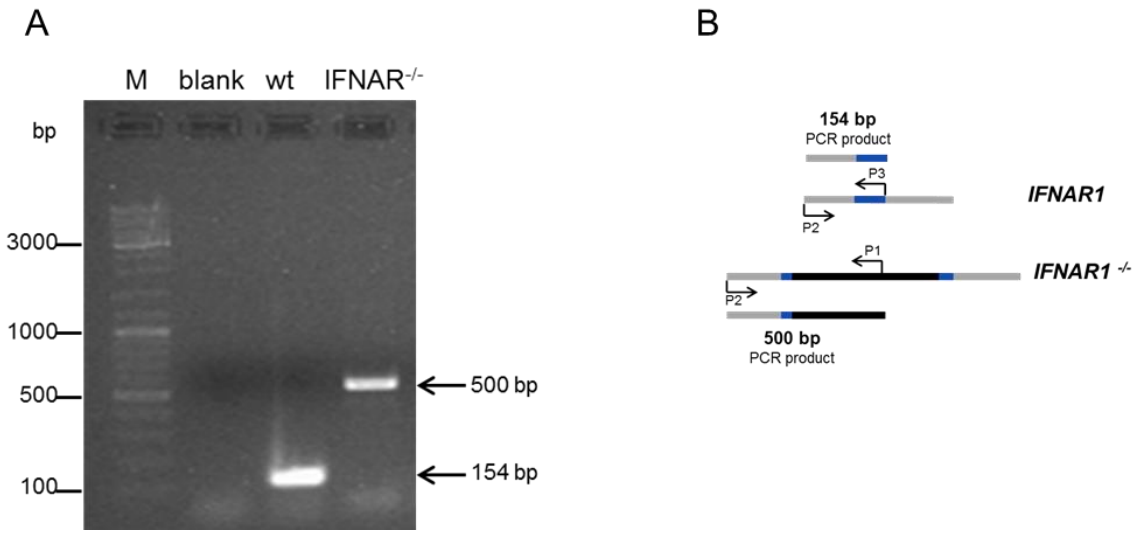

Figure 24: Genotypisation of IFNAR$^{-/-}$ animals. (A) Image of fluorescent signals indicating the position of PCR products after agarose gel electrophoresis. For the reactions, DNA from tissue lysates from wt or IFNAR$^{-/-}$ animals was used. (B) Scheme of the IFNAR$^{-/-}$ construct on exon III of the IFNAR1 gene, where a neomycin resistance gene insertion results in IFNAR1 gene disruption. The neomycin resistance gene is recognized by the primer 1, which in a combination with primer 2 upon PCR amplification results in a 500 bp fragment, confirming the IFNAR$^{-/-}$ knock out genotype. Blank sample contained H_2O instead of DNA template; bp indicates base pairs

3.5.2 Sting but not IFNAR is essential for the c-di-AMP-mediated enhancement of the humoral immune response

To address if the type I IFN pathways have an impact on the c-di-AMP-mediated enhancement of OVA-specific systemic humoral response, OVA-specific IgG titers were determined in serum samples of immunized mice by ELISA. To this end, the average titer value per experimental group was calculated, and the results were presented as fold of the titers detected in animals immunized with OVA alone. The obtained results clearly demonstrated that the c-di-AMP-mediated enhancement of the OVA-specific serum IgG titer observed in wt animals was lost in *Sting*$^{Gt/Gt}$ mice **(figure 25 A)**. However, the OVA-specific IgG titers were similar in wt and in IFNAR$^{-/-}$ mice **(figure 25 B)**.

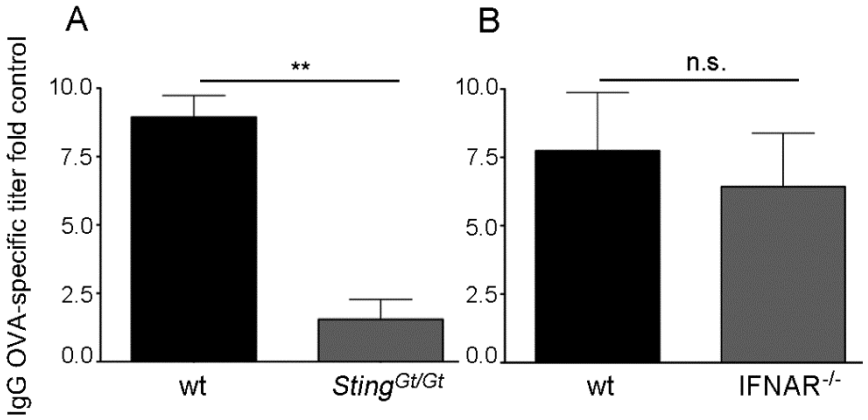

Figure 25: c-di-AMP enhances antigen-specific IgG responses in wt and IFNAR$^{-/-}$, but not in *Sting*$^{Gt/Gt}$ mice. Mice were immunized with OVA alone or OVA co-administered with c-di-AMP. Serum samples were then analysed by ELISA for the presence of OVA-specific total IgG. Titers were defined as the dilution factor of the assay sample with more than twice the readout value of the blank (absorbance of light of 405 nm wavelength). The average titer value per group is given as multiple of the value of the control group immunized with OVA alone. Results represent the response in wt vs. *Sting*$^{Gt/Gt}$ (A) and wt vs. IFNAR$^{-/-}$ (B). The error bars represent the SEM of three independent experiments where four or five animals per group were used. Statistical differences are indicated by ** for $p<0.01$, whereas n. s. indicates non-significant.

3.5.3 Sting but not IFNAR is essential for c-di-AMP-mediated enhancement of the proliferation capacity

The relevance of the type I IFN pathways for the c-di-AMP-mediated enhancement of OVA-specific cellular immune responses was evaluated. Spleen cells from immunized animals were re-stimulated with OVA *in vitro*. The proliferation of the re-stimulated cells was then measured using a ^{3}H-thymidine incorporation assay. The average count per minute value, proportional to the amount of ^{3}H-thymidine incorporated in cells, was calculated in each experimental group. Results are expressed as fold of response detected in animals immunized with OVA alone. The c-di-AMP-mediated enhancement of cell proliferation was considerably reduced in *Sting*$^{Gt/Gt}$ mice, as compared to values in samples from wt animals **(figure 26 A)**. In contrast, the extent of c-di-AMP-enhanced proliferation of OVA re-stimulated spleen cells derived from wt animals was similar to that observed in samples from IFNAR$^{-/-}$ mice **(figure 26 B).**

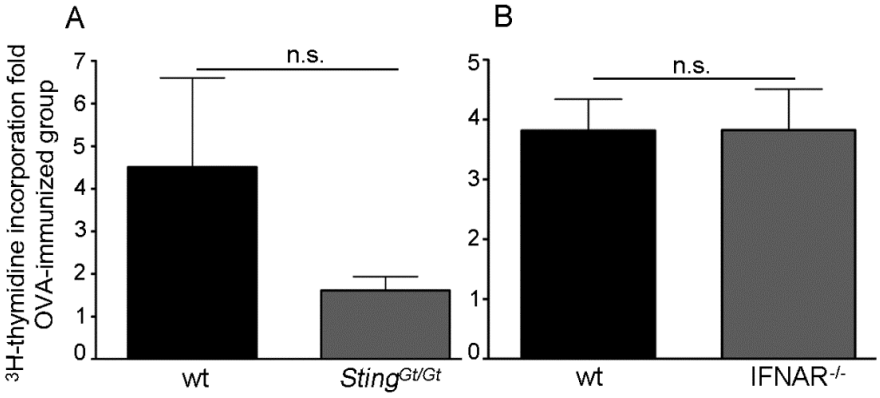

Figure 26: Incorporation of c-di-AMP in the immunization formulation results in enhanced antigen-specific proliferation of spleen cells from wt and IFNAR$^{-/-}$, but not *Sting*$^{Gt/Gt}$ mice. Spleen cells from mice immunized with OVA alone or co-administered with c-di-AMP were re-stimulated with OVA and analysed for their proliferative capacity using a ^{3}H-thymidine incorporation assay. The average value of the replicates in each group is given as multiple of the average value of the control group immunized with OVA alone. The error bars represent the SEM of three independent experiments where four or five animals per group were used; n. s. indicates non-significant.

3.5.4 Sting but not IFNAR is crucial for the c-di-AMP-mediated enhancement of Th1, Th2 and Th17 responses

To characterize the role played by the type I IFN pathways in the c-di-AMP-mediated enhancement of Th immune responses, the well accepted indicators of Th1 (IFN-γ, IL-2) or Th2 (IL-4) activity were determined. To this end, the production of cytokines by OVA-re-stimulated spleen cells obtained from wt mice and animals lacking functional Sting or IFNAR was measured using ELISPOT post immunization. The c-di-AMP-mediated enhancement in the numbers of IFN-γ, IL-2 and IL-4-producing cells observed in wt animals was lost in samples derived from *Sting*$^{Gt/Gt}$ mice **(figure 27, left panel).** In contrast, the results obtained in IFNAR$^{-/-}$ animals immunized with OVA and c-di-AMP showed a clear trend of higher numbers of IFN-γ, IL-2 and IL-4-secreting cells as compared to samples from wt mice **(figure 27, right panel)**.

Additional studies were performed to assess the production of selected cytokines in the CD4$^+$ T cell subset. To this end, intracellular staining of OVA-re-stimulated splenocytes was performed to evaluate the production of IL-17 and TNF-α in CD3$^+$/CD4$^+$ cells using flow cytometry. The c-di-AMP-mediated enhancement in the frequency of IL-17 positive cells within the CD3$^+$/CD4$^+$ cell fraction observed in wt mice was abolished in the samples obtained from *Sting*$^{Gt/Gt}$ animals, while it was preserved in IFNAR$^{-/-}$ mice-derived samples **(figure 28 A)**. Similarly to what was observed for the IFN-γ, IL-2 and IL-4 cytokine responses in the ELISPOT assay **(figure 27, right panel)**, in samples from

IFNAR$^{-/-}$ mice immunized with OVA and c-di-AMP a clear trend of higher frequency of IL-17-producing cells was observed when compared to samples derived from wt animals **(figure 28 A)**. The c-di-AMP-mediated enhancement in the frequency of TNF-α positive cells within the CD3^{+}/CD4^{+} cell fraction observed in wt mice was abolished in the samples derived from *Sting*$^{Gt/Gt}$ animals, whereas similar responses were detected in wt and IFNAR$^{-/-}$ animals **(figure 28 B)**.

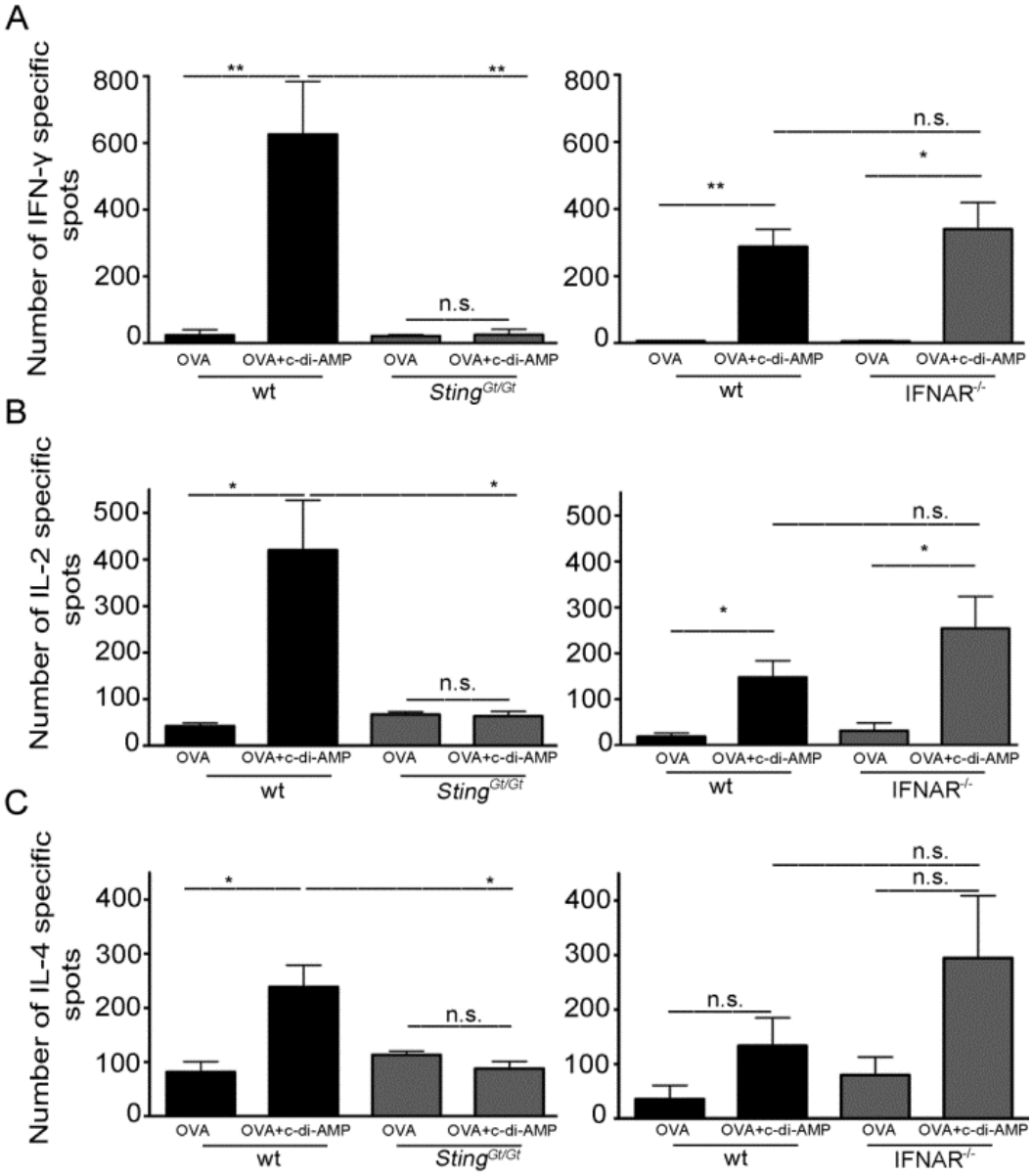

Figure 27: The c-di-AMP-mediated enhancement of IFN-γ, IL-2 and IL-4 responses is lost in *Sting*$^{Gt/Gt}$ but not in IFNAR$^{-/-}$ mice. Spleen cells from mice immunized with OVA alone or co-administered with c-di-AMP were re-stimulated with OVA and analyzed for specific cytokine production: IFN-γ (A), IL-2 (B) and IL-4 (C) using the ELISPOT assay. The results are expressed as average number of spots per 10^6 cells. The error bars represent the SEM of four (*Sting*$^{Gt/Gt}$) or three (IFNAR$^{-/-}$) independent experiments where four or five animals per group were used. Statistical differences are indicated by * for $p<0.05$, ** for $p<0.01$, whereas n. s. indicates non-significant.

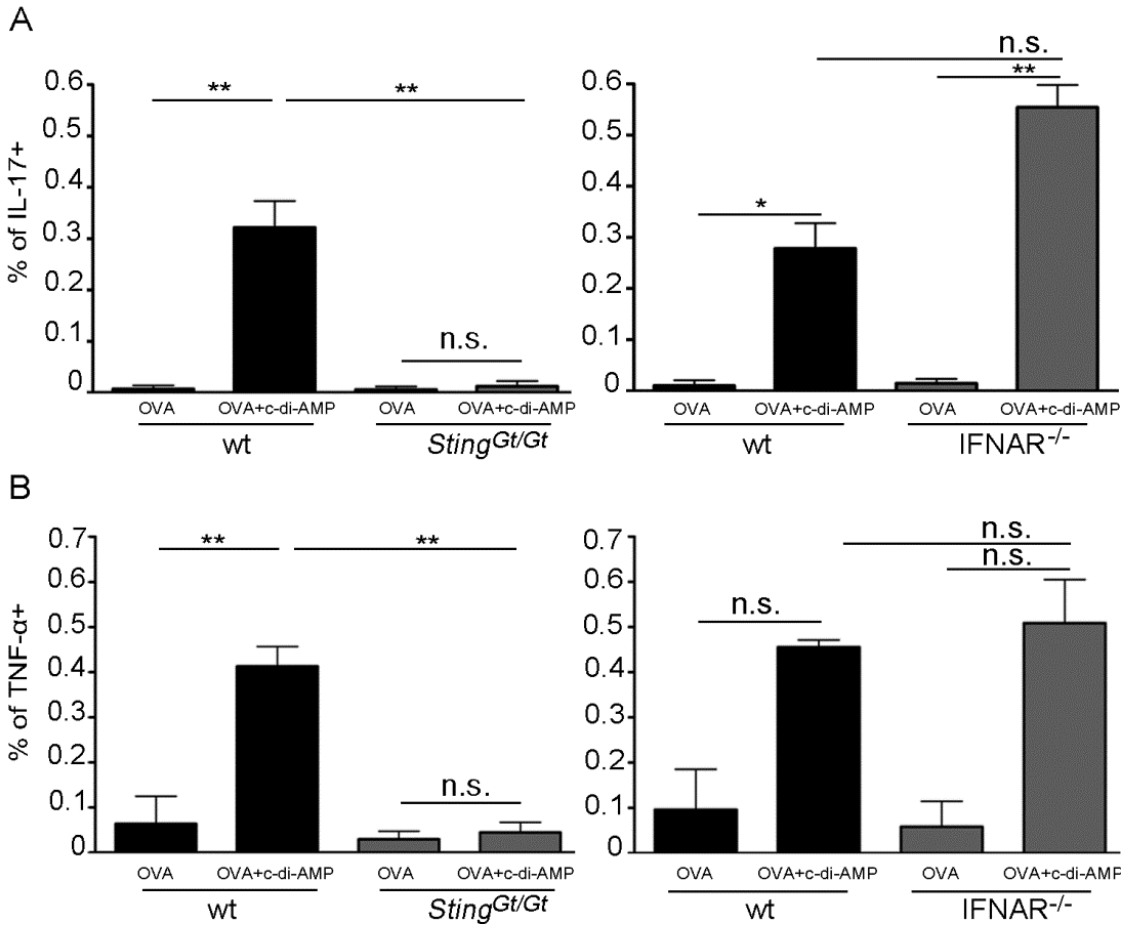

Figure 28: The c-di-AMP-mediated enhancement of IL-17 and TNF-α production is lost in *Sting*$^{Gt/Gt}$ but not in IFNAR$^{-/-}$ mice. Mice were immunized with OVA alone or co-administered with c-di-AMP. Spleen cells of the immunized mice were re-stimulated with OVA and analysed for the production of IL-17 (A) and TNF-α (B) by flow cytometry. Plots show the percentage of cells with intracellular fluorescent signals indicating the presence of IL-17 or TNF-α within gated CD3$^+$/CD4$^+$ cells. Error bars represent SEM of three (*Sting*$^{Gt/Gt}$) or two (IFNAR$^{-/-}$) independent experiments where four or five animals per group were used. Statistical differences are indicated by * for $p<0.05$ and ** for $p<0.01$, whereas n. s. indicates non-significant.

3.5.5 The role of Sting and IFNAR in the adjuvantictiy of cGAMP

To address the role played by the type I IFN pathways on the cGAMP-mediated enhancement of the adaptive immune responses, immunization experiments were performed in mice lacking a functional Sting or IFNAR. Animals were immunized with OVA or OVA co-administered with cGAMP and the immune responses were assessed according to the description given in **figure 10**. The data shown here represent three independent experiments in which the immune responses were compared in wt and *Sting*$^{Gt/Gt}$ animals, and one experiment in which responses in wt and IFNAR$^{-/-}$ animals were assessed. Each experiment contained four or five animals per group.

3.5.5.1 Sting is essential for cGAMP-mediated enhancement of antigen-specific IgG responses

To assess the impact of the type I IFN pathways on the cGAMP-mediated enhancement of humoral immune responses, OVA-specific IgG titers were determined in sera of immunized mice by ELISA. Average titer per experimental group was calculated and results were expressed as fold of the response detected in animals immunized with OVA alone. The obtained results demonstrated that, as observed for c-di-AMP, cGAMP-mediated enhancement of OVA-specific IgG response was lost in *Sting*$^{Gt/Gt}$ mice **(figure 29)**.

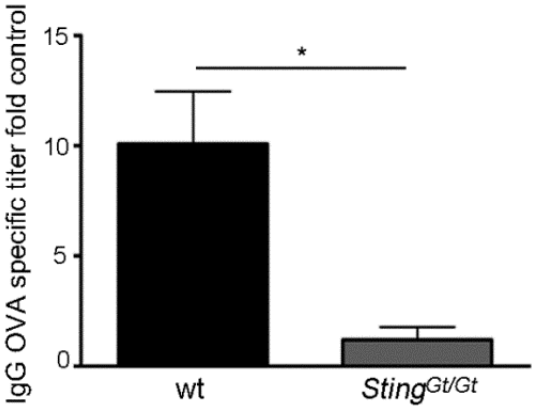

Figure 29: cGAMP enhances antigen-specific IgG responses in wt, but not in *Sting*$^{Gt/Gt}$ mice. Mice were immunized with OVA alone or OVA co-administered with cGAMP. Serum samples were then analyzed by ELISA for the presence of OVA-specific total IgG. Titers were defined as the dilution factor of the assay sample with more than twice the readout value of the blank (absorbance of light of 405 nm wavelength). The average titer value in each group is given as a multiple of the value in the control group in which mice were immunized with OVA alone. Results representing the response in wt vs. *Sting*$^{Gt/Gt}$ are shown. The error bars represent the SEM of three independent experiments where four or five animals per group were used. Statistical difference is indicated by * for $p<0.05$.

Subsequently, the immune responses were evaluated in IFNAR$^{-/-}$ mice. A preliminary experiment with four animals per group suggested that cGAMP-mediated enhancement of the OVA-specific IgG response in IFNAR$^{-/-}$ animals was slightly reduced when compared to that observed in wt animals **(figure 30)**. However, it was also clear that there is a residual retained adjuvanticity. Thus, it seems that type I IFN signaling contributes to some extent to the adjuvant activity of cGAMP.

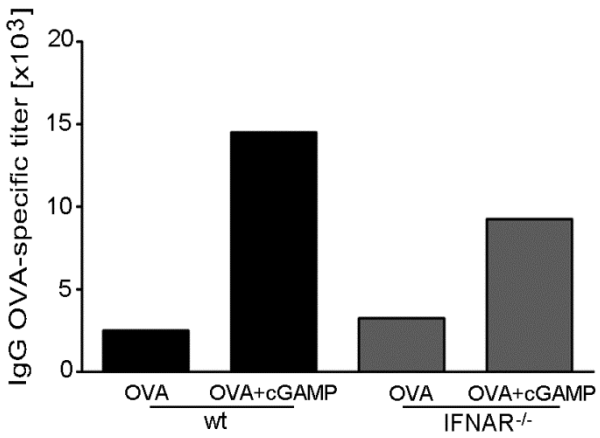

Figure 30: Antigen-specific IgG responses in wt and IFNAR$^{-/-}$ mice immunized with OVA alone or in a combination with cGAMP. Serum samples were analyzed by ELISA. For OVA-specific total IgG the titer was defined as the dilution factor of the assay sample with more than twice the readout value of the blank (absorbance of light of 405 nm wavelength). The average titer values of samples from individual animals are represented as columns. In the experiment were used four animals per group.

3.5.5.2 Sting is essential for cGAMP-mediated enhancement of Th1, Th2 and Th17 responses

Next, the indicators of Th1 (IFN-γ, IL-2), Th2 (IL-4) and Th17 (IL-17) activity were measured to assess the dependency of the cGAMP-mediated enhancement of Th responses on functional components of the type I IFN pathways. Thus, the production of cytokines by OVA-re-stimulated spleen cells from immunized wt mice and animals lacking functional Sting or IFNAR was measured using ELISPOT. The cGAMP-mediated enhancement in numbers of IFN-γ, IL-2, IL-4 and IL-17-producing cells observed in wt mice was lost in samples derived from *Sting*$^{Gt/Gt}$ animals **(figure 31)**. According to the results of the preliminary experiment using IFNAR$^{-/-}$ animals, cGAMP-mediated enhancement in numbers of IL-2, IL-4 and IL-17 producing cells seem to be preserved **(figure 32 B-D)**, whereas the number of IFN-γ producing cells was reduced as compared to the values observed in wt animals **(figure 32 A)**. This suggests that cGAMP-mediated activation of type I IFN contributes to Th1 polarization.

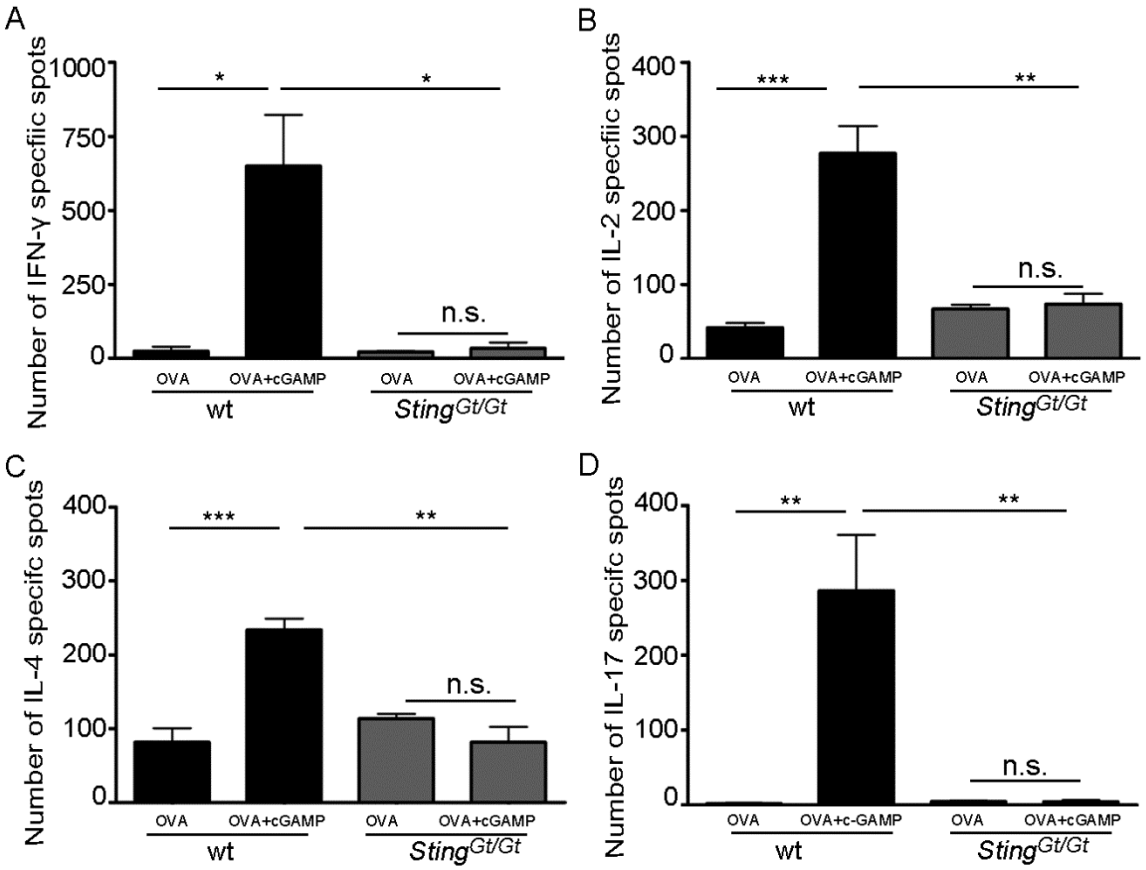

Figure 31: cGAMP enhances IFN-γ, IL-2, IL-4 and IL-17 production by OVA-re-stimulated spleen cells from immunized wt, but not *Sting*$^{Gt/Gt}$ mice. Spleen cells from mice immunized with OVA alone or co-administered with cGAMP were re-stimulated with OVA and analyzed for specific cytokine production: IFN-γ (A), IL-2 (B), IL-4 (C) and IL-17 (D) using the ELISPOT assay. The average number of spots is given for 10^6 cells. The error bars represent the SEM of four independent experiments where five animals per group were used. Statistical differences are indicated by * for $p<0.05$, ** for $p<0.01$, *** for $p<0.001$, whereas n. s. indicates non-significant.

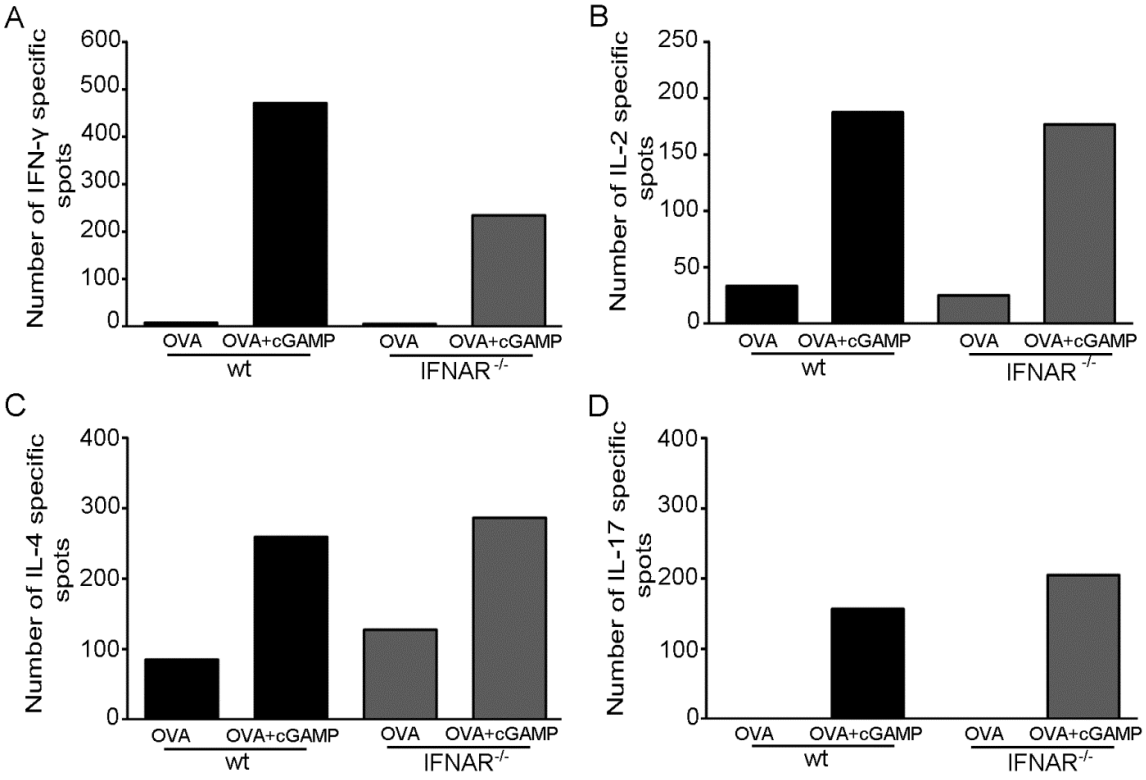

Figure 32: IFN-γ, IL-2, IL-4 and IL-17 production by OVA-re-stimulated spleen cells from wt and IFNAR$^{-/-}$ animals immunized with OVA alone or in a combination with cGAMP. Spleen cells from immunized mice were re-stimulated with OVA and analyzed for cytokine production: IFN-γ (A), IL-2 (B), IL-4 (C) and IL-17 (D) using the ELISPOT assay. The average number of spots is given for 10^6 cells. The columns represent average value of triplicates in one preliminary experiment where four animals per group were used.

4 DISCUSSION

The major objectives of this thesis were to: i) evaluate the adjuvant properties of cGAMP, ii) compare the immune modulatory properties of c-di-AMP and cGAMP and iii) investigate the role played by type I IFN induction and signaling pathways in the adjuvanticity of c-di-AMP and cGAMP. These questions were answered by performing *in vivo* immunization studies, where the model antigen OVA was applied by i.n. route alone or co-administered with CDN to wt mice or animals lacking functional Sting or IFNAR. After the completion of the immunization schedule, OVA-specific humoral and cellular responses were characterized. In addition, *in vitro* studies using BMDCs were performed to identify the parameters indicative for c-di-AMP and cGAMP immune stimulatory activity.

4.1 cGAMP is a potent candidate mucosal adjuvant able to evoke balanced humoral and cellular immune responses

In this thesis it was asked if cGAMP has immune modulatory properties when used as adjuvant. Immunization experiments were performed in which the model antigen OVA was administered alone or together with cGAMP to mice and the resulting adaptive immune responses were evaluated. Collectively, these data demonstrate the potency of cGAMP to enhance antigen-specific humoral and Th1/Th2/Th17 responses **(figure 11-13)**.

The increased production of specific IgA and IgG in animals treated with OVA and cGAMP as compared to mice receiving OVA alone **(figure 11)** demonstrates the adjuvant properties of cGAMP in terms of evoking enhanced antigen-specific humoral responses at mucosal and systemic levels. Production of secretory IgA is a hallmark of adaptive mucosal immunity and its ability to block the colonization of mucosal surfaces by pathogens contributes to prevent infections. Therefore, the ability of cGAMP to enhance the production of antigen-specific IgA suggests it as a promising tool to promote local protection at the mucosa. Re-stimulated spleen cells from animals immunized with OVA combined with cGAMP showed enhanced antigen-specific proliferation capacity **(figure 12)**, indicating that the incorporation of cGAMP into the immunization formulation can also potentiate cellular immune responses. Additional studies showed that the production of IFN-γ and IL-2 (indicators of Th1 response), IL-4 (indicator of Th2 response) and IL-17 (indicator of Th17 response) was also improved in

re-stimulated spleen cells from animals that received OVA and cGAMP **(figure 13)**. This demonstrates the ability of cGAMP to act as an enhancer of balanced Th1/Th2/Th17 responses. Th2 cell activity is known to promote Ig class switch in B cells to produce IgG1, whereas Th1 cell activity promotes Ig class switch leading to IgG2c production. Thus, the enhanced production of cytokines indicative for Th1 and Th2 responses is in agreement with the observed increment of IgG2c and IgG1 production in animals immunized with OVA and cGAMP **(figure 11 B-C)**. The model antigen OVA is described as a week immunogen [154], thereby mimicking the poor immunogenicity of antigens incorporated in subunit vaccines. Here, it was demonstrated that co-administration of cGAMP with OVA promotes a strong enhancement of OVA-specific humoral and cellular immune responses, suggesting its use as a valid candidate adjuvant for subunit vaccines. The desired vaccine-evoked immune response highly depends on the pathogen´s life style. Currently available vaccines promote a polarized humoral immune response that is sufficient to fight only some of the pathogens. For example, a vaccine-evoked long lasting humoral response sustained by Th2 cells is closely related to the protection against extracellular pathogens, such as *Corynebacterum diphteriae*, *Clostridium tetani* and *Bordetella pertussis* [155]. However, an immune response profile based only on antibody production is suboptimal in fighting pathogens that are not accessible to antibodies or in cases when both, antibody and cellular responses, such as Th17 [156-159] are required. The described cGAMP-mediated humoral and Th17 responses suggest a possible application of cGAMP in the development of vaccines against pathogens that need antibodies and Th17 responses to be fought, such as pneumococci [156]. To protect the host from intracellular pathogens hidden from antibodies inside of invaded cells, CTL activity is required (*e.g. M. tuberculosis*, *S. typhimurium*, *T. gondii,* human immunodeficiency virus). CTL development depends on the Th1 response. Therefore, the potency of cGAMP to enhance the Th1 response suggests its application in vaccines to fight intracellular pathogens. In addition to the demonstrated *in vivo* adjuvant efficacy of cGAMP in mice, its potency to activate human dendritic cells was reported [140]. This further supports the potential of cGAMP as a candidate adjuvant for human vaccines.

The cGAMP used in the studies presented in this thesis is a bacterial (3´,5´) isomer of the (2´, 5´)-cGAMP that is present in the cytosol of mammalian cells. The results presented here demonstrate that cGAMP can act as a PAMP, when administered extracellularly. For the (2´, 5´)-cGAMP Li *et al.* showed in a short term immunization experiment that intramuscular immunization of mice with OVA co-administered with

(2´,5´)-cGAMP enhanced the production of antigen-specific IgG1 in serum and IFN-γ and IL-2 by re-stimulated spleen cells, indicating its immune modulatory potential [160]. So far, the only known signaling axis that includes (2´,5´)-cGAMP is dsDNA-triggered cGAS-mediated (2´,5´)-cGAMP production that results in Sting-dependent IFN-β up-regulation [17, 18, 33-36]. Now, it is evident that even extracellular application of the cGAMP or (2´,5´)-cGAMP modulates the immune response. However, it is not known to which extent IFN-β is involved and what other pathways possibly contribute to their adjuvanticity. In this regard, it would be interesting to evaluate if the adjuvanticity of cGAMP and (2´,5´)-cGAMP rely on the same mechanisms, as well as to evaluate if there are any differences in terms of the molecular mode of action with respect to c-di-AMP and c-di-GMP (further discussed in the chapter 4.3).

4.2 The c-di-AMP and cGAMP exhibit different effector functions, rendering them as potential tools for fine-tuning immune responses following vaccination

Immunization experiments using OVA as a model antigen and c-di-AMP or cGAMP as adjuvants were further conducted in mice in order to explore the potential of the candidate adjuvants as tools for evoking differential immune responses. The data generated demonstrate that c-di-AMP is a more robust candidate adjuvant than cGAMP. In fact, slightly stronger humoral and Th1/Th2 responses were observed when using c-di-AMP as adjuvant as compared to those observed in mice receiving cGAMP **(figures 14-17)**. In addition, c-di-AMP also exhibits a significantly higher potency to enhance Th17 responses than cGAMP.

OVA-specific humoral immune responses of the immunized animals were quantified as titers of IgA and IgG. The incorporation of c-di-AMP or cGAMP in the immunization formulation resulted in enhanced titers of OVA-specific mucosal IgA and systemic IgG and its subclasses IgG1 and IgG2c (**figure 14)**, although slightly higher titers were obtained when using c-di-AMP. The proliferation capacity of antigen-re-stimulated spleen cells was also enhanced by both, c-di-AMP and cGAMP **(figure 15)**. The same was true for the numbers of antigen-specific cells producing IFN-γ and IL-2 (indicative for the Th1 cell phenotype) and IL-4 (indicative for the Th2 cell phenotype) **(figure 16 A-C)**. However, also here a trend can be observed for slightly superior responses, although statistically non-significant, in animals receiving c-di-AMP as adjuvant. Th1

activity promotes the development of a CTL response that is important to fight intracellular pathogens. Both, c-di-AMP and cGAMP enhance Th1 responses **(Figure 16 A-B)**, suggesting their use in vaccines fighting intracellular pathogens, which is barely achievable with currently available alum-containing vaccines [161].

The analysis of the IL-17 responses in immunized animals revealed that c-di-AMP is a more potent enhancer of Th17 responses than cGAMP **(figure 16 D, 17)**. IL-17 signaling can modulate Th1 responses [162] and mucosal immunity. It upregulates polymeric Ig receptor levels in mucosal epithelia [163] and promotes B-cell differentiation into IgA-secreting cells [164]. Interestingly, only minimal differences were observed in the Th1 and IgA responses promoted by c-di-AMP and cGAMP. This suggests that under our experimental conditions Th1 profiles and mucosal IgA responses do not depend on IL-17. One of the general goals of vaccination is to promote effector mechanisms leading to an efficient protective response without evoking mechanisms leading to potential adverse effects. This is a quite challenging task because the induction of the wrong Th profile in a particular context can lead to severe health problems. For example, a Th17 response seems to be required for vaccine-mediated protection against some pathogens (*e.g. Pseudomonas aeruginosa, M. tuberculosis* and *S. pneumonia*) [156, 159, 165-167]. However, a deregulated IL-17 production is responsible for immune pathology in chronic inflammatory and autoimmune diseases [168-170]. In this regard, arthritis is an IL-17-linked autoimmune disease that can develop after immunization and challenge with *Borrelia burgdorferi* in mice [171]. Furthermore, IL-17 production is related to the maintenance of encephalomyelitis in a murine model [172]. Thus, to minimize the health risks related to unnecessary induction of IL-17, cGAMP could be used in vaccine formulations for the pathogens where a strong Th17 response is not really needed, whereas c-di-AMP would be beneficial for the formulations against pathogens where it is needed for optimal host protection.

An important aspect of vaccine development is to reduce the risk of failure of candidate vaccines in late stages of clinical trials. Elucidation of the signaling network mediating the immune stimulatory effects of CDNs may facilitate the prediction of their safety profile and efficacy in humans. As a precondition to investigate the molecular mechanisms of their action, it is necessary to identify parameters indicative for CDN activity *in vitro*. Strong up-regulation of the surface expression of MHC class II and CD86, and induction of type I IFNs and IL-12/IL-23p40 expression in BMDCs after treatment with CDNs qualify these parameters and BMDCs as a suitable system for *in*

vitro investigation of CDNs **(figure 19-22)**. The identified markers of CDN activity can be used as readouts in future studies using specific inhibitors, allowing identification of molecular pathways triggered by CDNs. In the studies presented here, the treatment of BMDCs with CDNs did not result in IL-6 production **(figure 20 A, upper panel)**. This could be explained by two main reasons: i) IL-6 expression is not affected by the treatment of BMDCs with CDNs or ii) the applied experimental strategy was suboptimal for IL-6 detection. Kinetic analysis of IL-6 induction by CDNs would allow verifying if IL-6 is produced at an earlier time point than 16 h upon treatment, time at which the inhibitors of secretion were added to the cells. On the other hand, c-di-AMP was identified as a more potent inducer of IL-12/IL-23p40 expression in BMDCs than cGAMP **(figure 21, 20 A, lower panel)**. The p40 is a common protein subunit shared by IL-23 (p19p40) and IL-12 (p35p40) [173]. The used detection antibody against p40 does not allow distinction between IL-23 and IL-12. Therefore, the observed differences in IL-12/IL-23p40 expression by BMDCs after treatment with c-di-AMP and cGAMP cannot be exclusively attributed to either of these cytokines. Distinction between the two cytokines could be achieved by simultaneous detection of the p19 or p35 with the p40 subunit. However, flow cytometry assays allowing a reliable distinction between the IL-12 and IL-23 based on simultaneous detection of p19 or p35 with p40 need to be developed. Studies focused on specific detection of IL-12 and IL-23 mRNA may clarify which cytokine is affected by CDN treatments. The p40 can be present in a form of monomers or dimers and their ratio determines the bioactivity of IL-12 [174]. The p40 homodimer acts as a suppressor of IL-12 activity. IL-12 is a Th1 phenotype-promoting cytokine [175]. The results presented here **(figure 14 C, 16 A-B)** do not indicate strong differences in the capacity of c-di-AMP and cGAMP to enhance Th1 responses, as measured by the increase in IgG2c titers and the number of IFN-γ and IL-2 producing cells. Therefore, if it turns out that c-di-AMP and cGAMP differentially induce the IL-12 production further experiments will be needed to identify an immune response branch, other than Th1, that may be affected by the CDN-triggered production of IL-12. On the other hand, IL-23 seems to be important for the maintenance of Th17 response [68, 69]. Therefore, if the studies show that c-di-AMP and cGAMP can differentially affect IL-23 production by BMDCs, this could point to the underlying molecular mechanism for differential enhancement of Th17 responses observed *in vivo*.

Taken together, evoking balanced humoral and cellular responses with a fine-tuned level of IL-17 production is important for fighting many pathogens, but it is barely achievable with currently approved adjuvants. The results shown in this thesis indicate

c-di-AMP and cGAMP as a possible solution for this problem because both of them promote humoral and Th1/Th2 responses at similar and Th17 response at different levels. Therefore, depending on the need for a robust Th17 response, one could use c-di-AMP or cGAMP in vaccines. The identified parameters indicative for the c-di-AMP and cGAMP activity *in vitro* are crucial for further exploration of the pathways responsible for their adjuvanticity. To this end: i) specific indicators of the c-di-AMP or cGAMP activity *in vitro* can be used as readouts for elucidation the molecular cascade(s) triggered by CDNs resulting in up-regulation of a specific indicator or ii) *in vivo* studies using ko models can be applied to address if a specific indicator of the c-di-AMP or cGAMP activity *in vitro* is actually relevant for their efficacy as adjuvants. In this thesis, *in vivo* studies were conducted to address the relevance of type I IFN induction and signaling pathways for the adjuvanticity of c-di-AMP and cGAMP.

4.3 Sting is essential for the adjuvanticity of c-di-AMP and cGAMP

To address if the activation of type I IFN induction and signaling pathways was required for the adjuvant activities of c-di-AMP and cGAMP, immunization experiments were performed using mice lacking functional Sting or IFNAR. The data characterizing the humoral and cellular immune responses enhanced by the two candidate adjuvants shows that Sting is required for the adjuvanticity of c-di-AMP **(figure 25-28)** and cGAMP **(figure 29, 31)**. In contrast, IFNAR signaling seems to be dispensable for the adjuvanticity of c-di-AMP **(figure 25-28)** and, to some extent, also for cGAMP **(figure 30, 32)**.

Th cells are central players of the adaptive immunity. The c-di-AMP-mediated enhancement in the production of Th1, Th2 and Th17 cytokines was significantly impaired in *Sting*$^{Gt/Gt}$ animals, whereas it was preserved in animals lacking functional IFNAR signaling **(figure 27, 28 A)**. Similarly, cGAMP-mediated enhancement of Th1, Th2 and Th17 responses was impaired in *Sting*$^{Gt/Gt}$ animals **(figure 31)**. Preliminary experiments using cGAMP suggested that enhanced IL-2, IL-4 and IL-17 responses are preserved in IFNAR$^{-/-}$ animals, whereas IFN-γ is reduced **(figure 32)**. For c-di-GMP, Blaauboer *et al.* reported that enhanced humoral as well as Th responses were abolished in *Sting*$^{Gt/Gt}$ mice, whereas in IFNAR$^{-/-}$ mice they were enhanced to the same extent as those observed in wt animals [147].

Interestingly, IFNAR$^{-/-}$ animals immunized with the antigen co-administered with c-di-AMP have increased numbers of IL-4-producing T cells as compared to wt mice **(figure 27 C)**. This suggests an enhanced c-di-AMP-mediated Th2 activity in the absence of IFNAR signaling. This is in agreement with studies from Huber *et al.* describing type I IFN as a suppressor of Th2 responses, one of the major factors shaping the development of neutralizing antibodies [176]. Furthermore, a tendency of enhanced production of the Th1 indicators IL-2 and IFN-γ by IFNAR$^{-/-}$ animals was observed, whereas the TNF-α induction was the same as in wt animals immunized with the antigen and c-di-AMP **(figure 27 A-B, 28 B)**. A trend of enhanced c-di-AMP-mediated Th17 response in IFNAR$^{-/-}$ animals was also observed in comparison to wt animals **(figure 28 A)**. This could be due to an IFNAR-mediated suppression of the Th17 response, previously reported by Guo *et al.* [177]. Interestingly, no tendency towards an enhanced c-di-GMP-mediated Th1, Th2 and Th17 responses was observed in IFNAR$^{-/-}$ animals, when compared to responses in wt mice, as reported by Blaauboer *et al.* [147]. The same seems to be true for cGAMP in the preliminary experiment shown in **figure 32**. In fact, it also seems that the expansion of IFN-γ-producing cells is partially impaired in IFNAR$^{-/-}$ mice immunized using cGAMP as adjuvant. Therefore, the enhanced production of Th cytokines in the absence of IFNAR signaling seems to be a unique feature of c-di-AMP-adjuvanted immune responses.

Several reports described the potential of type I IFNs as enhancers of neutralizing antibody development [178-181]. Here, the c-di-AMP mediated enhancement of the systemic antigen-specific IgG response was dependent on Sting, but not on IFNAR **(figure 25)**. This result resembles the phenotype previously published [147], describing the lack of Sting as severely impairing the humoral responses enhanced by c-di-AMP. IL-4 production is a hallmark of Th2 activity which promotes the humoral response. Interestingly, a trend of enhanced c-di-AMP-mediated IgG response in IFNAR$^{-/-}$ animals was not observed when compared to wt mice, despite the fact that the enhanced number of IL-4-producing cells in IFNAR$^{-/-}$ mice was higher than that in wt animals **(figure 27 C)**.

In the preliminary experiment using cGAMP, Th2 and Th17 responses in IFNAR$^{-/-}$ animals were enhanced by cGAMP to a similar extent to those observed in wt animals (**figure 32 C-D)**. In contrast, the Th1 response was partially impaired, as indicated by a reduced IFN-γ production **(figure 32 A)**. The IgG titers were also lower in IFNAR$^{-/-}$ animals immunized with OVA and cGAMP than in wt animals **(figure 30)**. Therefore, it

seems that IFNAR might be required for cGAMP-mediated enhancement of IgG and Th1 responses. Similarly, in a short term immunization experiment using eukaryotic (2´,5´)-cGAMP, Li *et al.* reported significantly impaired IgG1 response in *Sting*$^{Gt/Gt}$ mice and reduced response in IFNAR$^{-/-}$ animals as compared to the response observed in wt animals [160]. Taken together, this data suggests that IFNAR-mediated signaling may differentially modulate the immune response profiles according to the specific CDN: down-regulation of c-di-AMP-mediated Th responses and the promotion of c-GAMP-mediated IgG and IFN-γ production.

Taken together, obtained results demonstrated that Sting is a crucial mediator of the adjuvanticity of c-di-AMP and cGAMP, suggesting that in this process Sting functions beyond its ability of inducing the production of type I IFNs. Although IFNAR is in part dispensable, IFNAR-mediated signaling seems to modulate the extent of c-di-AMP- and cGAMP-mediated enhancement of immune responses. The exact mechanisms of this modulation remain to be elucidated. Based on these findings and currently available knowledge on the stimulation of immune responses via the mucosa, a model of the c-di-AMP-mediated stimulation of immune responses following i.n. administration is proposed in **figure 33**. First, the antigen and c-di-AMP administered into the nasal cavity are transported from the apical to the basolateral side of the mucosal epithelium to reach the APCs which are part of the NALT. Most likely, this transport is done via M cell-mediated transcytosis. Then, OVA is internalized by APCs, processed and its peptides are presented on their surface in the context of MHC class II molecules that will allow the activation of OVA-specific T and B cells. Simultaneously, c-di-AMP triggers signals that lead to enhanced OVA-specific antibody production and Th1/Th2/Th17 cell development, characterized as a balanced immune response. This response is completely dependent on c-di-AMP-triggered activation of Sting, which is located in the membrane of ER. This implies that c-di-AMP has to be delivered to the cytosol of APCs, but does not exclude its potential to trigger signaling as well from the surface of APCs. It is not clear if c-di-AMP activates Sting by direct binding or indirectly. The presence of c-di-AMP also results in an enhanced surface expression of MHC class II, CD86 and CD80. This in turn, boosts the power of APCs to activate the naïve T and B cells present locally in the NALT. APCs also migrate to regional lymph nodes where they can cross-talk and activate naïve T and B cells. These initial events lead to the initiation of a balanced adaptive immune response, strongly dependent on Sting, but to a large extent independent of the biological activities of type I IFN.

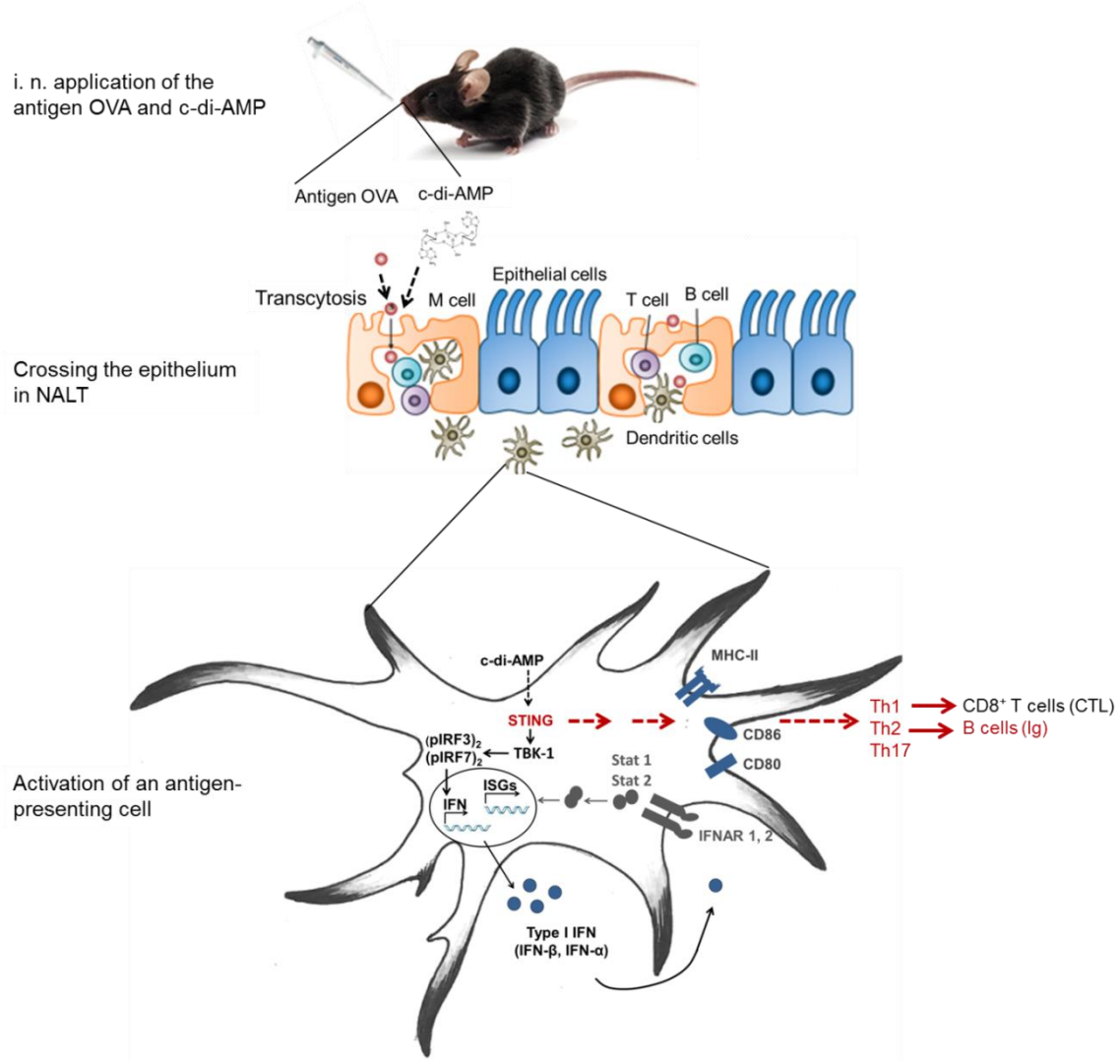

Figure 33: A model of the c-di-AMP-mediated enhancement of OVA-specific immune responses. Mice immunized by i.n. route with OVA co-administered with c-di-AMP as adjuvant develop enhanced adaptive immune responses (*i.e.* antibody production, Th1, Th2, Th17). OVA and c-di-AMP are administered into the nasal cavity of a mouse and have to cross the epithelium in the NALT from the apical side to the basolateral side (transcytosis) to reach APCs. APCs process OVA and c-di-AMP enhances their power to promote an OVA-specific immune response. The c-di-AMP-mediated activation of APCs is Sting-dependent and IFNAR-independent. The Th1 response promotes the development of cytotoxic T lymphocytes (CTL). Th2 response promotes the activation of B cells and production of protective antibodies (Ig). The picture of the mouse and the graphics of the NALT epithelium are adapted from [150] and [108], respectively.

Starting from the idea that IFN type I acts predominantly at the innate level to fight pathogens, it would be dispensable in a vaccination situation, when the goal is to build up an adaptive immune protection against a future encounter of a specific pathogen rather than evoking, for example, a direct antiviral response. However, the conclusions on the role of IFNAR-mediated signaling in the adjuvanticity of c-di-AMP presented in this thesis are based on measurements of humoral responses and Th cell activity.

The role of IFNAR in the c-di-AMP-mediated induction of long term memory and enhancement of a cytotoxic $CD8^+$ T cell response remains to be explored. Type I IFN may indirectly contribute to $CD8^+$ T cell priming. Archer *et al.* suggested that type I IFN suppresses *L. monocytogenes*-specific $CD8^+$ T cell priming via unknown mediators [146]. On the other hand, Zhang *et al.* suggested that the role of type I IFN in the development of a $CD8^+$ memory phenotype is mediated by IL-15 [182]. In this regard, it would be interesting to compare the potency of c-di-AMP to induce IL-15 secretion by APCs and to perform measurements of CTL activity in wt and $IFNAR^{-/-}$ animals to test if IFNAR is involved in c-di-AMP-mediated stimulation of CTL responses.

It has been described that Sting can activate IRF3 and/or NF-κB in a TBK-1-dependent manner, thereby resulting in IFN-β and/or TNF-α production [183]. This is in addition to its capacity to trigger ERK activation, as reported by Jin *et al.* [26]. Blaauboer *et al.* described that the non-canonical NF-κB activation by Sting results in TNF-α production [147]. This in turn acts via the tumor necrosis factor receptor (TNFR)1, being the critical mediator for the mucosal adjuvanticity of c-di-GMP and the IgG responses enhanced by c-di-AMP. However, the preserved enhancement of Th17 responses and the residual Th1, Th2 and humoral responses observed in $TNFR1^{-/-}$ animals suggest that molecular pathways functioning as mediators of the adjuvanticity of c-di-GMP cannot not be restricted to the alternative NF-κB-TNF-α pathway.

Negative [28, 30, 31, 184] and positive [29] regulators of Sting activity have been described. Some of them even differentially affect the ability of Sting to trigger IFN-β or TNF-α production [185], indicating that Sting activation may result in different cytokine profiles due to its regulation. In this thesis it was reported that the Th17 response is differentially enhanced by c-di-AMP and cGAMP **(figure 16 D, 17)** and Sting is critical for their ability to enhance Th17 responses **(figure 28 A, 31 D)**. Therefore, it would be interesting to explore if the differential enhancement of the Th17 response is a result of c-di-AMP and cGAMP interactions with different regulators of Sting.

4.4 Sting as a central molecule mediating the CDN immune stimulatory activity

Overstimulation of Sting can result in a chronic inflammatory state and the development of autoimmune diseases [186, 187]. For example, accumulation of non-processed DNA from apoptotic cells results in Sting-dependent overproduction of type I IFNs [186-189].

The c-di-AMP has been shown to induce IFN-β locally in the area of application and not systemically [153]. In addition, Sting is down-regulated after CDN treatment of APCs (Rueckert, unpublished data). Both observations may point to mechanisms ensuring host homeostasis and preventing the overproduction of inflammatory cytokines.

Translation of the findings related to Sting signaling from mouse to humans can be hampered by different sequences of human and murine Sting. For example, therapeutics acting via Sting, such as the antiviral drug CMA (10-carboxymethyl-9-acridanone) [190, 191] and the cancer therapeutic DMXAA (5,6-Dimetylxanthenone-4-acetic acid) [192] were successfully developed in murine models, but failed in human trials due to inability of binding to human Sting. However, it has been shown that c-di-AMP and cGAMP are able to activate human dendritic cells, implying their potential use in human vaccines [140, 153]. However, isoforms of human Sting with differential responsiveness to CDNs have been identified [193]. The prevalence of specific Sting haplotypes seems to be related to different ethnical backgrounds of individuals, as reported in a study where haplotypes of 1090 individuals were analyzed [193]. Therefore, it has to be expected that the responsiveness to CDN-adjuvanted vaccines in specific geographical regions would be defined by the frequency of prevalent Sting haplotypes. For example, Yi *et al.* showed that in the group of individuals with European ethnical background alleles encoding CDN-responsive Sting are prevalent, whereas the frequency of the allele encoding the isoform not responding to CDN is around 15% [193]. Similar frequency of non-responding Sting isoform was observed in the group of individuals with African background, indicating the percentage of the population that probably would not respond to CDN-adjuvanted vaccines. Therefore, to ensure the protection throughout the population, alternative vaccination approaches would be needed to induce protective immune responses in individuals not being able to respond to CDN-containing vaccines. Alternatively, medicinal chemistry can be exploited to generate CDN derivatives able to stimulate all Sting isoforms.

5 CONCLUSIONS AND OUTLOOK

The design of effective subunit vaccines requires availability of adjuvants capable of promoting humoral and cellular immune responses, not only systemically but also at the mucosal level. In this thesis it was demonstrated that the administration of cGAMP by i.n. route with the model antigen OVA to mice results in enhanced antigen-specific humoral responses at both systemic and mucosal level, as indicated by increased titers of serum IgG and mucosal IgA. In addition, it was observed an enhanced proliferation of splenocytes, as well as increment in the number of IFN-γ, IL-2, IL-4 and IL-17 producing cells. This, in turn indicates the capacity of cGAMP to induce balanced Th1/Th2/Th17 responses. These findings suggest that cGAMP is a promising candidate adjuvant for the design of mucosal subunit vaccines.

The adjuvant properties of c-di-AMP and cGAMP were then compared in mice. The obtained results showed that c-di-AMP is a more potent Th17 enhancer than cGAMP, whereas humoral and cellular responses were enhanced to a similar extent by the two CDNs. Collectively, these findings suggest that c-di-AMP and cGAMP can be used as tools for fine-tuning the Th17 responses, according to the specific clinical needs. For example, Th17 responses seem to be required for achieving efficient protection against pathogens such as *M. tuberculosis* and *S. pneumonia* [165, 194]. Further studies will be needed in order to assert the real value of c-di-AMP and cGAMP as adjuvants in terms of safety and efficacy for human vaccine in clinical trials. However the overall capacity of CDNs to promote both humoral and cellular responses to a similar extent appeals as extremely attractive for vaccine development. In fact, currently available adjuvants mainly promote humoral responses and there are few candidate adjuvants promoting the elicitation of both, cellular and humoral immunity [195]. Adjuvants promoting both, humoral and cellular responses would be key tools for the development of vaccines against persistent intracellular pathogens. In this particular setting, it would be essential to promote Th1 cell-facilitated CTL responses, which are able to kill infected cells. To further enhance the immune activity against intracellular pathogens, Th2 cell-potentiated humoral responses can be induced to inactivate the agents released from infected cells before they are able to enter bystander cells [196].

An up-regulated expression of MHC class II and CD86, together with an increased production of type I IFNs and IL-12/IL-23p40 was observed after BMDC treatment with c-di-AMP or cGAMP. These parameters can be used as readouts for future *in vitro*

studies using specific inhibitors of potentially involved pathways that may be triggered by CDNs to explore signaling cascades involved in the adjuvant activity of CDNs. Comparative studies revealed that c-di-AMP is a more potent inducer of IL-12/IL-23p40 production than cGAMP. This raises the question if their differential potencies to enhance a Th17 response *in vivo* may result from their differential induction of these cytokines. To this end, further experiments should elucidate if IL-12, IL-23 or just monomers or dimers of p40 are differentially up-regulated and if this contributes to the differential activation of Th17 responses.

Type I IFN induction and signaling pathways were tested as mediators of the adjuvanticity of c-di-AMP and cGAMP. The c-di-AMP- and cGAMP-mediated enhancement of antigen-specific IgG responses, spleen cell proliferation and cytokine production were impaired in the animals lacking functional Sting, but not in mice lacking IFNAR. This led to the conclusion that the adjuvant effects of c-di-AMP and cGAMP are Sting-dependent, whereas IFNAR seems to be largely dispensable for adjuvanticity. However, IFNAR-mediated signaling seems to modulate the stimulated responses. For example, IFNAR seems to be required for a robust stimulation of IFN-γ responses enhanced by cGAMP. Future investigation may be designed to identify signaling pathway(s) triggered by Sting that are responsible for the CDN-mediated enhancement of adaptive immune responses. Those studies should define the pathways responsible for the residual adjuvant activity of c-di-GMP observed in animals lacking signaling via TBK-1-dependent non-canonical NF-κB-TNF-α pathway, as well as the mechanisms responsible for CTL priming and stimulation of long term memory responses.

The identification of Sting as a key molecule mediating the adjuvanticity of c-di-AMP and cGAMP presented here and its differential responsiveness to CDNs in specific ethnical groups of human population [193] illustrate that integration of the knowledge about molecular mode of action of candidate adjuvants and population genetics may be potentially exploited for prediction of the efficacy of candidate vaccines in specific geographical regions. For this reason, the results presented in this thesis demonstrate that experimental concept of investigating molecular mode of action of candidate adjuvants represents a valuable approach in future research strategies that aim at rational vaccine design.

6 BIBLIOGRAPHY

1. Dranoff, G., *Cytokines in cancer pathogenesis and cancer therapy.* Nat Rev Cancer, 2004. **4**(1): p. 11-22.
2. Murphy, K.M., *Janeway's Immunobiology*. 2011: Taylor & Francis Group.
3. Dutton, R.W., *In vitro studies of immunological responses of lymphoid cells.* Adv Immunol, 1967. **6**: p. 253-36.
4. Unanue, E.R. and B.A. Askonas, *The immune response of mice to antigen in macrophages.* Immunology, 1968. **15**(2): p. 287-96.
5. Creagh, E.M. and L.A. O'Neill, *TLRs, NLRs and RLRs: a trinity of pathogen sensors that co-operate in innate immunity.* Trends Immunol, 2006. **27**(8): p. 352-57.
6. Akira, S., S. Uematsu, and O. Takeuchi, *Pathogen recognition and innate immunity.* Cell, 2006. **124**(4): p. 783-01.
7. Yoshida, K., T.K. van den Berg, and C.D. Dijkstra, *Two functionally different follicular dendritic cells in secondary lymphoid follicles of mouse spleen, as revealed by CR1/2 and FcR gamma II-mediated immune-complex trapping.* Immunology, 1993. **80**(1): p. 34-39.
8. Wykes, M., et al., *Dendritic cells interact directly with naive B lymphocytes to transfer antigen and initiate class switching in a primary T-dependent response.* J Immunol, 1998. **161**(3): p. 1313-19.
9. Batista, F.D., D. Iber, and M.S. Neuberger, *B cells acquire antigen from target cells after synapse formation.* Nature, 2001. **411**(6836): p. 489-94.
10. Medzhitov, R., *Recognition of microorganisms and activation of the immune response.* Nature, 2007. **449**(7164): p. 819-26.
11. Pomerantz, J.L. and D. Baltimore, *NF-kappaB activation by a signaling complex containing TRAF2, TANK and TBK1, a novel IKK-related kinase.* EMBO J, 1999. **18**(23): p. 6694-04.
12. Perry, A.K., et al., *The host type I interferon response to viral and bacterial infections.* Cell Res, 2005. **15**(6): p. 407-22.
13. Remoli, M.E., et al., *Selective expression of type I IFN genes in human dendritic cells infected with Mycobacterium tuberculosis.* J Immunol, 2002. **169**(1): p. 366-74.
14. Takaoka, A., et al., *DAI (DLM-1/ZBP1) is a cytosolic DNA sensor and an activator of innate immune response.* Nature, 2007. **448**(7152): p. 501-05.
15. Unterholzner, L., et al., *IFI16 is an innate immune sensor for intracellular DNA.* Nat Immunol, 2010. **11**(11): p. 997-04.
16. Zhang, Z., et al., *The helicase DDX41 senses intracellular DNA mediated by the adaptor STING in dendritic cells.* Nat Immunol, 2011. **12**(10): p. 959-65.
17. Sun, L., et al., *Cyclic GMP-AMP synthase is a cytosolic DNA sensor that activates the type I interferon pathway.* Science, 2013. **339**(6121): p. 786-91.
18. Wu, J., et al., *Cyclic GMP-AMP is an endogenous second messenger in innate immune signaling by cytosolic DNA.* Science, 2013. **339**(6121): p. 826-30.

19. Hardy, M.P., et al., *Characterization and transcriptional analysis of the mouse Chromosome 16 cytokine receptor gene cluster.* Mamm Genome, 2003. **14**(2): p. 105-18.

20. Owczarek, C.M., et al., *Cloning and characterization of soluble and transmembrane isoforms of a novel component of the murine type I interferon receptor, IFNAR 2.* J Biol Chem, 1997. **272**(38): p. 23865-70.

21. Ishikawa, H. and G.N. Barber, *STING is an endoplasmic reticulum adaptor that facilitates innate immune signalling.* Nature, 2008. **455**(7213): p. 674-78.

22. Sun, W., et al., *ERIS, an endoplasmic reticulum IFN stimulator, activates innate immune signaling through dimerization.* Proc Natl Acad Sci U S A, 2009. **106**(21): p. 8653-58.

23. Berry, M.P.R., et al., *An interferon-inducible neutrophil-driven blood transcriptional signature in human tuberculosis.* Nature, 2010. **466**(7309): p. 973-77.

24. Zhong, B., et al., *The adaptor protein MITA links virus-sensing receptors to IRF3 transcription factor activation.* Immunity, 2008. **29**(4): p. 538-50.

25. Tanaka, Y. and Z.J. Chen, *STING specifies IRF3 phosphorylation by TBK1 in the cytosolic DNA signaling pathway.* Sci Signal, 2012. **5**(214): p. ra20.

26. Jin, L., et al., *MPYS, a novel membrane tetraspanner, is associated with major histocompatibility complex class II and mediates transduction of apoptotic signals.* Mol Cell Biol, 2008. **28**(16): p. 5014-26.

27. Chen, H., et al., *Activation of STAT6 by STING is critical for antiviral innate immunity.* Cell, 2011. **147**(2): p. 436-46.

28. Zhong, B., et al., *The ubiquitin ligase RNF5 regulates antiviral responses by mediating degradation of the adaptor protein MITA.* Immunity, 2009. **30**(3): p. 397-07.

29. Tsuchida, T., et al., *The ubiquitin ligase TRIM56 regulates innate immune responses to intracellular double-stranded DNA.* Immunity, 2010. **33**(5): p. 765-76.

30. Saitoh, T., et al., *Atg9a controls dsDNA-driven dynamic translocation of STING and the innate immune response.* Proc Natl Acad Sci U S A, 2009. **106**(49): p. 20842-46.

31. Zhang, L., et al., *NLRC3, a member of the NLR family of proteins, is a negative regulator of innate immune signaling induced by the DNA sensor STING.* Immunity, 2014. **40**(3): p. 329-41.

32. Holm, C.K., et al., *Virus-cell fusion as a trigger of innate immunity dependent on the adaptor STING.* Nat Immunol, 2012. **13**(8): p. 737-43.

33. Gao, D., et al., *Cyclic GMP-AMP synthase is an innate immune sensor of HIV and other retroviruses.* Science, 2013. **341**(6148).

34. Diner, E.J., et al., *The innate immune DNA sensor cGAS produces a non-canonical cyclic-di-nucleotide that activates human STING.* Cell Rep, 2013. **3**(5): p. 1355-61.

35. Ablasser, A., et al., *cGAS produces a 2[prime]-5[prime]-linked cyclic dinucleotide second messenger that activates STING.* Nature, 2013. **498**(7454): p. 380-84.

36. Zhang, X., et al., *Cyclic GMP-AMP containing mixed phosphodiester linkages is an endogenous high affinity ligand for STING.* Mol Cell, 2013. **51**(2).

37. Lafferty, K.J. and A.J. Cunningham, *A new analysis of allogeneic interactions.* Aust J Exp Biol Med Sci, 1975. **53**(1): p. 27-42.

38. Acuto, O. and F. Michel, *CD28-mediated co-stimulation: a quantitative support for TCR signalling.* Nat Rev Immunol, 2003. **3**(12): p. 939-51.

39. Butte, M.J., et al., *Programmed Death-1 Ligand 1 Interacts Specifically with the B7-1 Costimulatory Molecule to Inhibit T Cell Responses.* Immunity, 2007. **27**(1): p. 111-22.

40. Waterhouse, P., et al., *Lymphoproliferative disorders with early lethality in mice deficient in Ctla-4.* Science, 1995. **270**(5238): p. 985-88.

41. He, T., et al., *CD4+ T cell acquisition of the bystander pMHC I colocalizing in the same immunological synapse comprising pMHC II and costimulatory CD40, CD54, CD80, OX40L, and 41BBL.* Biochem Biophys Res Commun, 2007. **362**(4): p. 822-28.

42. Gonzalez, S.F., et al., *Complement-dependent transport of antigen into B cell follicles .* J Immunol, 2010. **185**(5): p. 2659-64.

43. Catron, D.M., et al., *A protease-dependent mechanism for initiating T-dependent B cell responses to large particulate antigens.* J Immunol, 2010. **184**(7): p. 3609-17.

44. Cambier, J.C., C.M. Pleiman, and M.R. Clark, *Signal transduction by the B cell antigen receptor and its coreceptors.* Annu Rev Immunol, 1994. **12**: p. 457-86.

45. De Becker, G., et al., *Regulation of T helper cell differentiation in vivo by soluble and membrane proteins provided by antigen-presenting cells.* Eur J Immunol, 1998. **28**(10): p. 3161-71.

46. Sornasse, T., et al., *Antigen-pulsed dendritic cells can efficiently induce an antibody response in vivo.* J Exp Med, 1992. **175**(1): p. 15-21.

47. Litinskiy, M.B., et al., *DCs induce CD40-independent immunoglobulin class switching through BLyS and APRIL.* Nat Immunol, 2002. **3**(9): p. 822-29.

48. Halpern, M.S. and M.E. Koshland, *Novel subunit in secretory IgA.* Nature, 1970. **228**(5278): p. 1276-78.

49. Mestecky, J., J. Zikan, and W.T. Butler, *Immunoglobulin M and secretory immunoglobulin A: presence of a common polypeptide chain different from light chains.* Science, 1971. **171**(3976): p. 1163-65.

50. Brandtzaeg, P. and H. Prydz, *Direct evidence for an integrated function of J chain and secretory component in epithelial transport of immunoglobulins.* Nature, 1984. **311**(5981): p. 71-73.

51. Mostov, K., T. Su, and M. ter Beest, *Polarized epithelial membrane traffic: conservation and plasticity.* Nat Cell Biol, 2003. **5**(4): p. 287-93.

52. Raux, M., et al., *IgG subclass distribution in serum and various mucosal fluids of HIV type 1-infected subjects.* AIDS Res Hum Retroviruses, 2000. **16**(6): p. 583-94.

53. Wagner, D.K., et al., *Analysis of immunoglobulin G antibody responses after administration of live and inactivated influenza A vaccine indicates that nasal*

wash immunoglobulin G is a transudate from serum. J Clin Microbiol, 1987. **25**(3): p. 559-62.

54. Conley, M.E. and D.L. Delacroix, *Intravascular and mucosal immunoglobulin A: two separate but related systems of immune defense?* Ann Intern Med, 1987. **106**(6): p. 892-99.

55. Feili-Hariri, M., D.H. Falkner, and P.A. Morel, *Polarization of naive T cells into Th1 or Th2 by distinct cytokine-driven murine dendritic cell populations: implications for immunotherapy.* J Leukoc Biol, 2005. **78**(3): p. 656-64.

56. Seder, R.A. and W.E. Paul, *Acquisition of lymphokine-producing phenotype by CD4+ T cells.* Annu Rev Immunol, 1994. **12**: p. 635-73.

57. Grossman, W.J., et al., *The orphan granzymes of humans and mice.* Curr Opin Immunol, 2003. **15**(5): p. 544-52.

58. Yasukawa, M., et al., *Granule exocytosis, and not the fas/fas ligand system, is the main pathway of cytotoxicity mediated by alloantigen-specific CD4(+) as well as CD8(+) cytotoxic T lymphocytes in humans.* Blood, 2000. **95**(7): p. 2352-55.

59. Stinchcombe, J.C. and G.M. Griffiths, *Secretory mechanisms in cell-mediated cytotoxicity.* Annu Rev Cell Dev Biol, 2007. **23**: p. 495-17.

60. Russell, J.H. and T.J. Ley, *Lymphocyte-mediated cytotoxicity.* Annu Rev Immunol, 2002. **20**: p. 323-70.

61. Lowin, B., et al., *Cytolytic T-cell cytotoxicity is mediated through perforin and Fas lytic pathways.* Nature, 1994. **370**(6491): p. 650-52.

62. Wilson, D.C., S. Matthews, and G.S. Yap, *IL-12 signaling drives CD8+ T cell IFN-gamma production and differentiation of KLRG1+ effector subpopulations during Toxoplasma gondii Infection.* J Immunol, 2008. **180**(9): p. 5935-45.

63. Romani, L., et al., *Candida albicans-specific Ly-2+ lymphocytes with cytolytic activity.* Eur J Immunol, 1991. **21**(6): p. 1567-70.

64. Flynn, S., et al., *CD4 T cell cytokine differentiation: the B cell activation molecule, OX40 ligand, instructs CD4 T cells to express interleukin 4 and upregulates expression of the chemokine receptor, Blr-1.* J Exp Med, 1998. **188**(2): p. 297-04.

65. Mowen, K.A. and L.H. Glimcher, *Signaling pathways in Th2 development.* Immunol Rev, 2004. **202**: p. 203-22.

66. Yang, L., et al., *IL-21 and TGF-beta are required for differentiation of human T(H)17 cells.* Nature, 2008. **454**(7202): p. 350-52.

67. Hirahara, K., et al., *Signal transduction pathways and transcriptional regulation in Th17 cell differentiation.* Cytokine Growth Factor Rev, 2010. **21**(6): p. 425-34.

68. Mangan, P.R., et al., *Transforming growth factor-beta induces development of the T(H)17 lineage.* Nature, 2006. **441**(7090): p. 231-34.

69. Chen, Y., et al., *Anti-IL-23 therapy inhibits multiple inflammatory pathways and ameliorates autoimmune encephalomyelitis.* J Clin Invest, 2006. **116**(5): p. 1317-26.

70. Harrington, L.E., et al., *Interleukin 17-producing CD4+ effector T cells develop via a lineage distinct from the T helper type 1 and 2 lineages.* Nat Immunol, 2005. **6**(11): p. 1123-32.

71. Ye, P., et al., *Requirement of interleukin 17 receptor signaling for lung CXC chemokine and granulocyte colony-stimulating factor expression, neutrophil recruitment, and host defense.* J Exp Med, 2001. **194**(4): p. 519-27.

72. Black, R.E., et al., *Global, regional, and national causes of child mortality in 2008: a systematic analysis.* Lancet, 2010. **375**(9730): p. 1969-87.

73. Vitoria, M., et al., *The global fight against HIV/AIDS, tuberculosis, and malaria: current status and future perspectives.* Am J Clin Pathol, 2009. **131**(6): p. 844-48.

74. Hornef, M.W., et al., *Bacterial strategies for overcoming host innate and adaptive immune responses.* Nat Immunol, 2002. **3**(11): p. 1033-40.

75. Rosenberger, C.M. and B.B. Finlay, *Phagocyte sabotage: disruption of macrophage signalling by bacterial pathogens.* Nat Rev Mol Cell Biol, 2003. **4**(5): p. 385-96.

76. Hilleman, M.R., *Strategies and mechanisms for host and pathogen survival in acute and persistent viral infections.* Proc Natl Acad Sci U S A, 2004. **101** Suppl 2: p. 14560-66.

77. Sorci, G., S. Cornet, and B. Faivre, *Immune evasion, immunopathology and the regulation of the immune system*. Pathogens. 2013 Mar;2(1):71-91. doi:10.3390/pathogens2010071.

78. Finlay, B.B. and G. McFadden, *Anti-immunology: evasion of the host immune system by bacterial and viral pathogens.* Cell, 2006. **124**(4): p. 767-82.

79. Davies, J. and D. Davies, *Origins and evolution of antibiotic resistance.* Microbiol Mol Biol Rev, 2010. **74**(3): p. 417-33.

80. Berzofsky, J.A., et al., *Progress on new vaccine strategies against chronic viral infections.* J Clin Invest, 2004. **114**(4): p. 450-62.

81. Ehreth, J., *The global value of vaccination.* Vaccine, 2003. **21**(7-8): p. 596-00.

82. Lamm, M.E., *Interaction of antigens and antibodies at mucosal surfaces.* Annu Rev Microbiol, 1997. **51**: p. 311-40.

83. Barackman, J.D., G. Ott, and D.T. O'Hagan, *Intranasal immunization of mice with influenza vaccine in combination with the adjuvant LT-R72 induces potent mucosal and serum immunity which is stronger than that with traditional intramuscular immunization.* Infect Immun, 1999. **67**(8): p. 4276-79.

84. Di Tommaso, A., et al., *Induction of antigen-specific antibodies in vaginal secretions by using a nontoxic mutant of heat-labile enterotoxin as a mucosal adjuvant.* Infect Immun, 1996. **64**(3): p. 974-79.

85. Kaul, D. and P.L. Ogra, *Mucosal responses to parenteral and mucosal vaccines.* Dev Biol Stand, 1998. **95**: p. 141-46.

86. Neutra, M.R. and J.P. Kraehenbuhl, *The role of transepithelial transport by M cells in microbial invasion and host defense.* J Cell Sci Suppl, 1993. **17**: p. 209-15.

87. Fubara, E.S. and R. Freter, *Protection against enteric bacterial infection by secretory IgA antibodies.* J Immunol, 1973. **111**(2): p. 395-03.

88. Stokes, C.R., J.F. Soothill, and M.W. Turner, *Immune exclusion is a function of IgA.* Nature, 1975. **255**(5511): p. 745-46.

89. Williams, R.C. and R.J. Gibbons, *Inhibition of bacterial adherence by secretory immunoglobulin A: a mechanism of antigen disposal.* Science, 1972. **177**(4050): p. 697-99.

90. Fokkens, W.J. and R.A. Scheeren, *Upper airway defence mechanisms.* Paediatr Respir Rev, 2000. **1**(4): p. 336-41.

91. Neutra, M.R., E. Pringault, and J.P. Kraehenbuhl, *Antigen sampling across epithelial barriers and induction of mucosal immune responses.* Annu Rev Immunol, 1996. **14**: p. 275-00.

92. Turnberg, L.A., *Gastric mucosal defence mechanisms.* Scand J Gastroenterol Suppl, 1985. **110**: p. 37-40.

93. Cerutti, A., *The regulation of IgA class switching.* Nat Rev Immunol, 2008. **8**(6): p. 421-34.

94. Kraehenbuhl, J.P. and M.R. Neutra, *Transepithelial transport and mucosal defence II: secretion of IgA.* Trends Cell Biol, 1992. **2**(6): p. 170-74.

95. Yokoyama, Y. and Y. Harabuchi, *Intranasal immunization with lipoteichoic acid and cholera toxin evokes specific pharyngeal IgA and systemic IgG responses and inhibits streptococcal adherence to pharyngeal epithelial cells in mice.* Int J Pediatr Otorhinolaryngol, 2002. **63**(3): p. 235-41.

96. Kweon, M.-N., *Recent progress in mucosal immunology and vaccine development.* Exp Mol Med, 2014. **46**: p. e86.

97. Johansson, E.L., et al., *Comparison of different routes of vaccination for eliciting antibody responses in the human stomach.* Vaccine, 2004. **22**(8): p. 984-90.

98. Kozlowski, P.A., et al., *Comparison of the oral, rectal, and vaginal immunization routes for induction of antibodies in rectal and genital tract secretions of women.* Infect Immun, 1997. **65**(4): p. 1387-94.

99. Sabin, A.B., *Oral poliovirus vaccine: history of its development and use and current challenge to eliminate poliomyelitis from the world.* J Infect Dis, 1985. **151**(3): p. 420-36.

100. Hirabayashi, Y., et al., *Comparison of intranasal inoculation of influenza HA vaccine combined with cholera toxin B subunit with oral or parenteral vaccination.* Vaccine, 1990. **8**(3): p. 243-48.

101. Kanesaki, T., et al., *Effectiveness of enteric immunization in the development of secretory immunoglobulin A response and the outcome of infection with respiratory syncytial virus.* J Virol, 1991. **65**(2): p. 657-63.

102. Kurono, Y., et al., *Nasal immunization induces Haemophilus influenzae-specific Th1 and Th2 responses with mucosal IgA and systemic IgG antibodies for protective immunity.* J Infect Dis, 1999. **180**(1): p. 122-32.

103. Del Giudice, G., M. Pizza, and R. Rappuoli, *Mucosal delivery of vaccines.* Methods, 1999. **19**(1): p. 148-55.

104. Forssell, H., *Gastric mucosal defence mechanisms: a brief review.* Scand J Gastroenterol Suppl, 1988. **155**: p. 23-28.

105. Chen, L., et al., *Enhanced nasal mucosal delivery and immunogenicity of anti-caries DNA vaccine through incorporation of anionic liposomes in chitosan/DNA complexes.* PLoS One, 2013. **8**(8): p. e71953.

106. Wu, H.Y., H.H. Nguyen, and M.W. Russell, *Nasal lymphoid tissue (NALT) as a mucosal immune inductive site.* Scand J Immunol, 1997. **46**(5): p. 506-13.

107. Kuper, C.F., et al., *The role of nasopharyngeal lymphoid tissue.* Immunol Today, 1992. **13**(6): p. 219-24.

108. Xu, Y., P.W. Yuen, and J.K. Lam, *Intranasal DNA vaccine for protection against respiratory infectious diseases: The Delivery Perspectives.* Pharmaceutics, 2014. **6**(3): p. 378-15.

109. Pavot, V., et al., *New insights in mucosal vaccine development.* Vaccine, 2012. **30**(2): p. 142-54.

110. Lauring, A.S., J.O. Jones, and R. Andino, *Rationalizing the development of live attenuated virus vaccines.* Nat Biotech, 2010. **28**(6): p. 573-79.

111. Murphy, T.V., et al., *Intussusception among infants given an oral rotavirus vaccine.* N Engl J Med, 2001. **344**(8): p. 564-72.

112. Rueckert, C. and C.A. Guzman, *Vaccines: from empirical development to rational design.* PLoS Pathog, 2012. **8**(11): p. e1003001.

113. Vogel, F.R., *Adjuvants in perspective.* Dev Biol Stand, 1998. **92**: p. 241-48.

114. Lycke, N., T. Tsuji, and J. Holmgren, *The adjuvant effect of Vibrio cholerae and Escherichia coli heat-labile enterotoxins is linked to their ADP-ribosyltransferase activity.* Eur J Immunol, 1992. **22**(9): p. 2277-81.

115. Holmgren, J., N. Lycke, and C. Czerkinsky, *Cholera toxin and cholera B subunit as oral-mucosal adjuvant and antigen vector systems.* Vaccine, 1993. **11**(12): p. 1179-84.

116. Jagusztyn-Krynicka, E.K., J.E. Clark-Curtiss, and R. Curtiss, 3rd, *Escherichia coli heat-labile toxin subunit B fusions with Streptococcus sobrinus antigens expressed by Salmonella typhimurium oral vaccine strains: importance of the linker for antigenicity and biological activities of the hybrid proteins.* Infect Immun, 1993. **61**(3): p. 1004-15.

117. Mutsch, M., et al., *Use of the inactivated intranasal influenza vaccine and the risk of Bell's palsy in Switzerland.* N Engl J Med, 2004. **350**(9): p. 896-03.

118. Brewer, J.M., et al., *In interleukin-4-deficient mice, alum not only generates T helper 1 responses equivalent to freund's complete adjuvant, but continues to induce T helper 2 cytokine production.* Eur J Immunol, 1996. **26**(9): p. 2062-66.

119. Grun, J.L. and P.H. Maurer, *Different T helper cell subsets elicited in mice utilizing two different adjuvant vehicles: the role of endogenous interleukin 1 in proliferative responses.* Cell Immunol, 1989. **121**(1): p. 134-45.

120. Brewer, J.M., et al., *Aluminium hydroxide adjuvant initiates strong antigen-specific Th2 responses in the absence of IL-4- or IL-13-mediated signaling.* J Immunol, 1999. **163**(12): p. 6448-54.

121. Quan, F.S., et al., *Mucosal adjuvants for influenza virus-like particle vaccine.* Viral Immunol, 2013. **26**(6): p. 385-95.

122. Clapp, T., et al., *Vaccines with aluminum-containing adjuvants: optimizing vaccine efficacy and thermal stability.* J Pharm Sci, 2011. **100**(2): p. 388-01.

123. Rappuoli, R., et al., *Vaccines for the twenty-first century society.* Nat Rev Immunol, 2011. **11**(12): p. 865-72.

124. Ross, P., et al., *Regulation of cellulose synthesis in Acetobacter xylinum by cyclic diguanylic acid.* Nature, 1987. **325**(6101): p. 279-81.

125. Witte, G., et al., *Structural biochemistry of a bacterial checkpoint protein reveals diadenylate cyclase activity regulated by DNA recombination intermediates.* Mol Cell, 2008. **30**(2): p. 167-78.

126. Davies, B.W., et al., *Coordinated regulation of accessory genetic elements produces cyclic di-nucleotides for V. cholerae virulence.* Cell, 2012. **149**(2): p. 358-70.

127. Chen, L.H., et al., *Cyclic di-GMP-dependent signaling pathways in the pathogenic Firmicute Listeria monocytogenes.* PLoS Pathog, 2014. **10**(8): p. e1004301.

128. Hong, Y., et al., *Cyclic di-GMP mediates Mycobacterium tuberculosis dormancy and pathogenecity.* Tuberculosis (Edinb), 2013. **93**(6): p. 625-34.

129. Tamayo, R., et al., *Role of cyclic Di-GMP during el tor biotype Vibrio cholerae infection: characterization of the in vivo-induced cyclic Di-GMP phosphodiesterase CdpA.* Infect Immun, 2008. **76**(4): p. 1617-27.

130. Schwartz, K.T., et al., *Hyperinduction of host beta interferon by a Listeria monocytogenes strain naturally overexpressing the multidrug efflux pump MdrT.* Infect Immun, 2012. **80**(4): p. 1537-45.

131. Woodward, J.J., A.T. Iavarone, and D.A. Portnoy, *c-di-AMP secreted by intracellular Listeria monocytogenes activates a host Type I interferon response.* Science, 2010. **328**(5986): p. 1703-05.

132. Yang, J., et al., *Deletion of the cyclic di-AMP phosphodiesterase gene (cnpB) in Mycobacterium tuberculosis leads to reduced virulence in a mouse model of infection.* Mol Microbiol, 2014. **93**(1): p. 65-79.

133. Biolog, G. *Biolog products*. 2015 [cited 2015 30.3.2015]; Chemical structures of cyclic di-nucleotides]. Available from: http://www.biolog.de/products/eshop/product/C_088/.

134. Burdette, D.L., et al., *STING is a direct innate immune sensor of cyclic di-GMP.* Nature, 2011. **478**(7370): p. 515-18.

135. Sauer, J.D., et al., *The N-ethyl-N-nitrosourea-induced Goldenticket mouse mutant reveals an essential function of Sting in the in vivo interferon response to Listeria monocytogenes and cyclic dinucleotides.* Infect Immun, 2011. **79**(2): p. 688-94.

136. Jin, L., et al., *MPYS is required for IFN response factor 3 activation and type I IFN production in the response of cultured phagocytes to bacterial second messengers cyclic-di-AMP and cyclic-di-GMP.* J Immunol, 2011. **187**(5): p. 2595-01.

137. Parvatiyar, K., et al., *The helicase DDX41 recognizes the bacterial secondary messengers cyclic di-GMP and cyclic di-AMP to activate a type I interferon immune response.* Nat Immunol, 2012. **13**(12): p. 1155-61.

138. Karaolis, D.K., et al., *Bacterial c-di-GMP is an immunostimulatory molecule.* J Immunol, 2007. **178**(4): p. 2171-81.

139. Ebensen, T., et al., *Bis-(3',5')-cyclic dimeric adenosine monophosphate: strong Th1/Th2/Th17 promoting mucosal adjuvant.* Vaccine, 2011. **29**(32): p. 5210-20.

140. Skrnjug, I., C.A. Guzman, and C. Ruecker, *Cyclic GMP-AMP displays mucosal adjuvant activity in mice.* PLoS One, 2014. **9**(10): p. e110150.

141. Huang, Y.-H., et al., *The structural basis for the sensing and binding of cyclic di-GMP by STING.* Nat Struct Mol Biol, 2012. **19**(7): p. 728-30.

142. Ouyang, S., et al., *Structural analysis of the STING adaptor protein reveals a hydrophobic dimer interface and mode of cyclic di-GMP binding.* Immunity, 2012. **36**(6): p. 1073-86.

143. Gratz, N., et al., *Group A streptococcus activates type I interferon production and MyD88-dependent signaling without involvement of TLR2, TLR4, and TLR9.* J Biol Chem, 2008. **283**(29): p. 19879-87.

144. Xiao, Z., et al., *Programming for CD8 T cell memory development requires IL-12 or type I IFN.* J Immunol, 2009. **182**(5): p. 2786-94.

145. Kaplan, A., et al., *Failure to induce IFN-beta production during Staphylococcus aureus infection contributes to pathogenicity.* J Immunol, 2012. **189**(9): p. 4537-45.

146. Archer, K.A., J. Durack, and D.A. Portnoy, *STING-dependent type I IFN production inhibits cell-mediated immunity to Listeria monocytogenes.* PLoS Pathog, 2014. **10**(1): p. e1003861.

147. Blaauboer, S.M., V.D. Gabrielle, and L. Jin, *MPYS/STING-mediated TNF-alpha, not type I IFN, is essential for the mucosal adjuvant activity of (3'-5')-cyclic-di-guanosine-monophosphate in vivo.* J Immunol, 2014. **192**(1): p. 492-02.

148. Muller, U., et al., *Functional role of type I and type II interferons in antiviral defense.* Science, 1994. **264**(5167): p. 1918-21.

149. Inagawa, H., C. Kohchi, and G. Soma, *Oral administration of lipopolysaccharides for the prevention of various diseases: benefit and usefulness.* Anticancer Res, 2011. **31**(7): p. 2431-36.

150. Charles River, U. *Products_basic research_mouse model*. 2015 [cited 2015 30.3.2015.]; Available from: http://www.criver.com/products-services/basic-research/find-a-model/c57bl-6-e-mouse.

151. Nimmerjahn, F. and J.V. Ravetch, *Divergent immunoglobulin g subclass activity through selective Fc receptor binding.* Science, 2005. **310**(5753): p. 1510-12.

152. Zhou, L., et al., *IL-6 programs T(H)-17 cell differentiation by promoting sequential engagement of the IL-21 and IL-23 pathways.* Nat Immunol, 2007. **8**(9): p. 967-74.

153. Skrnjug, I., et al., *The mucosal adjuvant cyclic di-AMP exerts immune stimulatory effects on dendritic cells and macrophages.* PLoS One, 2014. **9**(4): p. e95728.

154. Slutter, B., et al., *Conjugation of ovalbumin to trimethyl chitosan improves immunogenicity of the antigen.* J Control Release, 2010. **143**(2): p. 207-14.

155. Plotkin, S.A., *Vaccines: correlates of vaccine-induced immunity.* Clin Infect Dis, 2008. **47**(3): p. 401-09.

156. Lu, Y.J., et al., *Interleukin-17A mediates acquired immunity to pneumococcal colonization.* PLoS Pathog, 2008. **4**(9): p. e1000159.

157. Malley, R., et al., *Antibody-independent, interleukin-17A-mediated, cross-serotype immunity to pneumococci in mice immunized intranasally with the cell wall polysaccharide.* Infect Immun, 2006. **74**(4): p. 2187-95.

158. DeLyria, E.S., R.W. Redline, and T.G. Blanchard, *Vaccination of mice against H pylori induces a strong Th-17 response and immunity that is neutrophil dependent.* Gastroenterology, 2009. **136**(1): p. 247-56.

159. Priebe, G.P., et al., *IL-17 is a critical component of vaccine-induced protection against lung infection by lipopolysaccharide-heterologous strains of Pseudomonas aeruginosa.* J Immunol, 2008. **181**(7): p. 4965-75.

160. Li, X.D., et al., *Pivotal roles of cGAS-cGAMP signaling in antiviral defense and immune adjuvant effects.* Science, 2013. **341**(6152): p. 1390-94.

161. Montomoli, E., et al., *Current adjuvants and new perspectives in vaccine formulation.* Expert Rev Vaccines, 2011. **10**(7): p. 1053-61.

162. Muranski, P. and N.P. Restifo, *Essentials of Th17 cell commitment and plasticity.* Blood, 2013. **121**(13): p. 2402-14.

163. Jaffar, Z., et al., *Cutting edge: lung mucosal Th17-mediated responses induce polymeric Ig receptor expression by the airway epithelium and elevate secretory IgA levels.* J Immunol, 2009. **182**(8): p. 4507-11.

164. Doreau, A., et al., *Interleukin 17 acts in synergy with B cell-activating factor to influence B cell biology and the pathophysiology of systemic lupus erythematosus.* Nat Immunol, 2009. **10**(7): p. 778-85.

165. Moffitt, K.L., et al., *T(H)17-based vaccine design for prevention of Streptococcus pneumoniae colonization.* Cell Host Microbe, 2011. **9**(2): p. 158-65.

166. Scriba, T.J., et al., *Distinct, specific IL-17- and IL-22-producing CD4+ T cell subsets contribute to the human anti-mycobacterial immune response.* J Immunol, 2008. **180**(3): p. 1962-70.

167. de Cassan, S.C., et al., *Investigating the induction of vaccine-induced Th17 and regulatory T cells in healthy, Mycobacterium bovis BCG-immunized adults vaccinated with a new tuberculosis vaccine, MVA85A.* Clin Vaccine Immunol, 2010. **17**(7): p. 1066-73.

168. Waite, J.C. and D. Skokos, *Th17 response and inflammatory autoimmune diseases.* Int J Inflam, 2012. **2012**: p. 819467.

169. Leipe, J., et al., *Role of Th17 cells in human autoimmune arthritis.* Arthritis Rheum, 2010. **62**(10): p. 2876-85.

170. Miossec, P. and J.K. Kolls, *Targeting IL-17 and TH17 cells in chronic inflammation.* Nat Rev Drug Discov, 2012. **11**(10): p. 763-76.

171. Burchill, M.A., et al., *Inhibition of interleukin-17 prevents the development of arthritis in vaccinated mice challenged with Borrelia burgdorferi.* Infect Immun, 2003. **71**(6): p. 3437-42.

172. Komiyama, Y., et al., *IL-17 plays an important role in the development of experimental autoimmune encephalomyelitis.* J Immunol, 2006. **177**(1): p. 566-73.

173. Cua, D.J., et al., *Interleukin-23 rather than interleukin-12 is the critical cytokine for autoimmune inflammation of the brain.* Nature, 2003. **421**(6924): p. 744-48.

174. Klinke, D.J., 2nd, *The ratio of P40 monomer to dimer is an important determinant of IL-12 bioactivity.* J Theor Biol, 2006. **240**(2): p. 323-35.

175. McKnight, A.J., et al., *Effects of IL-12 on helper T cell-dependent immune responses in vivo.* J Immunol, 1994. **152**(5): p. 2172-79.

176. Huber, J.P. and J.D. Farrar, *Regulation of effector and memory T-cell functions by type I interferon.* Immunology, 2011. **132**(4): p. 466-74.

177. Guo, B., E.Y. Chang, and G. Cheng, *The type I IFN induction pathway constrains Th17-mediated autoimmune inflammation in mice.* J Clin Invest, 2008. **118**(5): p. 1680-90.

178. Bach, P., et al., *Vesicular stomatitis virus glycoprotein displaying retrovirus-like particles induce a type I IFN receptor-dependent switch to neutralizing IgG antibodies.* J Immunol, 2007. **178**(9): p. 5839-47.

179. Le Bon, A., et al., *Type i interferons potently enhance humoral immunity and can promote isotype switching by stimulating dendritic cells in vivo.* Immunity, 2001. **14**(4): p. 461-70.

180. Proietti, E., et al., *Type I IFN as a natural adjuvant for a protective immune response: lessons from the influenza vaccine model.* J Immunol, 2002. **169**(1): p. 375-83.

181. Su, C., et al., *IFN-alpha as an ddjuvant for adenovirus-vectored FMDV subunit vaccine through improving the generation of T follicular helper cells.* PLoS One, 2013. **8**(6): p. e66134.

182. Zhang, X., et al., *Potent and selective stimulation of memory-phenotype CD8+ T cells in vivo by IL-15.* Immunity, 1998. **8**(5): p. 591-99.

183. Abe, T. and G.N. Barber, *Cytosolic-DNA-mediated, STING-dependent proinflammatory gene induction necessitates canonical NF-kappaB activation through TBK1.* J Virol, 2014. **88**(10): p. 5328-41.

184. Konno, H., K. Konno, and Glen N. Barber, *Cyclic dinucleotides trigger ULK1 (ATG1) phosphorylation of STING to prevent sustained innate immune signaling.* Cell, 2013. **155**(3): p. 688-98.

185. Chen, H., et al., *An alternative splicing isoform of MITA antagonizes MITA-mediated induction of type I IFNs.* J Immunol, 2014. **192**(3): p. 1162-70.

186. Ahn, J., et al., *STING manifests self DNA-dependent inflammatory disease.* Proc Natl Acad Sci U S A, 2012. **109**(47): p. 19386-91.

187. Gall, A., et al., *Autoimmunity initiates in nonhematopoietic cells and progresses via lymphocytes in an interferon-dependent autoimmune disease.* Immunity, 2012. **36**(1): p. 120-31.

188. Abe, T., et al., *STING recognition of cytoplasmic DNA instigates cellular defense.* Mol Cell, 2013. **50**(1): p. 5-15.

189. Stetson, D.B., et al., *Trex1 prevents cell-intrinsic initiation of autoimmunity.* Cell, 2008. **134**(4): p. 587-98.

190. Kramer, M.J., J.L. Taylor, and S.E. Grossberg, *Induction of interferon in mice by 10-carboxymethyl-9-acridanone.* Methods Enzymol, 1981. **78**(Pt A): p. 284-87.

191. Cavlar, T., et al., *Species-specific detection of the antiviral small-molecule compound CMA by STING.* Embo j, 2013. **32**(10): p. 1440-50.

192. Conlon, J., et al., *Mouse, but not human STING, binds and signals in response to the vascular disrupting agent 5,6-dimethylxanthenone-4-acetic acid.* J Immunol, 2013. **190**(10): p. 5216-25.

193. Yi, G., et al., *Single nucleotide polymorphisms of human STING can affect innate immune response to cyclic dinucleotides.* PLoS One, 2013. **8**(10): p. e77846.

194. Monin, L., et al., *Immune requirements for protective Th17 recall responses to Mycobacterium tuberculosis challenge.* Mucosal Immunol, 2015.

195. Petrovsky, N. and J.C. Aguilar, *Vaccine adjuvants: Current state and future trends.* Immunol Cell Biol, 2004. **82**(5): p. 488-96.

196. Casadevall, A., *Antibody-mediated immunity against intracellular pathogens: two-dimensional thinking comes full circle.* Infect Immun, 2003. **71**(8): p. 4225-28.